AD-A044 261 DAVID W TAYLOR NAVAL SHIP RESEARCH AND DEVELOPMENT CE--ETC F/G 1/3
SEAWORTHINESS CHARACTERISTICS OF A 2900 TON SMALL WATERPLANE AR--ETC(U)
SEP 76 J A KALLIO

UNCLASSIFIED SPD-620-03 NL

1 OF 2
ADA
044261

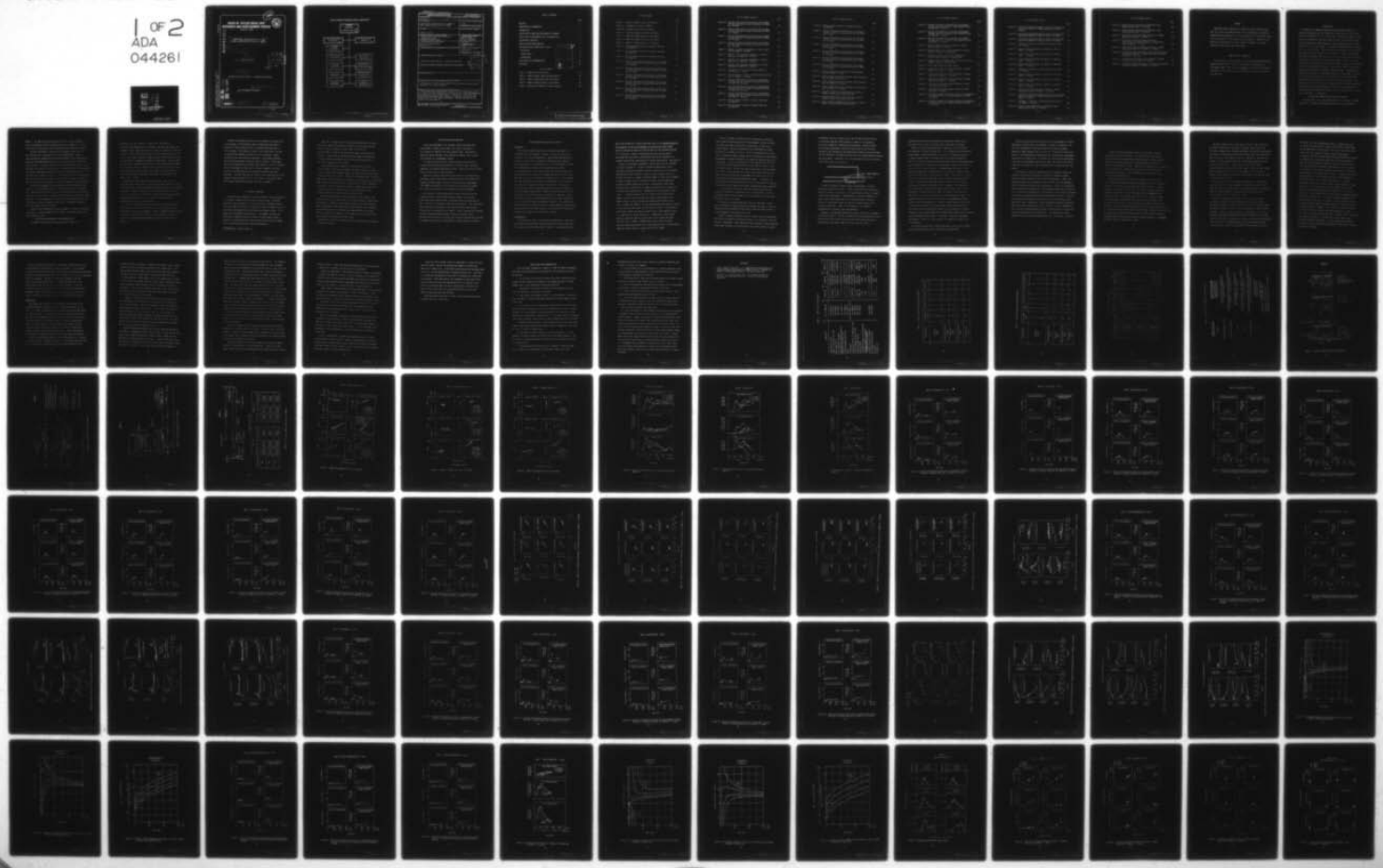

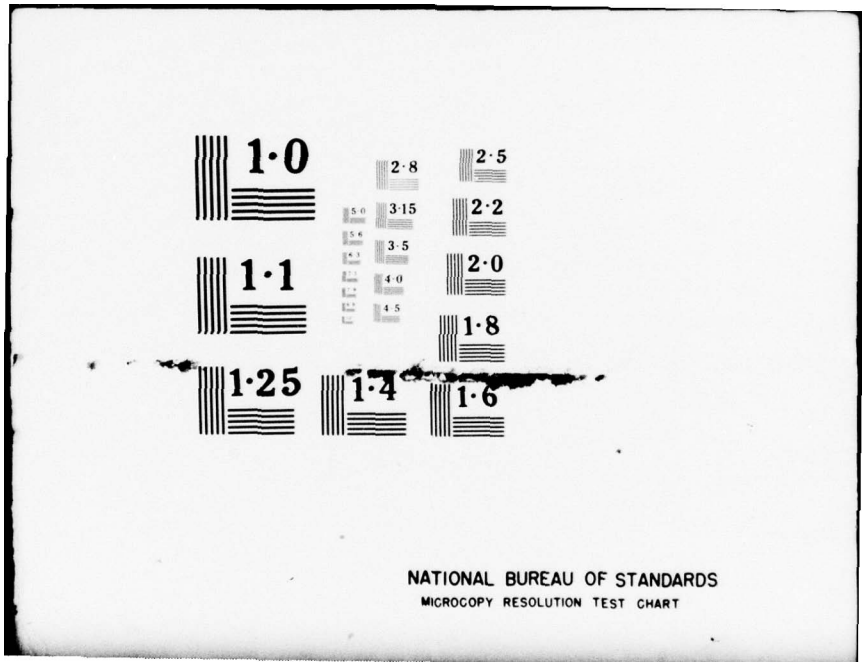
1·0
1·1
1·25
1·4
1·6
1·8
2·0
2·2
2·5
2·8
3·15
3·5
4·0
4·5
5·0
5·6
NATIONAL BUREAU OF STANDARDS
MICROCOPY RESOLUTION TEST CHART

SPD-620-03

DAVID W. TAYLOR NAVAL SHIP RESEARCH AND DEVELOPMENT CENTER

Bethesda, Md. 20084

SEAWORTHINESS CHARACTERISTICS OF A 2900 TON SMALL WATERPLANE AREA TWIN HULL (SWATH)

Final rept.,

by

James A. Kallio

F43421

APPROVED FOR PUBLIC RELEASE: DISTRIBUTION UNLIMITED

ZF43421001

SHIP PERFORMANCE DEPARTMENT

SEP 1976 | 123 p. | SPD-620-03

389 694

SEAWORTHINESS CHARACTERISTICS OF A 2900 TON SMALL WATERPLANE AREA TWIN HULL (SWATH)

MAJOR DTNSRDC ORGANIZATIONAL COMPONENTS

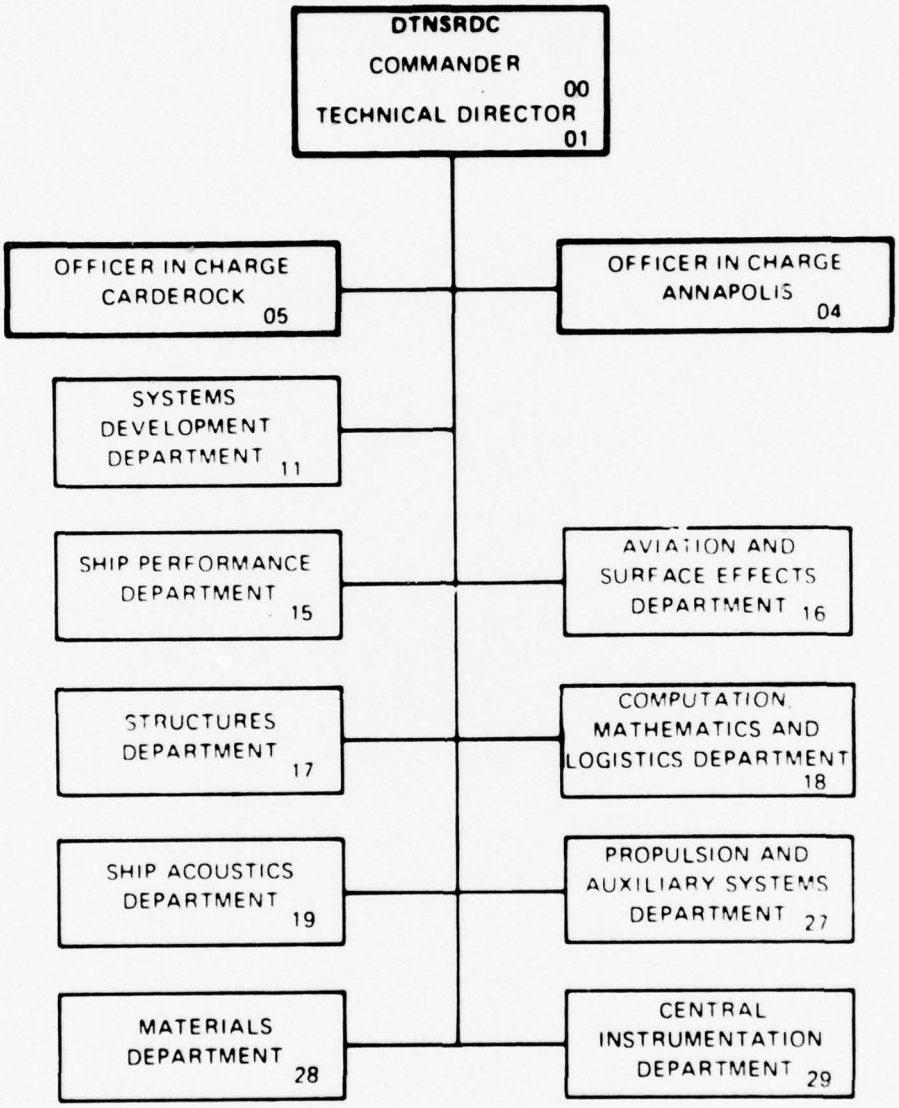

UNCLASSIFIED

SECURITY CLASSIFICATION OF THIS PAGE (When Data Entered)

REPORT DOCUMENTATION PAGE		READ INSTRUCTIONS BEFORE COMPLETING FORM
1. REPORT NUMBER SPD-620-03	2. GOVT ACCESSION NO.	3. RECIPIENT'S CATALOG NUMBER
4. TITLE (and Subtitle) Seaworthiness Characteristics of a 2900 Ton Small Waterplane Area Twin Hull (SWATH)		5. TYPE OF REPORT & PERIOD COVERED Final 6. PERFORMING ORG. REPORT NUMBER
7. AUTHOR(s) James A. Kallio		8. CONTRACT OR GRANT NUMBER(s)
9. PERFORMING ORGANIZATION NAME AND ADDRESS David W. Taylor Naval Ship Research and Development Center Bethesda, Maryland 20084		10. PROGRAM ELEMENT, PROJECT, TASK AREA & WORK UNIT NUMBERS Element 62543N Work Unit 1507-200 Task Area ZF43421001
11. CONTROLLING OFFICE NAME AND ADDRESS Naval Sea Systems Command Washington, D. C.		12. REPORT DATE September 1976 13. NUMBER OF PAGES 113
14. MONITORING AGENCY NAME & ADDRESS(if different from Controlling Office)		15. SECURITY CLASS. (of this report) UNCLASSIFIED 15a. DECLASSIFICATION/DOWNGRADING SCHEDULE

16. DISTRIBUTION STATEMENT (of this Report)

APPROVED FOR PUBLIC RELEASE: DISTRIBUTION UNLIMITED

17. DISTRIBUTION STATEMENT (of the abstract entered in Block 20, if different from Report)

18. SUPPLEMENTARY NOTES

19. KEY WORDS (Continue on reverse side if necessary and identify by block number)

SWATH Motions and Acclerations; Three Strut Configurations, Bow and Stern Horizontal Fins; Impact Pressures

20. ABSTRACT (Continue on reverse side if necessary and identify by block number)

Experiments were conducted with a model of a small waterplane area twin hull craft, with three different strut configurations, in both the Maneuvering and Seakeeping Facility and Carriage II of the David W. Taylor Naval Ship Research and Development Center (DTNSRDC) to determine craft motions and acceleration at various speeds and headings. Data were obtained in both regular and random seaways.

DD FORM 1 JAN 73 1473 EDITION OF 1 NOV 65 IS OBSOLETE
S/N 0102-014-6601

UNCLASSIFIED

SECURITY CLASSIFICATION OF THIS PAGE (When Data Entered)

TABLE OF CONTENTS

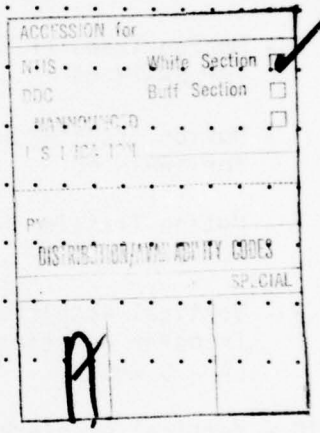

LIST OF TABLES

LIST OF FIGURES

LIST OF FIGURES (Cont'd)

LIST OF FIGURES (Cont'd)

LIST OF FIGURES (Cont'd)

LIST OF FIGURES (Cont'd)

LIST OF FIGURES (Cont'd)

ABSTRACT

Experiments were conducted with a model of a small waterplane area twin hull craft, with three different strut configurations, in both the Maneuvering and Seakeeping Facility and Carriage II of the David W. Taylor Naval Ship Research and Development Center (DTNSRDC) to determine craft motions and acceleration at various speeds and headings. Data were obtained in both regular and random seaways.

ADMINISTRATIVE INFORMATION

This project was jointly funded by the Systems Development Department, Advanced Concepts Office, David W. Taylor Naval Ship Research and Development Center, under work unit 1170-090 and by the Ship Performance Department's High Performance Vehicle Hydrodynamics Program under work unit 1507-200.

INTRODUCTION

An experimental seakeeping program was conducted with a model of a small waterplane area twin hull (SWATH) with three different strut configurations, represented by a 1:22.5 scale model, designated as SWATH 6. Experiments were conducted in head, bow quartering, beam, stern quartering and following regular and random seaways at speeds corresponding to full scale speeds of 0, 10, 20 and 28 knots. Calm water experiments were also conducted at 0, 10, 20 and 28 knots. These experiments were conducted with the model free running, without restraint, in six degrees of freedom. Measurements were made of the seaway, the craft pitch, roll, yaw, heave, surge, sway, relative motion near the bow, roll acceleration (angular) as well as vertical acceleration at three places along the craft length, surge, and sway acceleration and stern horizontal fin angle. Pressures due to wave impacting were measured at four locations along the bridging structure. Investigations were made of the effect of longitudinal metacentric height ($\overline{GM}_L$), characteristic of the three different strut configurations, on the craft motions, accelerations and impact pressures at various headings and speeds. This report consists of running trim and sinkage data from calm water experiments, motion transfer functions determined from regular wave experiments and significant double amplitudes of motions and impact pressure data collected during experiments in random waves.

DESCRIPTION OF MODEL AND EXPERIMENTAL EQUIPMENT

The model used in this investigation was a 22.5 scale model, DTNSRDC Model 5337, of a 2900 ton developmental SWATH type craft designated as

SWATH 6. The model was constructed such that any of three different strut configurations could be attached to one set of lower hulls. Craft particulars for the various strut configurations are presented in Table 1.

The major difference in characteristics imparted to the craft by the different strut configurations is the longitudinal $\overline{GM}$. Figure 1 shows the physical dimensions for the three different craft configurations. Note that while SWATH 6A and 6B have only one strut per hull, 6C has two struts per hull. Also note (Table 1) that all configurations used a set of horizontal stabilizer fins (two per hull, inboard) and those for 6A had about 40% greater projected area than those used on configurations 6B and 6C. Fin shape and size is shown in Figure 2. The forward fins on all configurations were fixed at zero angle of attack while the angle of attack on the aft set was variable and could be changed by means of a remotely controlled actuator.

The port and starboard hull-strut combinations were attached to each other by a rigid bridging structure. Diaphragm type pressure transducers were attached on the flat bottom portion near the bow and on the curved bow section of this structure, at locations shown by Figure 1b, to measure impact pressures. A strain gaged panel section on the flat bottom portion of this structure was also used to measure impact loads. No attempt was made to scale the rigidity of this structure.

Propulsion was provided by two five horsepower D.C. motors, one housed in each hull. Since the model was free running, controllable rudders were used to maintain course.

DESCRIPTION OF MEASUREMENTS AND INSTRUMENTATION

The SWATH 6A experiments were conducted with the model self

propelled and free running. Tether lines, required for acceleration and deceleration of the model, and motor power cables and transducer signal cables were the only connections between the model and carriage. These lines and cables were slack during data collection and did not affect model responses. Model speed was controlled manually and was regulated in accordance with preset carriage speed. Thus the model was kept fairly stationary with respect to the carriage and model speed was relatively constant. However, during some head sea conditions with severe impacting, and during some stern quartering and following sea conditions there was considerable surge motion and the tether lines became taut at times.

Course was maintained by means of yaw and sway signal inputs to the rudder servo control device. Heave, surge, sway and relative motion at the bow as well as wave height were measured by ultrasonic displacement transducers. Heave was measured at the longitudinal center of gravity (LCG) on the centerline, surge at the aft edge of the bridging structure, and relative bow motion 9 ft (2.8m) forward of the front edge of the bridging structure, on the centerline.

Pitch, roll, and yaw were measured by vertical gyroscopes mounted near the LCG just to port of the centerline. Roll acceleration was measured by an angular accelerometer. Vertical accelerations were measured at the bow, at the LCG and at the stern at the locations indicated in Figure 1a. Surge and sway accelerometer locations are also given in Figure 1a.

Although the bridging structure did not necessarily represent that of a prototype, it did provide a means of determining the order of magnitude of impact pressure which a prototype might experience in various seaways. No attempt was made to scale the bridging structure to simulate the vibratory characteristics of a prototype. Impact pressures on this structure were measured by strain-gaged diaphragm type pressure transducers located as shown in Figure 1b. These gages, designed and manufactured at DTNSRDC, were rated at 0 to 5 psi (34.5k Pa) with a flat response to 1500 hz and a natural frequency of at least 25,000 hz, and thus were more than adequate to measure the impact phenomena. The panel load gage was simply a strain gaged section of the plywood bridging structure, 9.4 ft (2.9m) square. The maximum range and freuqency response of the panel load gage is unknown.

EXPERIMENTAL PROCEDURE

Experiments were conducted on the three different strut configurations in calm water, regular and long crested irregular waves. Calm water experiments were conducted at 10, 20 and 28 knots to determine running trim and sinkage for various trim moments and stern fin angles. During all experiments the forward fins were fixed at zero angle of attack. Trim moments were produced by moving ballast. Trim moments and stern fin angles which produced a near zero running trim were chosen, based on experience, for each particular speed such that neither the trim moment nor fin angle were excessively large (See Reference 1).*

* References are listed on page 24.

Once the trim moments and fin angles were established, calm water runs were conducted during which the model was force pulsed manually near its natural frequency in pitch, heave or roll at the various speeds in order to determine motion decay curves and natural periods. In some cases at the 20 and 28 knot speeds, the motion was so highly damped that determination of the natural heave and pitch period was impossible by this method.

Experiments were then conducted in regular and long crested irregular waves at the various headings and speeds indicated in Tables 2 and 3. Nominal wave steepness ($2\zeta_A/\lambda$) for the regular wave experiments ranged from about 1/50 to 1/90. In addition, experiments were conducted in head regular seas at 20 knots and in beam seas at 0 knots in near synchronous wave conditions for heave and roll, respectively, at several steepnesses to provide a linearity check on the motions. Regular wave experiments in head seas were also conducted on each strut configuration with various combinations of the horizontal stabilizer fins.

Irregular wave experiments were conducted at various headings and speeds (See Table 3) to obtain statistical data on motions, accelerations and frequency of impact on the bridging structure. For each condition about 150 samples of peak-to-peak motions were obtained since experience has shown that realistic inferences about the population may be made from this sample size. However, not all sample sizes in some quartering and following sea conditions were this large.

Note that for strut 6A a linearity check in random waves was conducted at 0 knots in head seas.

DATA COLLECTION AND REDUCTION

During the experiments, the transducer signals were amplified and recorded in analog form on paper strip chart (including an oscillograph for impacts) and analog magnetic tape. The system for measuring impacts provided a flat response to 1500 hz, which is more than adequate for the phenomena studied.

Calm water running trim and sinkage and regular wave data were recorded and analyzed by the Interdata 70 on the carriage providing immediate high quality experimental results. Natural period oscillation data were read from strip chart records.

Reduction of regular wave data by the Interdata 70 provided motion amplitudes, phases, mean offsets, amplitudes of the first harmonic wave frequency and the transfer function for each particular measurement. The immediate availability of this data on the carriage was used to plan future run conditions as the experimental program proceeded.

Data obtained in random waves were analyzed in both the time and frequency domains by the CDC 6700 computer program. This analysis yields mean values, power spectra, histograms and Fourier transforms as well as statistical information about the time histories. Only significant double amplitudes (the average of the one-third highest peak-to-peak fluctuations) are presented in this report. Impact pressure data obtained in random waves were extracted manually from oscillograph records. Absolute vertical motions at the bow, the LCG and at the stern were obtained by integrating the vertical accelerations at these respective locations.

PRESENTATION AND DISCUSSION OF RESULTS

CALM WATER

The trim and sinkage results from calm water experiments at 10 20 and 28 knots are presented in Figures 3, 4 and 5 for strut configurations A, B and C respectively. These figures show the effect of stern fin angle and trim moment on running trim and sinkage for the various speeds. At 10 knots there is little trim moment or stern fin angle effect on running trim or sinkage for any of the strut configurations. At 20 and 28 knots craft trim and sinkage are very responsive to a change in trim moment and stern fin angle, somewhat more so for strut configuration A than for B or C. Note, however, the total projected aft fin area for configuration A is 40% greater than that for configurations B and C (See Table 1). There was no vertical plane instability demonstrated for any strut configuration at any of the speeds investigated. There was also no indication that any of the stern fins had approached or reached stall condition. Heave, pitch and roll natural periods determined from calm water experiments at 0, 10, 20 and 28 knots are presented in Table 4. Also presented in Table 4 are the trim moment and stern fin angle needed for approximately zero running trim, which were used for a particular strut configuration and particular speed for all experiments in waves.

REGULAR WAVES

The regular wave data in this report are presented as a function of wave length, and the motions nondimensionalized as transfer functions in accordance with the scheme shown in Table 5. The observations made

during the discussion of regular wave data refer to the maximum dimensionless response and not to the response to any particular wave length. Vertical acceleration data and linearity data are not nondimensionalized for discussion. However, dimensionless absolute vertical motions calculated from the vertical accelerations do give an indication of a transfer function type relationship for vertical acceleration. (See Table 5).

Results of experiments conducted in regular head seas are presented in Figures 6 through 23. Figures 6 through 8 present heave, pitch and relative bow motion transfer function in head seas at various speeds. Nondimensional heave decreases slightly as speed increases from 0 to 28 knots for strut A , changes little with speed for strut B but increases as speed increases from 0 to 20 knots for strut C and then decreases slightly as speed increases to 28 knots. Dimensionless relative bow motion decreases significantly as speed increases from 0 to 28 knots for all three strut configurations. Nondimensional pitch decreases significantly as speed increases from 0 to 28 knots for all three struts. However, pitch is not very large at any speed in wave lengths up to 2000 ft (610m) for strut A because the resonant wave length for this strut is longer than 2000 ft. At zero knots dimensionless heave for strut C is less than for strut B which is less than for strut A. At 20 and 28 knots heave is about the same for struts B and C, while heave for strut A is lower than for either strut B or C. Dimensionless relative bow motion is about the same for struts B and C at all speeds and lowest for strut A at all speeds. Nondimensional pitch follows the above trend for relative bow motion for a given speed but pitch is significantly lower for strut A than for struts B and C at all speeds.

Figures 9 through 18 present vertical accelerations at the bow, the LCG and the stern and the vertical displacement transfer functions calculated from these accelerations, respectively, in head seas at various speeds. Vertical accelerations and displacements are about the same at all speeds for strut A. Vertical accelerations for struts B and C increase as speed increases from 0 to 20 knots while the vertical displacements are about the same at all speeds for these two strut configurations. Vertical accelerations at zero speed are about the same for all three struts but are less for strut A than for struts B and C at 20 and 28 knots. At zero knots the maximum vertical CG displacement for strut C is less than that for struts A and B, which are about the same. Vertical bow and stern displacement for struts B and C at 20 and 28 knots follow the trend observed for heave. The scatter in the acceleration data around the peak for the 20 knot condition reflects the results of the linearity experiments conducted near heave reasonance.

It is noted that for a given speed and strut configuration the vertical accelerations and absolute vertical displacements at the bow are greater than at the LCG which in turn are greater than at the stern, except for strut C at 0 knots.

The results of the above mentioned linearity experiments in head seas at 20 knots for heave resonance wave lengths are shown in Figure 19. The motions and accelerations remain quite linear with wave height for a wave steepness in the range of 60 to 120.

Figures 20 through 23 present results of regular head sea experiments during which the effect of different combinations of horizontal stabilizer fins was investigated. These experiments were conducted in wave conditions around heave resonance for the particular strut configuration and speed.

Experimental results for strut A at 10 and 20 knots and struts B and C at 20 knots show that the existence of a bow fin is responsible for quite a reduction in motions and accelerations. Motion pictures of calm water experiments indicate this may be due to the fact that the bow fin was located near the longitudinal position on the strut where the flow velocity of the wave coming off the strut leading edge was downward. See sketch below. Variations in fin size examined on strut configuration A had little effect on the motions.

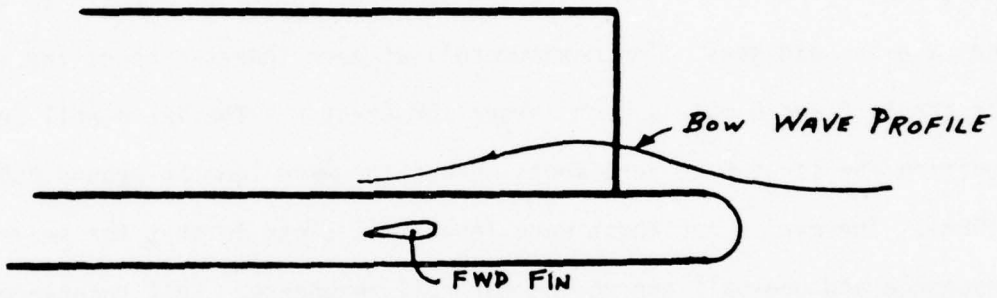

Figures 24 through 27 present results of experiments in regular bow quartering seas at 20 knots. Figure 24 shows that the highest heave, relative bow motion, pitch and roll, are experienced by struts C, B and A in that order respectively. Although there is not much difference in heave, relative bow motion and roll for the three struts, pitch for strut A is significantly lower than pitch for struts B and C as was the case in head seas. There is no difference in roll angular acceleration for the three strut configurations.

Vertical accelerations and absolute vertical motions are presented in Figures 25 through 27. Vertical accelerations and displacements are about the same for struts B and C at 20 knots while the vertical bow and CG accelerations are slightly lower for strut A than for B and C.

Accelerations and absolute displacement at the bow are greater than at the stern for all struts, as was the case in head seas at 20 knots.

Results of regular wave experiments in beam seas at 0 and 20 knots are presented in Figures 28 through 38. For all three strut configurations maximum heave, relative bow motion, roll and roll acceleration decrease as speed increases from 0 to 20 knots while yaw follows the opposite trend. At 0 knots the maximum relative bow motion and roll acceleration are about the same for all three strut configurations. Heave at zero speed is about the same for struts A and B and somewhat lower for strut C as was the case in head seas. The maximum roll at zero speed is about the same for struts A and C but is much larger for strut B. The large roll transfer function for strut B at zero knots occurs for wave lengths around 350 ft (106m). The period for these wave lengths is close to that for heave resonance and one-half the period for roll resonance. Roll resonance is not reached until the wave length reaches about 1400 ft (427m). During experiments in waves near 350 ft (106m) the craft rolled slightly for about five or six cycles and then the roll angles became very large. This unstable character of the roll motion is due to a phenomenon called the Mathieu instability (Reference 2). When the natural period of one motion is twice that of another (or the two natural periods are nearly equal) the motion with the longer natural period can be excited at its resonant frequency in near resonant waves for the other mode of motion due to nonlinear coupling between the two motions. This effect is even more pronounced when damping is small, as is the case for roll damping of a SWATH craft at zero speed.

At 20 knots maximum heave, relative bow motion, roll and roll acceleration are about the same for all three strut configurations.

Vertical accelerations and absolute vertical displacements in regular beam seas at 0 and 20 knots are presented in Figures 31 through 36. For all strut configurations the maximum acceleration and displacements decrease as speed increases from 0 to 20 knots. At both zero and 20 knots there is little difference in accelerations for any particular longitudinal location for all three struts. At 20 knots for struts A and B the maximum stern and bow displacements are about the same. At 0 knots for all three struts and at 20 knots for strut C the bow motion is larger than the stern motion.

The scatter in the zero speed data near roll resonance reflects the results of the linearity experiments conducted at these wave lengths. Figure 37 presents results of these linearity experiments. Heave, stern acceleration and stern displacement are quite linear for wave steepnesses from 70 to 200 for all three strut configurations. Roll, roll acceleration, vertical bow and CG accelerations and displacements show some nonlinearities for all three strut configurations. Nonlinearities in roll and roll acceleration for the large wave heights are most pronounced for strut C. This may be explained by the nature of the roll motion in very long wave at both zero and 20 knots. Observation of these experiments show that although the wave form for the long waves was nearly sinusoidal, the roll response was not. With waves coming from the port beam, the craft would roll up as the wave crest passed under the starboard hull. The resultant roll trace appeared flat on the maximum starboard down side of the trace. See sketch.

Figures 38 through 46 present results of experiments in regular stern quartering seas at 20 knots. The maximum pitch, yaw, relative bow motion and roll acceleration are about the same for struts B and C. There are not enough yaw and roll acceleration data for strut A to compare it with the other struts. Heave and roll motions are about the same for all three struts. Relative bow motion and pitch are larger for strut A than for B and C. This is probably due to the larger stern fin used with configuration A.

The determination of the location of the peak for the pitch and relative bow motion transfer functions and perhaps for the roll transfer function is difficult as may be seen from the data scatter around wave lengths of 200 to 300 ft (61 to 91m). The nature of the quartering sea phenomena, presented in Figures 41 through 43, may be responsible for the data scatter in that narrow wave length region. For small changes in the wave length around 200 ft (61m) there are large changes in the encounter period (Figure 41) and the encounter frequency (Figure 42) at 20 knots. Also note that the encounter period for this wave length is near pitch resonance for all three struts. These phenomena, coupled with the fact that in quartering seas there are large excusions in surge (and thus relative ship-wave velocity, Figure 43) which tend to produce changes in the apparent encounter frequency, produce this scatter.

The maximum heave for all three struts is less in stern quartering seas than in head, bow or beam seas at 20 knots. (See Figures 6-10, 24, 28-30) Maximum pitch, relative bow motion, roll and roll acceleration are greater in stern quartering seas than in head, bow or beam seas at 20 knots for strut A (See Figures 6, 24, 28). Maximum roll and pitch are greater in stern quartering seas than in head, bow or beam seas at 20 knots for struts B and C (See Figures 7-8, 24, 29-30). Roll acceleration and relative bow motion are lower in beam seas than in head bow or quartering seas for strut B (See Figures 7, 24, 29) but are larger in stern quartering seas than in head, bow or beam seas for strut C (See Figures 8, 24, 30).

Vertical acceleration and absolute displacements in regular stern quartering seas at 20 knots presented in Figures 44 through 46 are about the same for all three struts. Maximum accelerations and displacements for various headings at 20 knots follow the trend for heave above (Figures 11, 14, 17, 25-27, 32, 34, 36).

Results of experiments in regular following seas at 20 knots, presented in Figure 47, indicate maximum pitch, heave and relative bow motion are larger for strut A than for strut B. Not enough reliable data were collected for strut C to determine the peak of these transfer functions. Pertinent to this discussion is the behavior of the craft in following seas and the attendant difficulties in obtaining usable data from a tethered model. Because of the large surge excusions experienced by SWATH type craft in following seas due to the long encounter periods, it was difficult to keep the surging model from exceeding the slack in

the tether lines and instrumentation cables. Attempts were made to control the surge motion by manually controlling the model power during experiments on struts B and C but this too was difficult and quite unrealistic because a sudden increase in motor power to keep the craft from surging aftward would make the bow rise sharply, thus debasing pitch and relative bow motion and bow acceleration data. The data presented for these two struts are from portions of the experimental runs during which model power was fairly constant. In an effort to cope with this excessive surge motion, a different approach was taken to acquire data on strut A. Instead of maintaining a wave steepness of 1/60 for these experiments, wave steepness was decreased to about 1/80 by lowering wave height. As a result, model power could be held constant though the model would still surge about 50 ft (17m) fore and aft in cyclical fashion with the waves. Since the surge problem was successfully handled for this strut configuration, it was decided to try controlling pitch attitude by manually controlling the stern fins. At near zero encounter frequencies the craft was very responsive to fin control. Active control of the fins at other encounter frequencies produced about a 40% reduction in peak to peak pitch motion. However, it was difficult to manually control the craft for more than eight or nine wave encounters at a time. This problem of obtaining useful data from a tethered craft in following seas indicate the need for a reliable radio control model system with data telemetry capabilities. If such a system were available, collection of quality data would not depend upon compromising realistic experimental techniques.

Vertical acceleration and vertical displacement transfer functions are not presented for following seas for two major reasons. First, because of the languid motion and the reduced wave height in following seas experiments, the vertical accelerations are small, (in the order of 0.05 to 0.1 g) and hence difficult to measure. Secondly, the encounter frequencies are very small for most wave lengths (about .2 rad/sec) and near zero for the shorter wave lengths and thus hard to measure accurately. Since the calculation of vertical displacements involves division by the encounter frequency squared (ω_e^4 in the spectral calculations), again a very small number, the vertical displacements could not be accurately calculated.

RANDOM WAVES

Experiments were conducted in long crested irregular waves at the speeds and headings indicated in Table 3. Zero speed spectra for Sea State 3, 5, 6 and 7 representative of those used during these experiments are shown in Figure 51. Though these spectra do not exactly duplicate theoretical Pierson-Moskowitz spectra, they are realistic and do contain sufficient energy in the frequency range to excite the present models and elicit motion responses. Data presented in this report are the significant double amplitudes (average of the one-third highest peak to peak excusions) of motions and accelerations. Impact pressure data are presented as frequency of impacting and impact pressure histograms.

Results of experiments conducted in head random waves at 0, 20 and 28 knots are presented in Figures 52 through 70. Significant heave and pitch for all three struts follow the speed effect trends observed for the

regular wave data in head seas. However, there appears to be no speed effect on significant relative bow motion for all three struts. The observations made about heave, pitch and relative bow motion comparing the three struts at a given speed in head regular waves hold true in random head seas. There appears to be little speed effect on surge for all struts in Sea State 6 and for struts A and B in Sea State 7 while surge increases as speed increases from 0 to 28 knots for strut C in Sea State 7. Figure 52 also indicates that heave, pitch, and relative bow motion are quite linear with significant wave height up to about 25 ft (7.6m) for strut A at zero speed.

Figures 57 through 61 present significant vertical accelerations and displacements experienced by the craft operating in random head seas at various speeds. Vertical displacements follow the speed effect trend observed in regular head seas for struts A and C, and increase as speed increases from 0 to 20 knots for strut B. At zero speed the vertical accelerations and displacements are about the same for struts A and B and for strut C are slightly less than for A and B. At 20 and 28 knots the significant accelerations and displacements are about the same for struts B and C and lowest for strut A.

Figures 62 through 70 present impact pressure data obtained during experiments in random head seas at 20 and 28 knots. Figures 62 shows that struts B and C experienced the most frequent impacts at gage 4 during experiments in head Sea State 7 at 20 knots. Figures 63 through 66 show the pressure distribution of the impact pressure samples recorded in head Sea State 7 at 20 knots. The N in the figure indicates the number of

pressure samples recorded at the particular gage location. The frequency of occurrence is calculated by dividing the number of pressure samples which fell within the boundaries of a particular pressure range, by N, and multiplying by 100. The maximum pressures experienced by the bridging structure for strut configurations B and C are higher than those for strut configuration A. Although some impact pressures are as high as 35 psi (241 kPa), most are less than 15 psi (103 kPa) in head Sea State 7 at 20 knots. Note that both Figures 65 and 66 show data for strut C but the significant wave height generating the data in Figure 66 is slightly higher than for that in Figure 65. Also, panel load gage data was obtained at the higher wave height. As mentioned before, the panel load gage seemed to be quite stiff and was frequently inoperative. In general, the pressure magnitudes recorded on gage 4, located in the center of the strain-gaged panel load section of the bridging structure, were from two to five times higher than those recorded over the area of the panel load gage itself. It should be noted here however, that most sample sizes are somewhat small and experience has shown that for cases when the sample size of impact pressures is less than about 50, caution should be used in drawing conclusions from the data.

Figures 67 through 70 present impact pressure data obtained during experiments in head Sea State 6 at 28 knots. Figure 67 shows little difference in frequency of impact between strut configurations except at gages 2 and 4 where strut configuration C had significantly more frequent impacts than did strut configurations A and B.

Figures 68 through 70 show the distribution of the pressure samples recorded in head Sea State 6, 28 knot conditions. Sample size is too small to draw any conclusions about pressure distributions on strut config-

urations A and B. Though some pressure magnitudes for strut configuration C reach 20 psi (138 kPa), most fall below 10 psi (69 kPa).

Results of experiments in bow quartering seas at 20 knots are presented in Figures 71 through 76. Figures 71 and 72 indicate little difference in significant motions and accelerations between the three strut configurations except for bow acceleration and displacement which are smaller for strut A than for struts B and C. This was the trend in regular waves also.

Impact pressure data obtained during these experiments in bow quartering Sea State 7 at 20 knots are presented in Figures 73 through 76. Strut configuration B experiences more frequent bridging structure impacts than does configuration C, and configuration A has the lowest frequency of impact.

Histograms of the impact pressure magnitude distribution, Figures 74 through 76 do not represent an adequate size for drawing conclusions. Though some pressure magnitudes were as high as 40 psi (276 kPa), most were below 20 psi (138 kPa).

Results of experiments conducted in random beam seas at 20 knots are presented in Figures 76 and 77. Motion and accelerations are about the same for all three struts except significant roll acceleration appears to be higher for strut C than for struts A and B. The "roll and hold" motion displayed by strut configuration C in regular waves was also present in random waves.

Results of experiments in random stern quartering seas at 20 knots are presented in Figures 78 and 79. Motions and accelerations follow the trends observed in regular waves except significant roll and roll acceleration appear lower for strut C than for struts A and B and vertical displacements are highest for strut configuration A.

Figures 80 and 81 present results of experiments in random following seas at 20 knots. Motions and accelerations appear to be about the same for all three struts. CG and stern acceleration and displacement data for strut C are not presented due to transducer malfunctions. Once again it is noted that the behavior of the craft in following seas leaves much to be desired. There were several runs attempted in a Sea State 4 with strut configuration A but the surge motion was still large and it was difficult to keep the model from being restrained by the tether lines. Again, had the craft been radio controlled and free to surge, more realistic data could have been obtained.

Note that significant pitch is larger in both stern quartering and following seas than in head seas.

CONCLUSIONS AND RECOMMENDATIONS

From experiments conducted on a model of a 2900 ton SWATH developmental craft with three different strut configurations, the following conclusions may be drawn:

1. In calm water, at 20 knots and above, the craft's running trim and sinkage are very responsive to changes in trim moment and stern fin angle, somewhat more so for configuration A with the large fins.

2. There were no indications of vertical plane instability for any craft configuration at any speed in calm water.

3. Some natural periods were difficult, if not impossible, to determine from calm water oscillation experiments because of the highly damped nature of the craft.

4. Pitch motion for strut configuration A which had the smallest longitudinal metacentric height was significantly lower than for B and C in head and bow seas for wave lengths shorter than 2000 ft (610 m) because the very long natural pitch period of configuration A. Pitch motion for strut configurations B and C decreases significantly as speed increases from zero to 28 knots.

5. Motions and accelerations in head regular seas at 20 knots are quite linear in near heave resonance wave lengths for wave steepnesses in the range of 1/60 to 1/20 for all three struts.

6. Experiments in regular head seas show that the bow fin is quite effective in reducing motions at 10 and 20 knots near heave resonance. The fin size has no appreciable effect on motions but the longitudinal location of the bow fin may.

7. Though maximum roll motion near roll resonance is about the same for all three strut configurations at zero speed in beam seas, strut

configuration B exhibits very low roll damping at encounter frequencies near one-half its natural roll frequency.

8. The roll motion for strut configuration C in regular beam seas at both zero and 20 knots is characterized by a "roll and hold" response resulting in a flat response on the down run of the cycle.

9. Roll motion for all three struts decreases appreciably as speed increases from zero to 20 knots in wave lengths near roll resonance.

10. Roll, roll acceleration and some vertical accelerations and displacements are non-linear in near roll resonant wave lengths at zero speed.

11. Pitch, roll and roll acceleration are significantly larger in stern quartering than bow quartering seas at 20 knots.

12. Pitch and relative bow motion are much larger in following seas than in head seas at 20 knots, especially for strut configuration A which had a longitudinal metacentric height only one-half that for configurations B and C. Heave follows a trend opposite to that above.

13. Craft surge motions in stern quartering and following seas are generally so extreme that the collection of quality data by use of a tethered model is severely hampered. However, surge motion in regular following seas for configuration A was reduced to a tenable level by decreasing the wave slope, thus providing an opportunity to conduct experiments with active fin control. The craft's pitch attitude was very responsive to manual fin control at near zero encounter frequencies. Active fin control at several other encounter frequencies produced about a 40% reduction in peak to peak pitch motions. Because SWATH craft exhibit larger pitch and surge motions at the above headings and since active fin control may be a promising method to reduce pitch motions, it is recommended that experiments be conducted with a radio control model which would remove the encumbrances of tether lines and transducer cables, while also providing a means for use of more sophisticated active fin control techniques.

REFERENCES

1. Kallio, James A. and Ricci, J.J. "Seaworthiness Characteristics of a Small Waterplane Area Twin-Hull (SWATH IV) Part II" DTNSRDC SPD Research and Development Report No. SPD 620-02, May 1976.

2. Paulling, J.R. and Rosenberg, R.M., "On Unstable Ship Motions Resulting from Nonlinear Coupling," Journal of Ship Research, June 1959.

TABLE 1 - SWATH 6 Craft Particulars

PARTICULAR	UNIT OF MEASURE	STRUT 6A	STRUT 6B	STRUT 6C
Length Overall (LOA)	Feet (Meter)	———	240.0(73.15)	———
Length at the Waterline (LWL)	Feet (Meter)	172.3(52.50)	208.0(63.40)	197.5(60.20)
Beam (Lower Hull)	Feet (Meter)	———	15.0(4.57)	———
Strut Thickness (maximum)	Feet (Meter)	7.25(2.21)	6.00(1.83)	8.47(2.58)
Midship Maximum Breadth (Bridging Structure or at Lower Hull)	Feet (Meter)	———	90.0(27.43)	———
Distance Between Centerlines	Feet (Meter)	———	75.0(22.86)	———
Draft	Feet (Meter)	———	26.67(8.13)	———
Displacement	Long Ton (Metric Ton)	———	2900 (2946)	———
Longitudinal CG Aft of Lower Hull Nose	Feet (Meter)	116.3(35.45)	115.3(35.14)	113.9(34.72)
Vertical Center of Gravity ($\overline{KG}$)	Feet (Meter)	———	34.0(10.36)	———
Longitudinal $\overline{GM}$ (Design)	Feet (Meter)	20(6.10)	38(11.6)	45(13.7)
Transverse $\overline{GM}$	Feet (Meter)	11.06(3.37)	10.60(3.23)	10.94(3.33)
Longitudinal Radius of Gyration/LOA		0.233	0.245	0.242
$\frac{\text{Transverse Radius of Gyration}}{\text{Centerline Hull Spacing}}$		0.528	0.530	0.519
Bridging Structure Clearance	Feet (Meter)	———	20(6.10)	———
Deck Height Above Baseline	Feet (Meter)	———	60.67(18.49)	———
C_{wp} Strut		0.85	0.85	0.68
C_p Lower Hull		———	0.85	———

TABLE 2 - SWATH 6 Regular Wave Experiment Matrix

Ship Heading	Ship Speed Knot	Strut 6A	Strut 6B	Strut 6C
Head Sea (180°)	0	X	X	X
	10	X		
	20	X	X	X
	28	X	X	X
Bow Quartering Sea (135°)	20	X	X	X
Beam Sea (90°)	0	X	X	X
	20	X	X	X
Stern Quartering Sea (45°)	20	X	X	X
Following Sea (0°)	20	X	X	X

TABLE 3 - SWATH 6 Random Wave Experiment Matrix

Ship Heading	Ship Speed Knot	Sea State	Strut 6A	Strut 6B	Strut 6C
Head Sea (180°)	0	3	X		
	0	5	X		
	0	6	X	X	X
	0	7	X	X	X
	20	7	X	X	X
	28	6	X	X	X
Bow Quartering Sea (135°)	20	6	X		
	20	7	X	X	X
Beam Sea (90°)	20	6	X	X	X
Stern Quartering Sea (45°)	20	5	X	X	X
Following Sea (0°)	20	6	X	X	X

TABLE 4 - SWATH 6 Natural Periods in Calm Water

Ship Speed Knot	Trim Moment Ft.-Ton (kn-km)	Stern Fin Angle Trailing Edge Up = +	STRUT 6A			STRUT 6B			STRUT 6C		
			Heave Sec.	Pitch Sec.	Roll Sec.	Heave Sec.	Pitch Sec.	Roll Sec.	Heave Sec.	Pitch Sec.	Roll Sec.
0	0	0	10.10	13.70	17.0	9.64	13.60	16.7	10.13	12.70	19.3
10	572 Aft (177)	+2.0 Deg.	9.70	11.30*	19.5						
20	4434 Aft (1373)	+5.0 Deg.	10.60	11.80*	19.0*						
28	4434 Aft (1373)	-1.0 Deg.	11.60*	14.50*	20.2						
10	191 Aft (59)	0 Deg.				11.80	14.70	19.7			
20	3814 Aft (1161)	+4.0 Deg.				9.80*	10.40*	19.5			
28	3814 Aft (1181)	-2.5 Deg.				10.20	10.60	19.5			
10	596 Aft (185)	0 Deg.							9.50	11.40	21.4
20	3194 Aft (989)	+3.0 Deg.							10.50	10.54*	22.7
28	3194 Aft	-2.0 Deg.							10.20	10.10*	26.0

TABLE 5 - Definition of SWATH 6 Transfer Functions

TRANSFER FUNCTION	NONDIMENSIONALIZATION
Heave	$\frac{\text{Heave Amplitude (m)}}{\text{Wave Amplitude (m)}}$
Relative Bow Motion (RBM)	$\frac{\text{Relative Bow Motion Amplitude (m)}}{\text{Wave Amplitude (m)}}$
Vertical Displacement	$\frac{\text{Vertical Acceleration Amplitude (g)} \times 9.8\ \text{m/sec}^2/\text{g}}{\omega_e^2\ (\text{sec}^{-2}) \times \text{Wave Amplitude (m)}}$
Pitch	$\frac{\text{Pitch Amplitude (rad)} \times \text{Ship Length (m)}}{2 \times \text{Wave Amplitude (m)}}$
Roll	$\frac{\text{Roll Amplitude (rad)} \times \text{Hull Cemterline Spacing (m)}}{2 \times \text{Wave Amplitude (m)}}$
Roll Acceleration	$\frac{\text{Roll Acceleration Amplitude (rad/sec}^2) \times \text{Wave Length (m)}}{2\pi\omega_e^2\ (\text{sec}^{-2}) \times \text{Wave Amplitude (m)}}$
Yaw	$\frac{\text{Yaw Amplitude (rad)}}{\text{Wave Slope (rad)}}$

$$\text{Wave Slope} = \frac{2\pi \times \text{Wave Amplitude (m)}}{\text{Wave Length (m)}}$$

Ship Length = 240.0 ft (73.15 m)

Hull Centerline Spacing = 75.0 ft (22.86 m)

SWATH 6

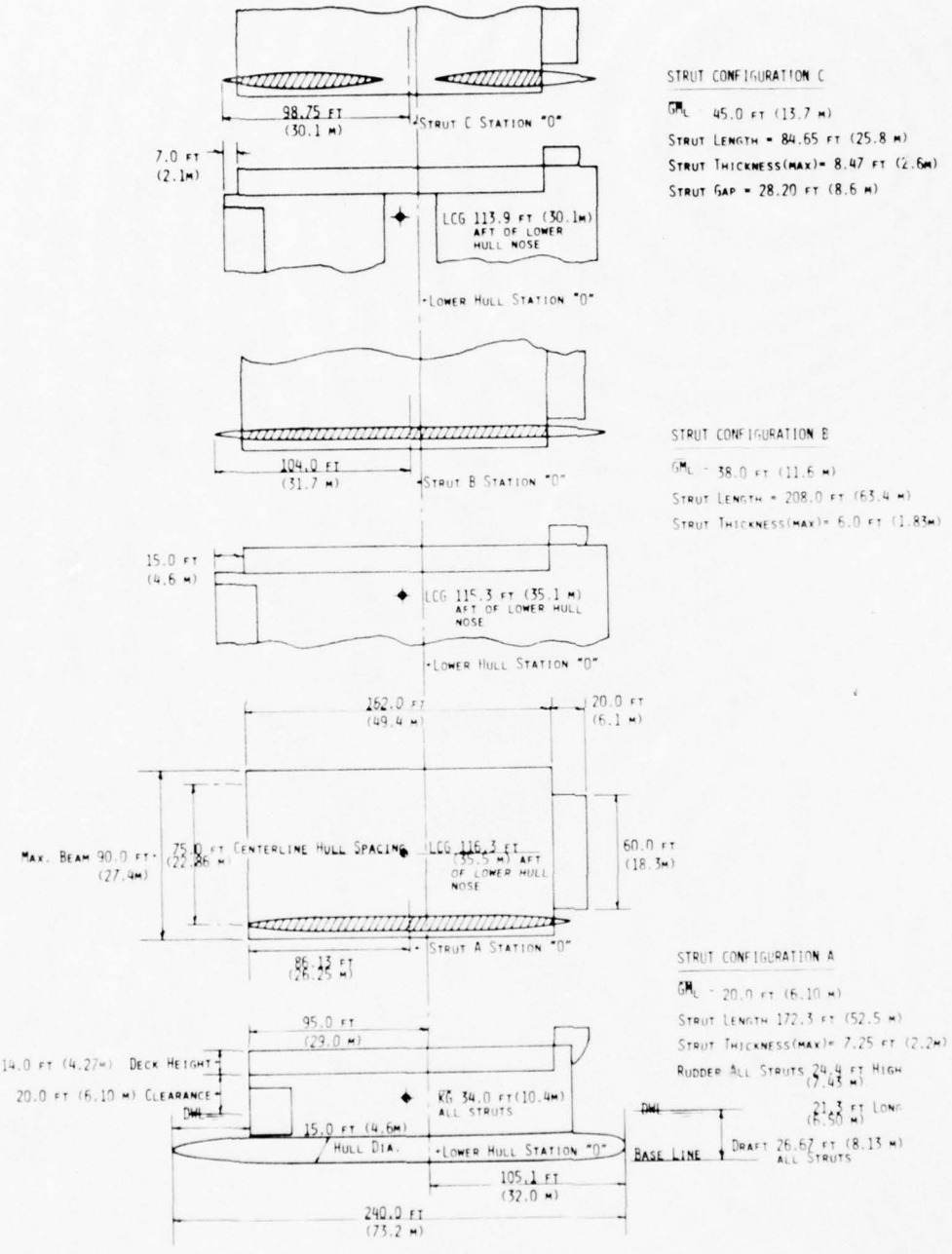

Figure 1 - Sketch of SWATH 6 Strut Configurations

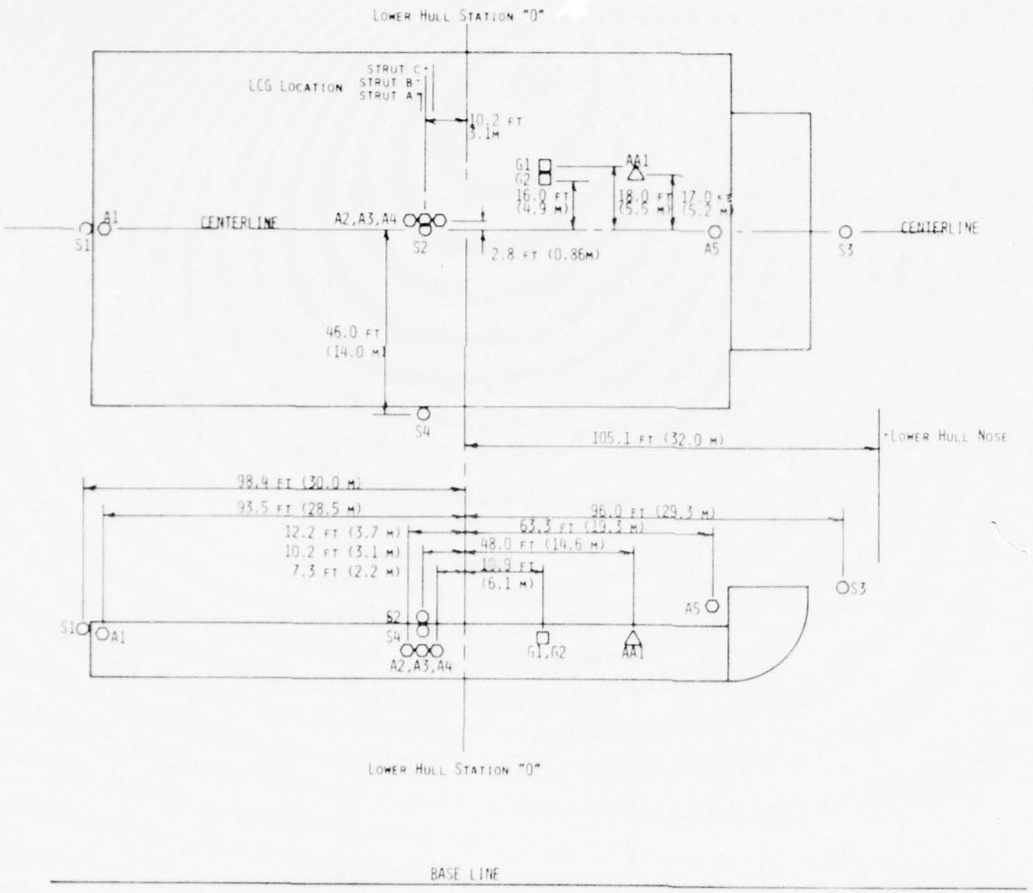

SWATH 6

○ A1 Vertical Stern Acceleration
○ A2 Surge Acceleration
○ A3 Vertical CG Acceleration
○ A4 Sway Acceleration
○ A5 Vertical Bow Acceleration

○ S1 Surge Motion
○ S2 Heave Motion
○ S3 Relative Bow Motion
○ S4 Sway Motion

□ G1 Yaw Angle
□ G2 Pitch and Roll Angle

△ AA1 Roll Acceleration

Figure 1a - Transducer Locations on SWATH 6

SWATH 6

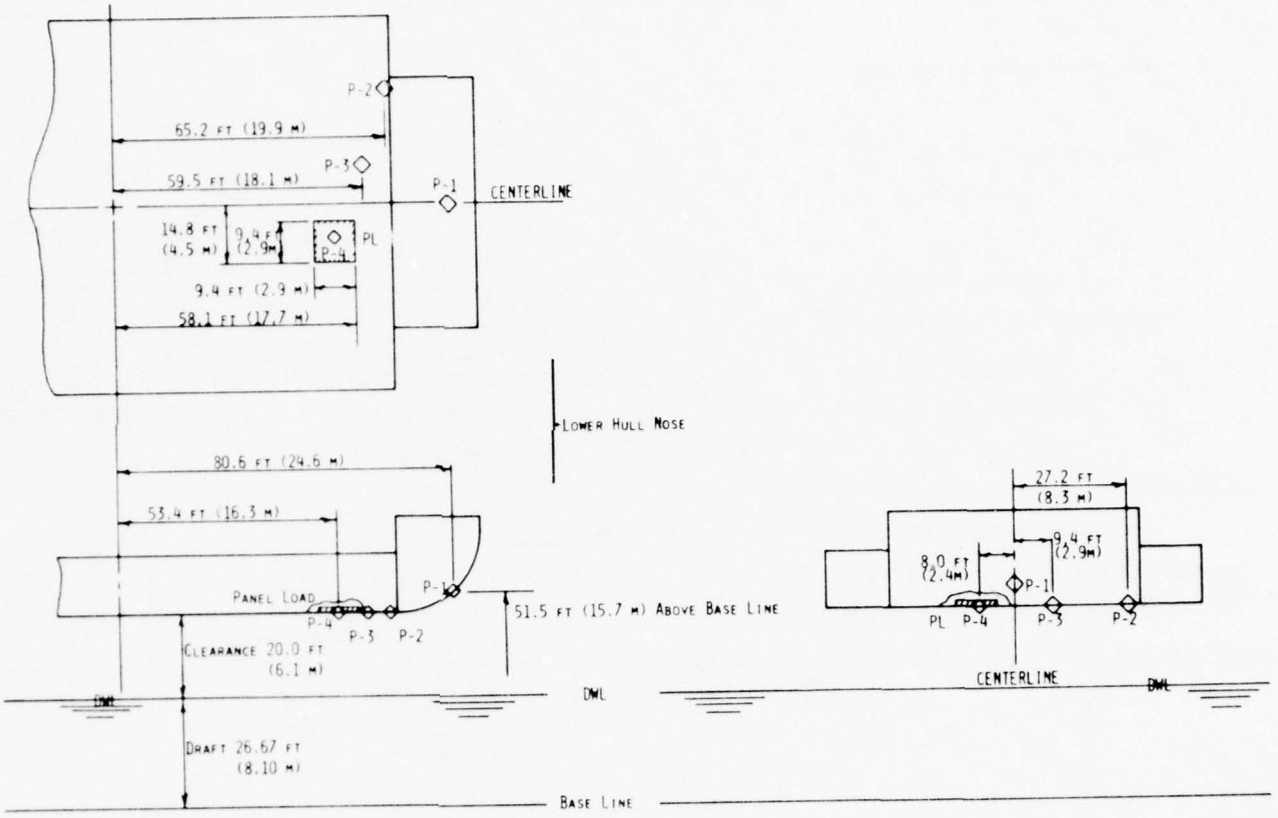

Figure 1b - Pressure Gage Locations on SWATH 6

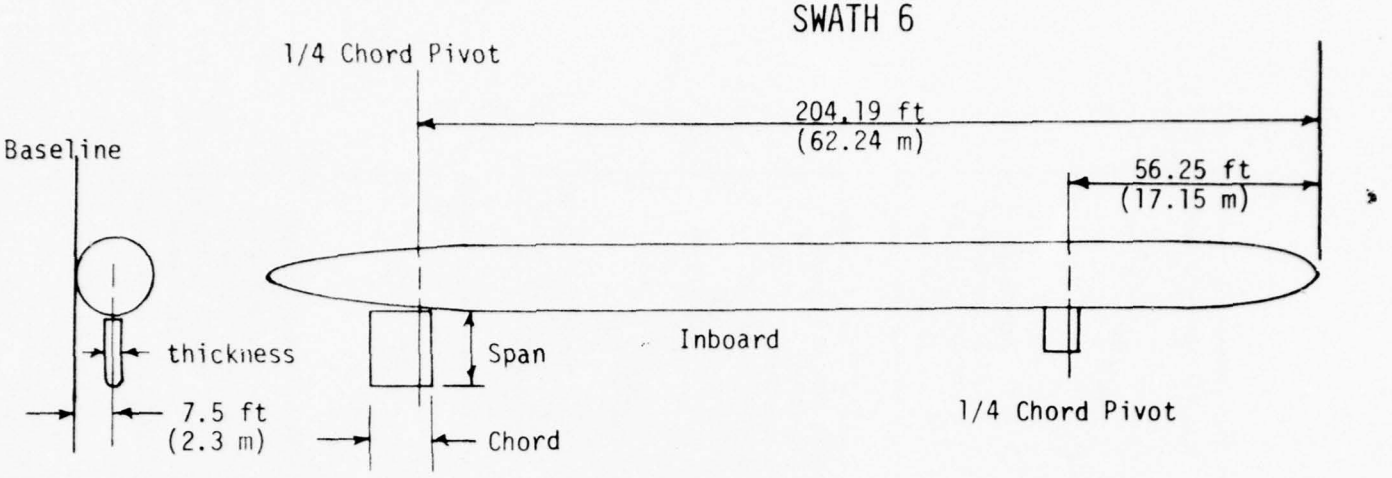

Fin Section NACA 64-015

Configuration	AFT FIN			FORWARD FIN		
	Chord	Span	Thickness(max)	Chord	Span	Thickness(max)
6A	14.7 ft (4.48m)	17.6 ft (5.36m)	2.20 ft (0.67m)	8.50 ft (2.59m)	10.2 ft (3.11m)	1.27 ft (0.39m)
6B	12.3 ft (3.73m)	14.7 ft (4.48m)	1.83 ft (0.56m)	7.10 ft (2.16m)	8.50 ft (2.59m)	1.06 ft (0.32m)
6C	12.3 ft (3.73m)	14.7 ft (4.48m)	1.83 ft (0.56m)	7.10 ft (2.16m)	8.50 ft (2.59m)	1.06 ft (0.32m)

Figure 2 - Fin Size, Shape and Location on SWATH 6

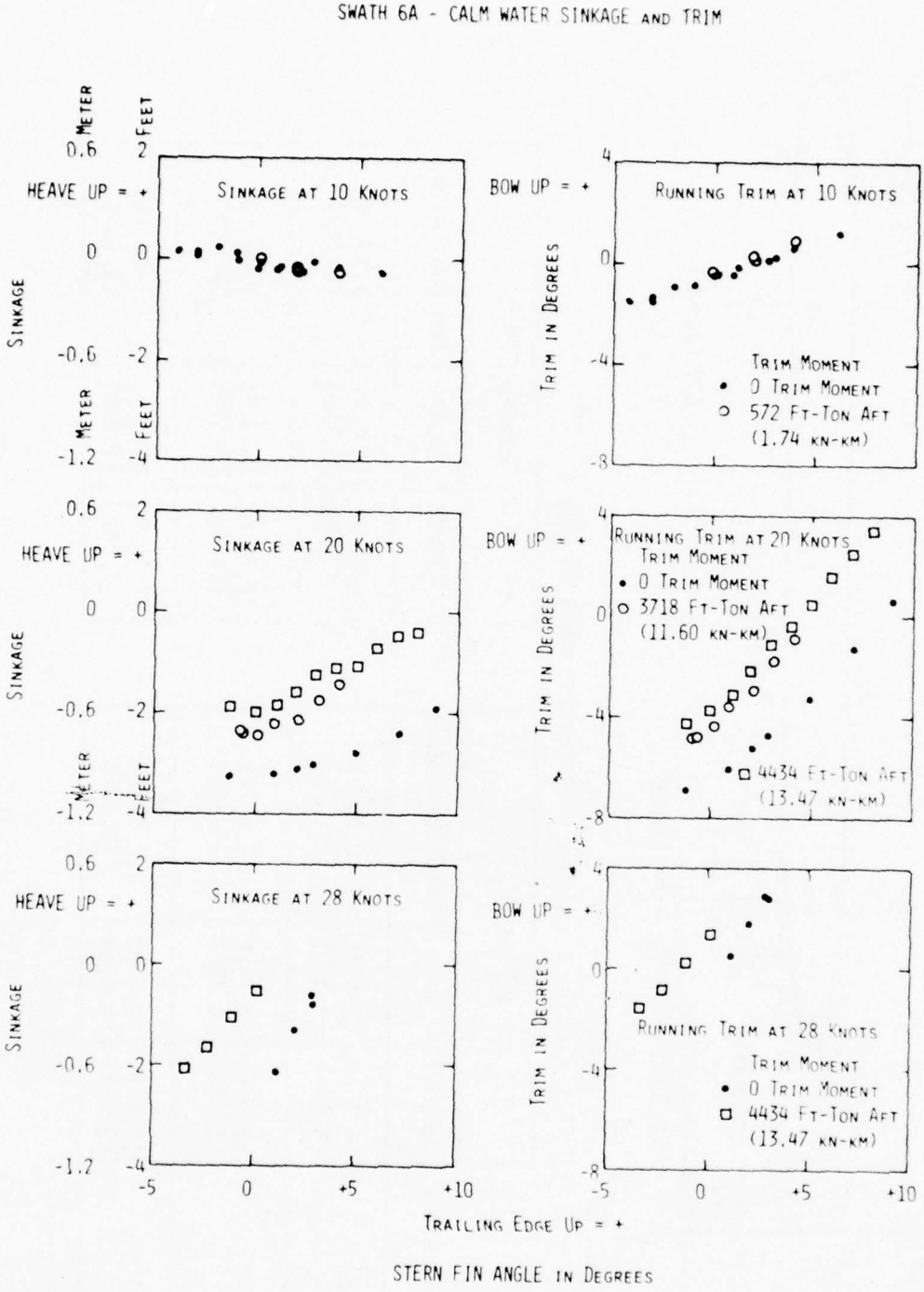

Figure 3 - SWATH 6A Sinkage and Trim in Calm Water

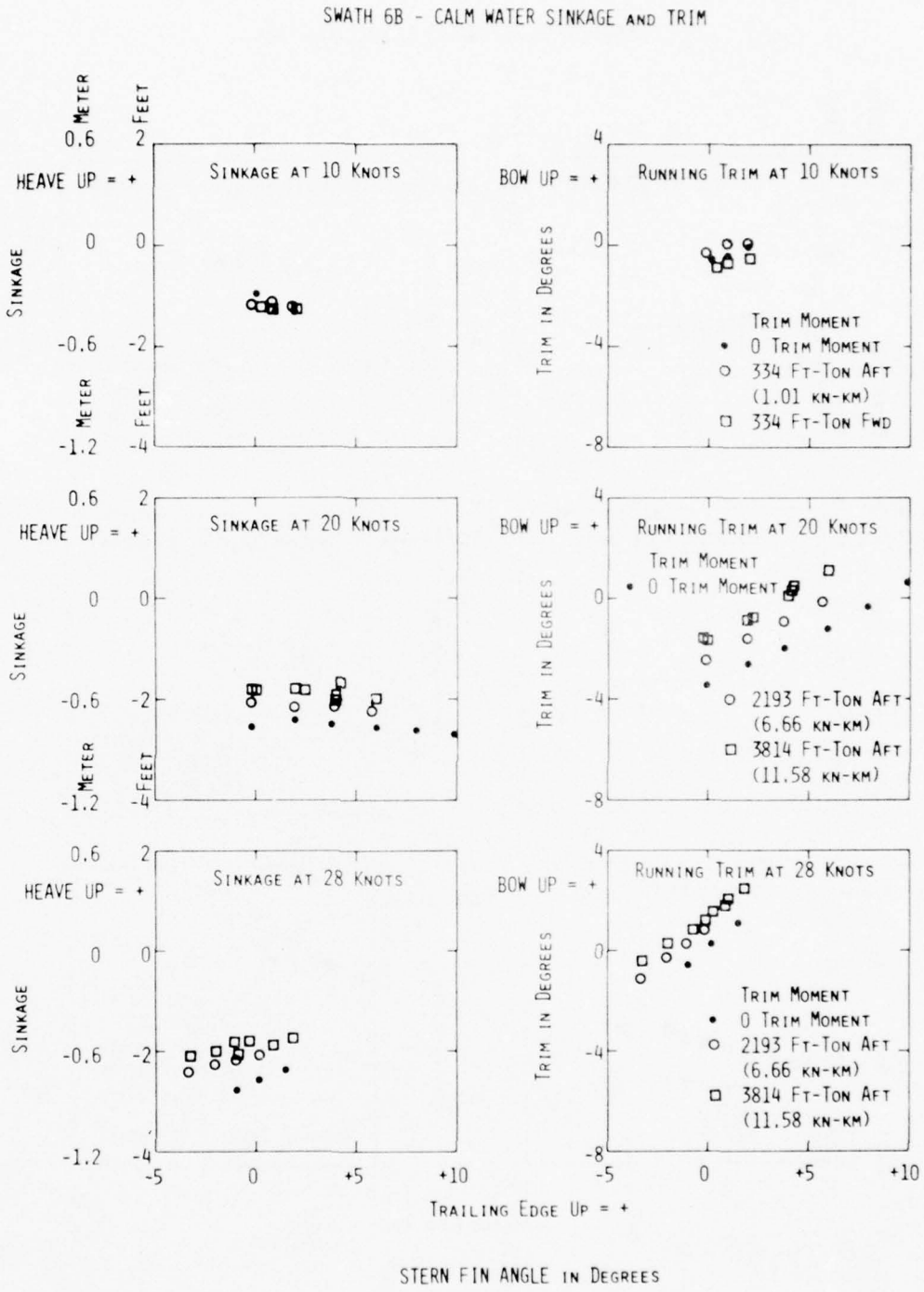

Figure 4 - SWATH 6B Sinkage and Trim in Calm Water

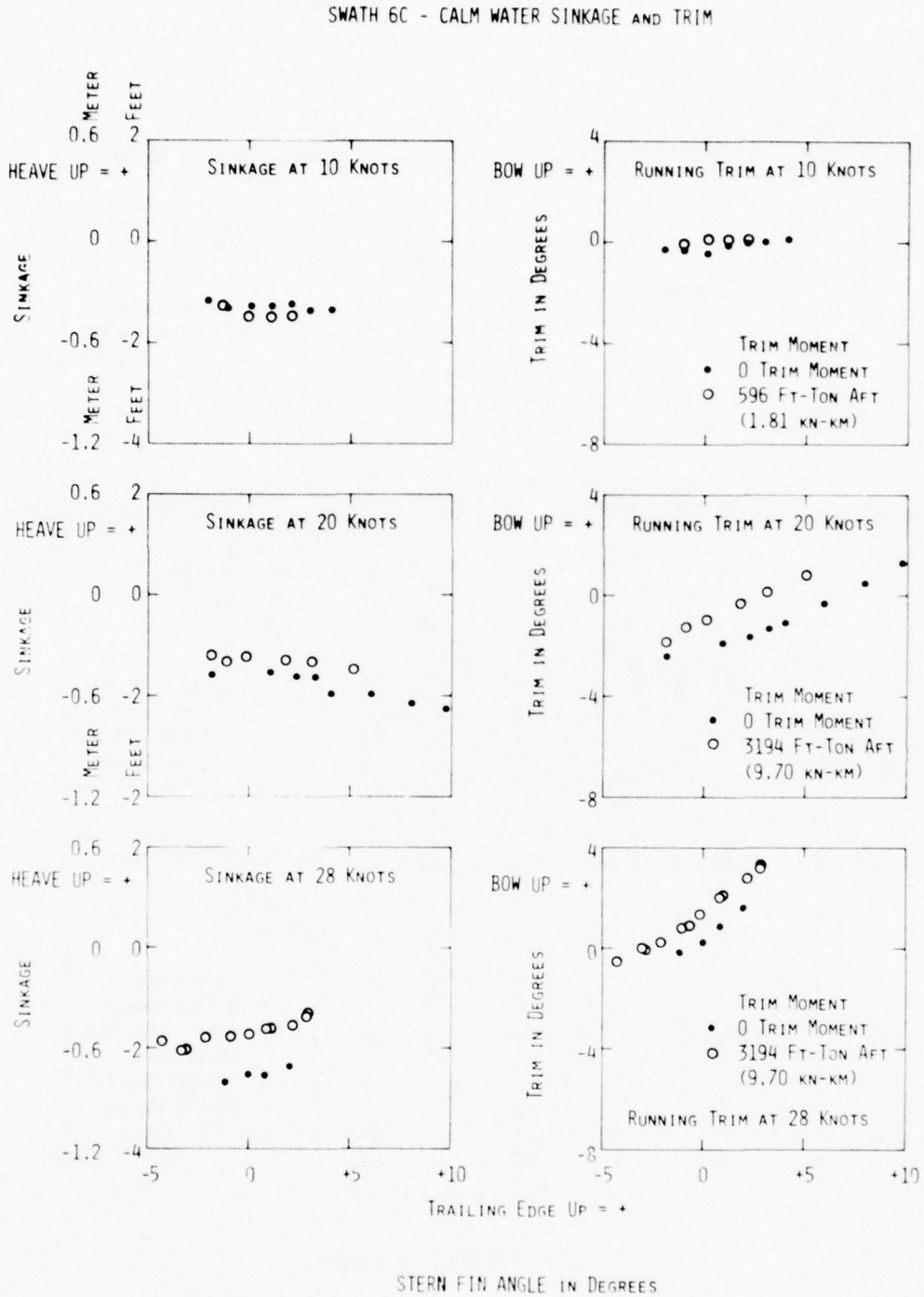

Figure 5 - SWATH 6C Sinkage and Trim in Calm Water

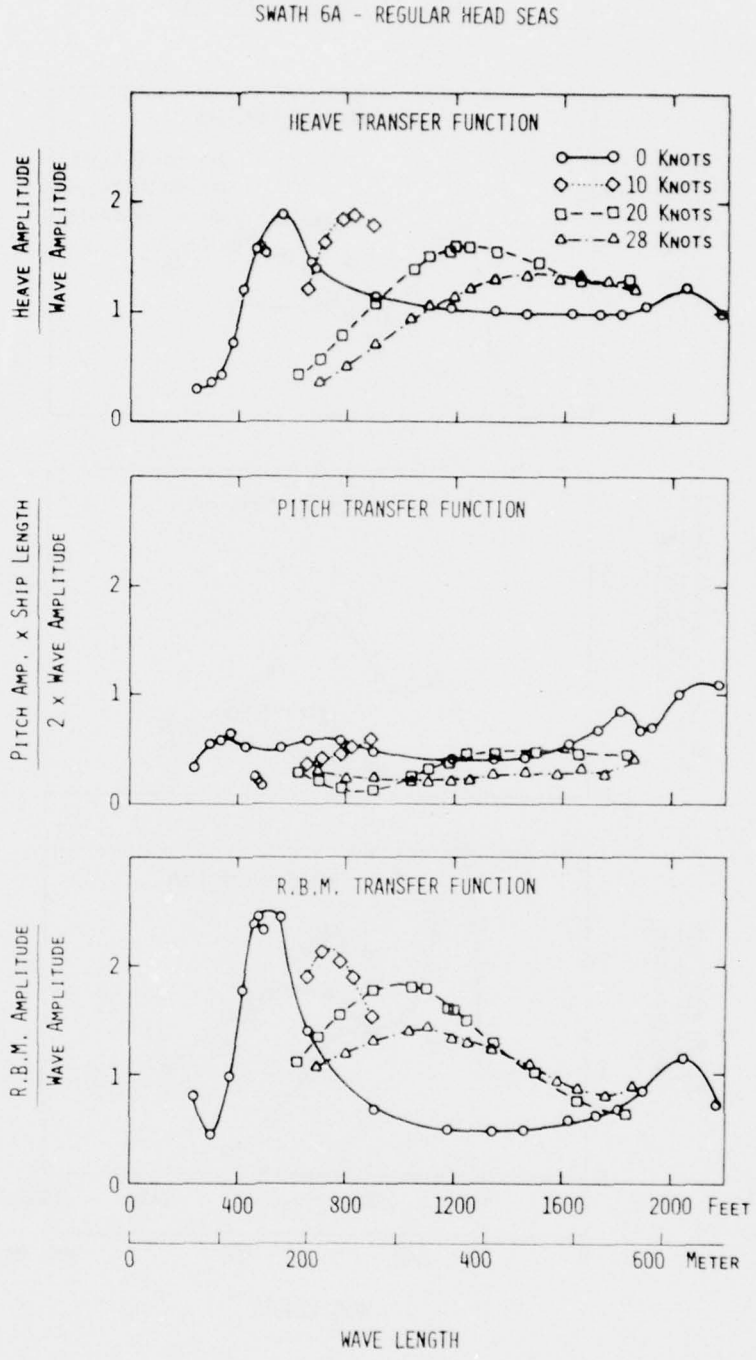

Figure 6 - Motion Transfer Functions in Regular Head Seas for SWATH 6A

SWATH 6B - REGULAR HEAD SEAS

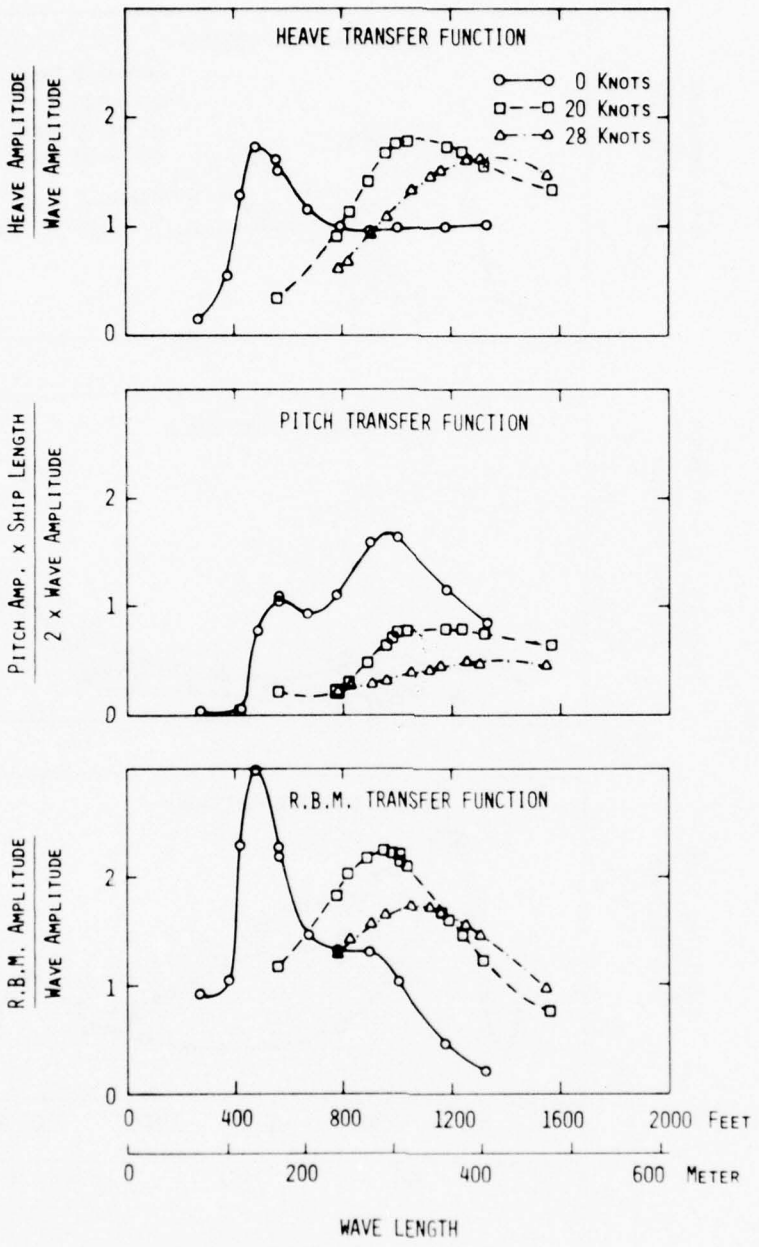

Figure 7 - Motion Transfer Functions in Regular Head Seas for SWATH 6B

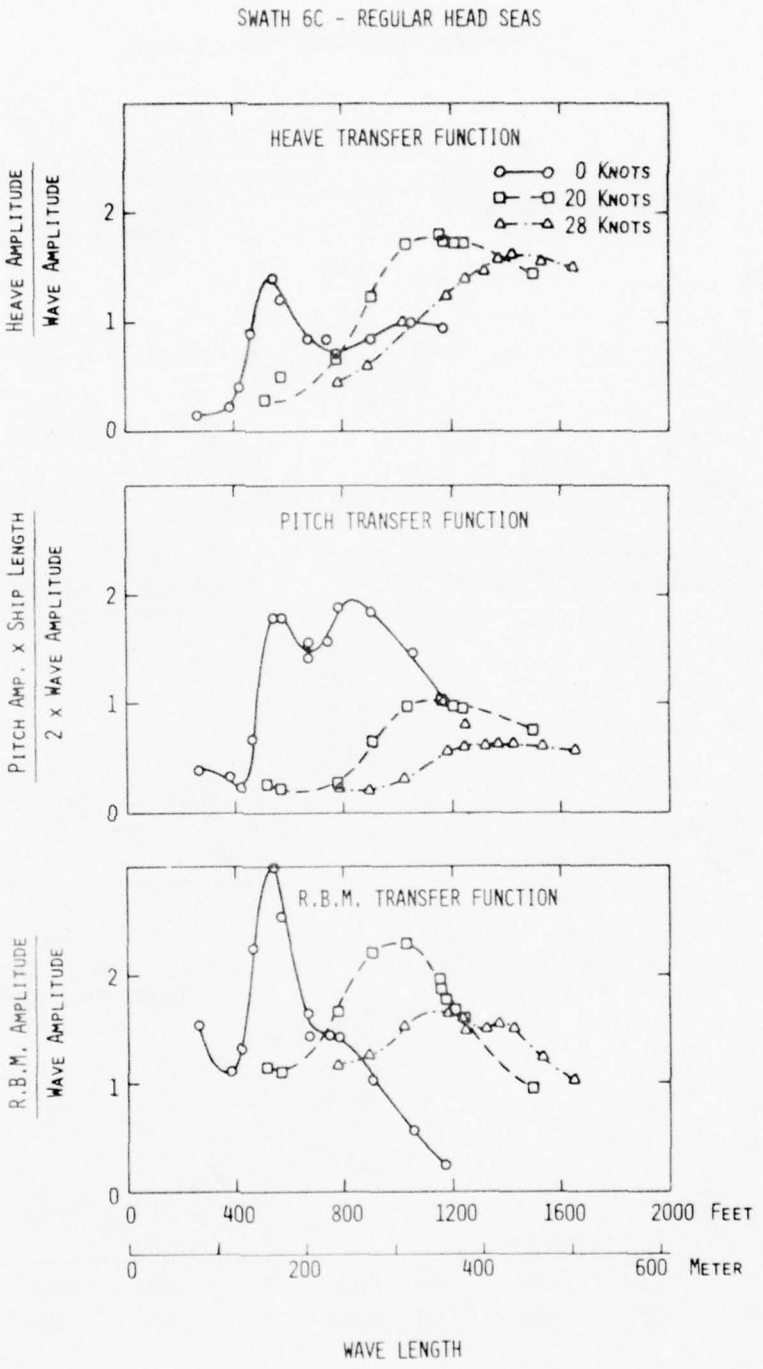

Figure 8 - Motion Transfer Functions in Regular Head Seas for SWATH 6 C

SWATH 6A - REGULAR HEAD SEAS - 0 KNOTS

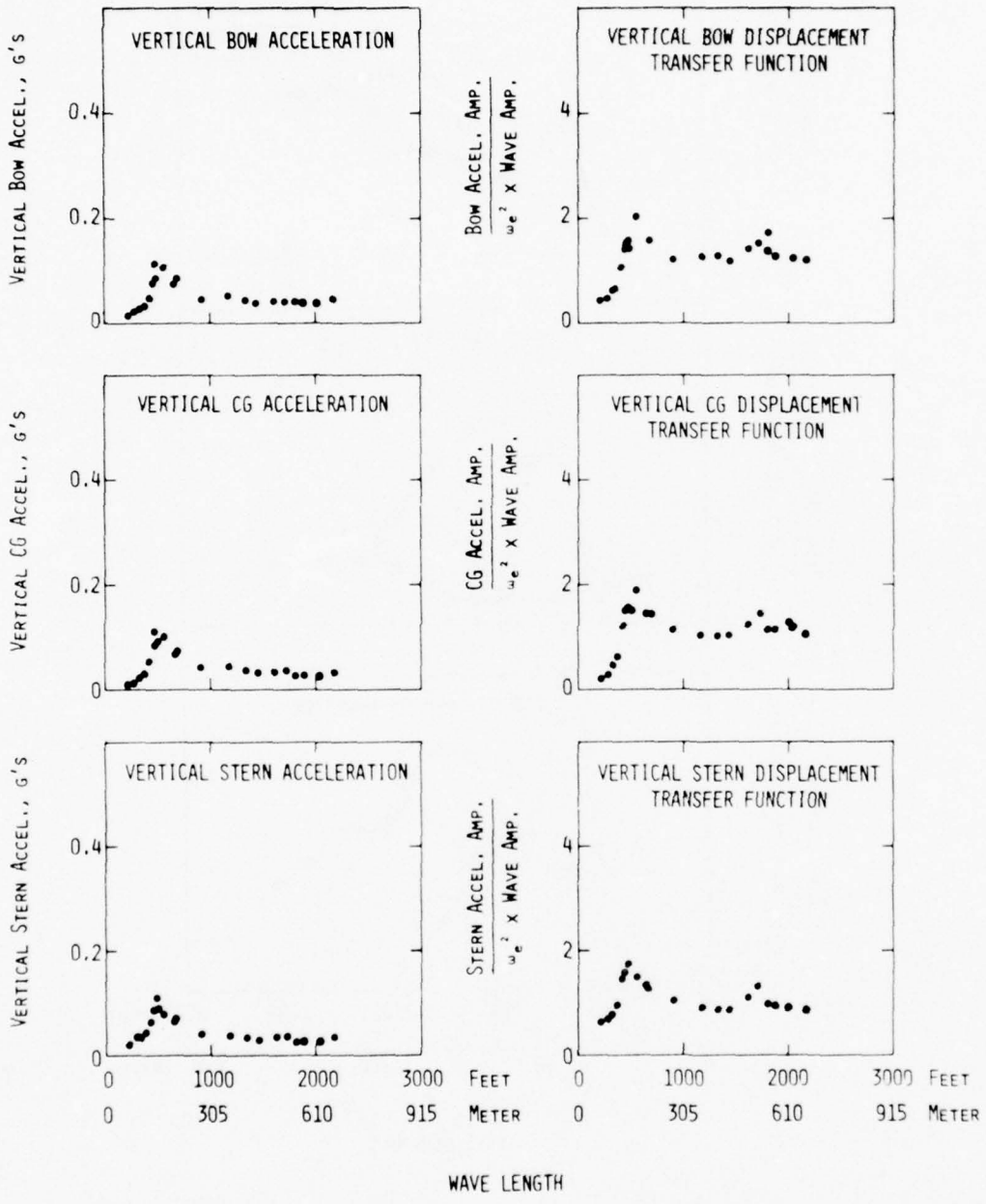

Figure 9 - Vertical Accelerations and Vertical Displacement Transfer Functions in Regular Head Seas for SWATH 6A - 0 Knots

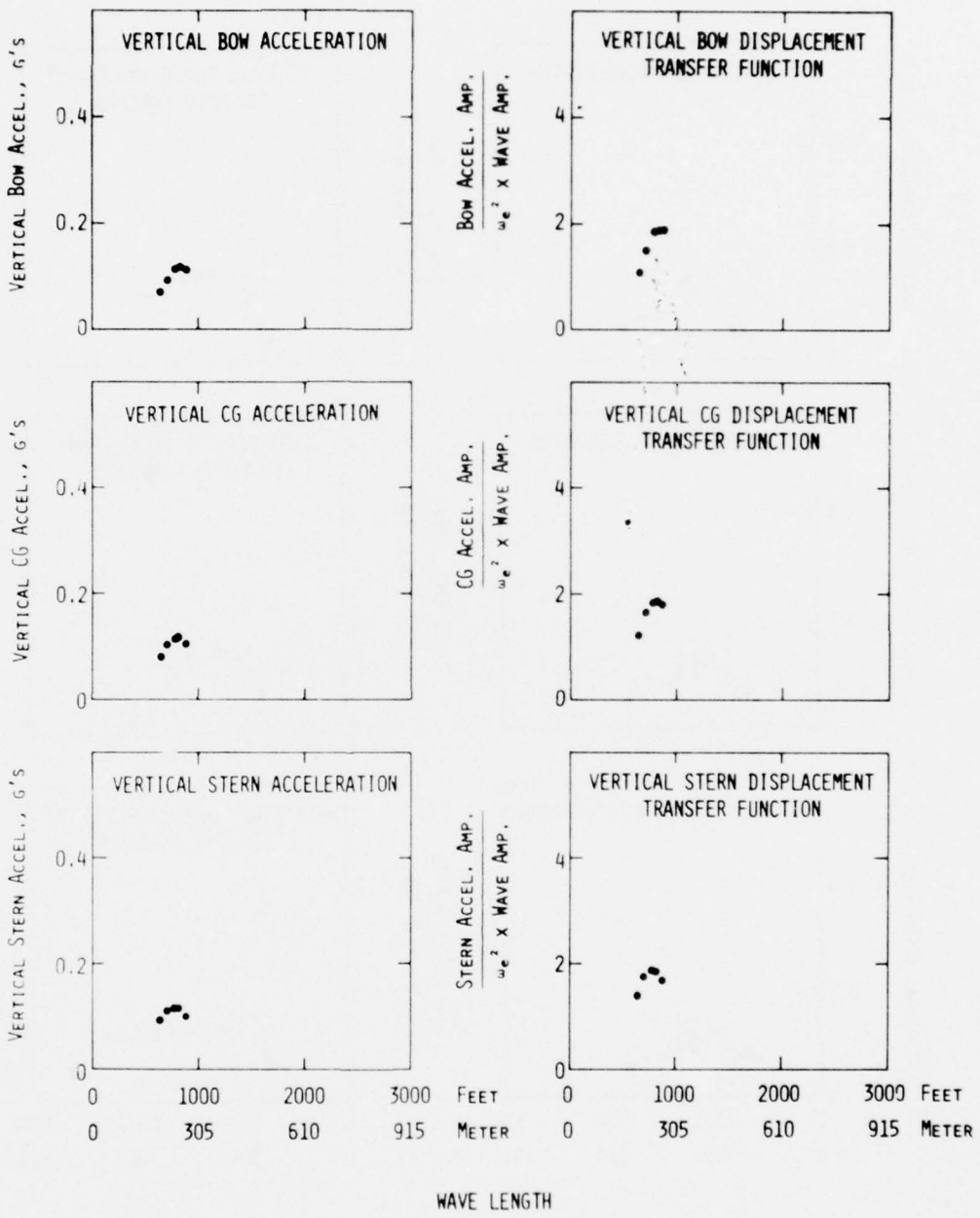

Figure 10 - Vertical Accelerations and Vertical Displacement Transfer Functions in Regular Head Seas for SWATH 6A - 10 Knots

SWATH 6A - REGULAR HEAD SEAS - 20 KNOTS

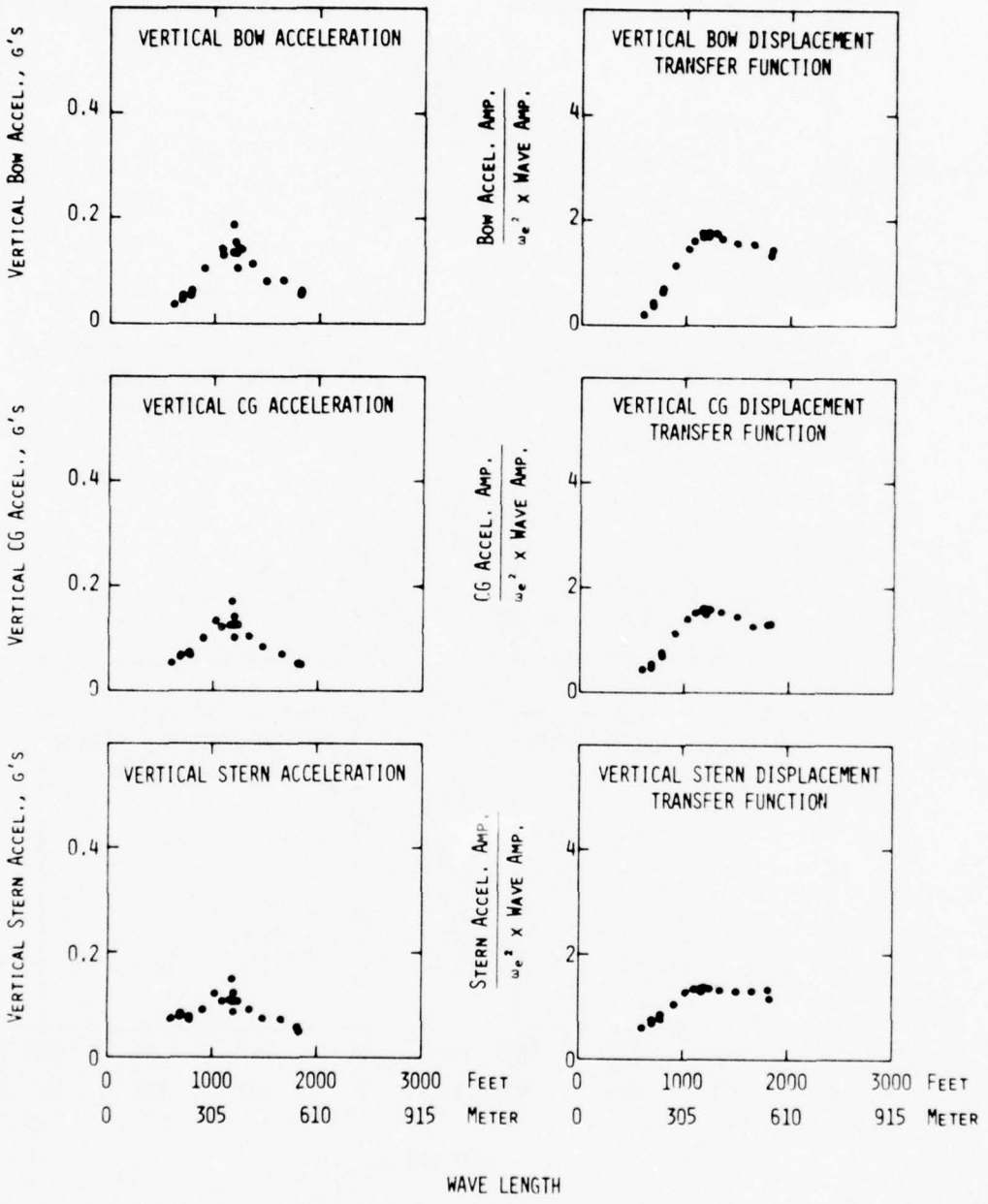

Figure 11 - Vertical Accelerations and Vertical Displacement Transfer Functions in Regular Head Seas for SWATH 6A - 20 Knots

SWATH 6A - REGULAR HEAD SEAS - 28 KNOTS

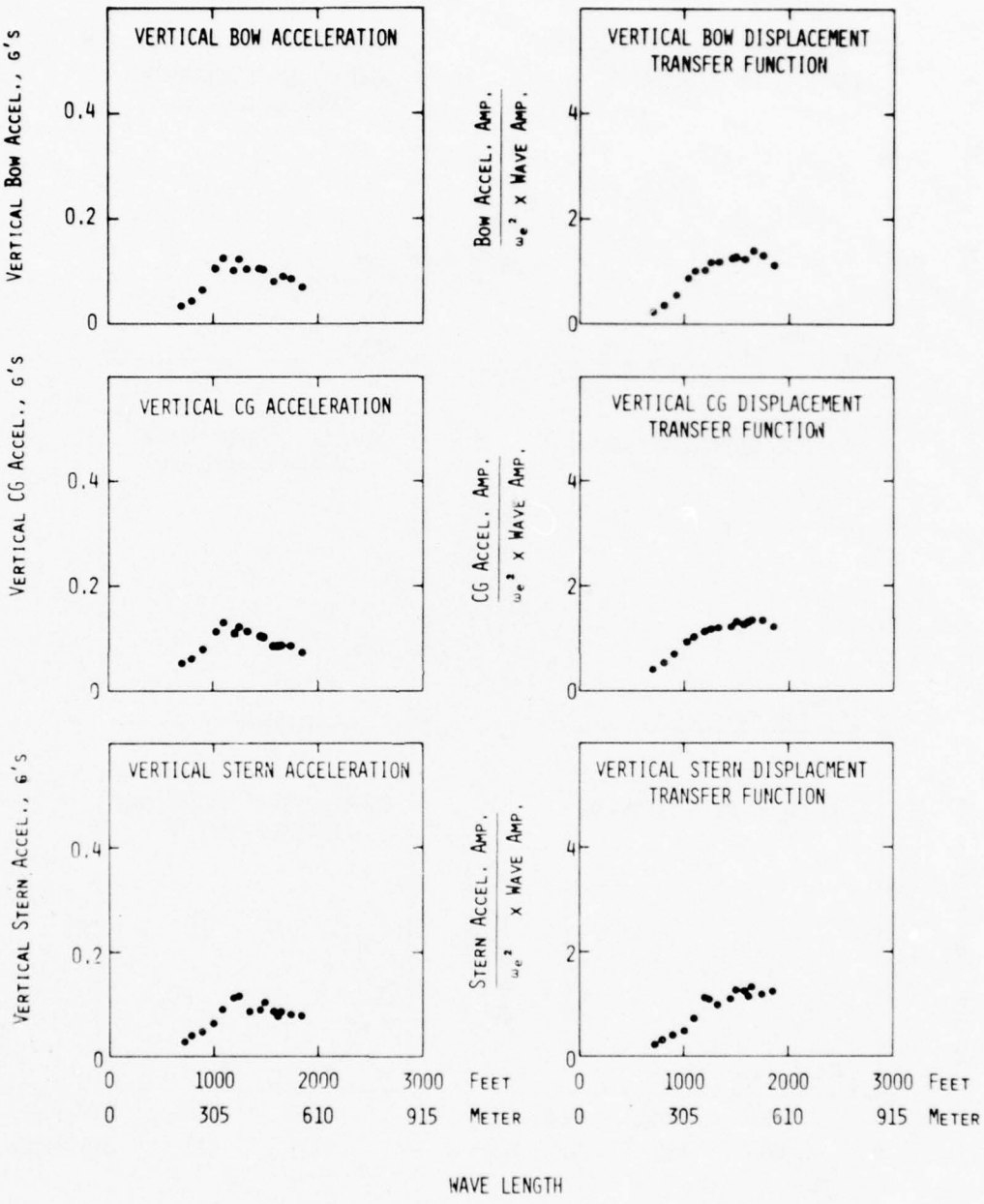

Figure 12 - Vertical Accelerations and Vertical Displacement Transfer Functions in Regular Head Seas for SWATH 6A - 28 Knots

SWATH 6B - REGULAR HEAD SEAS - 0 KNOTS

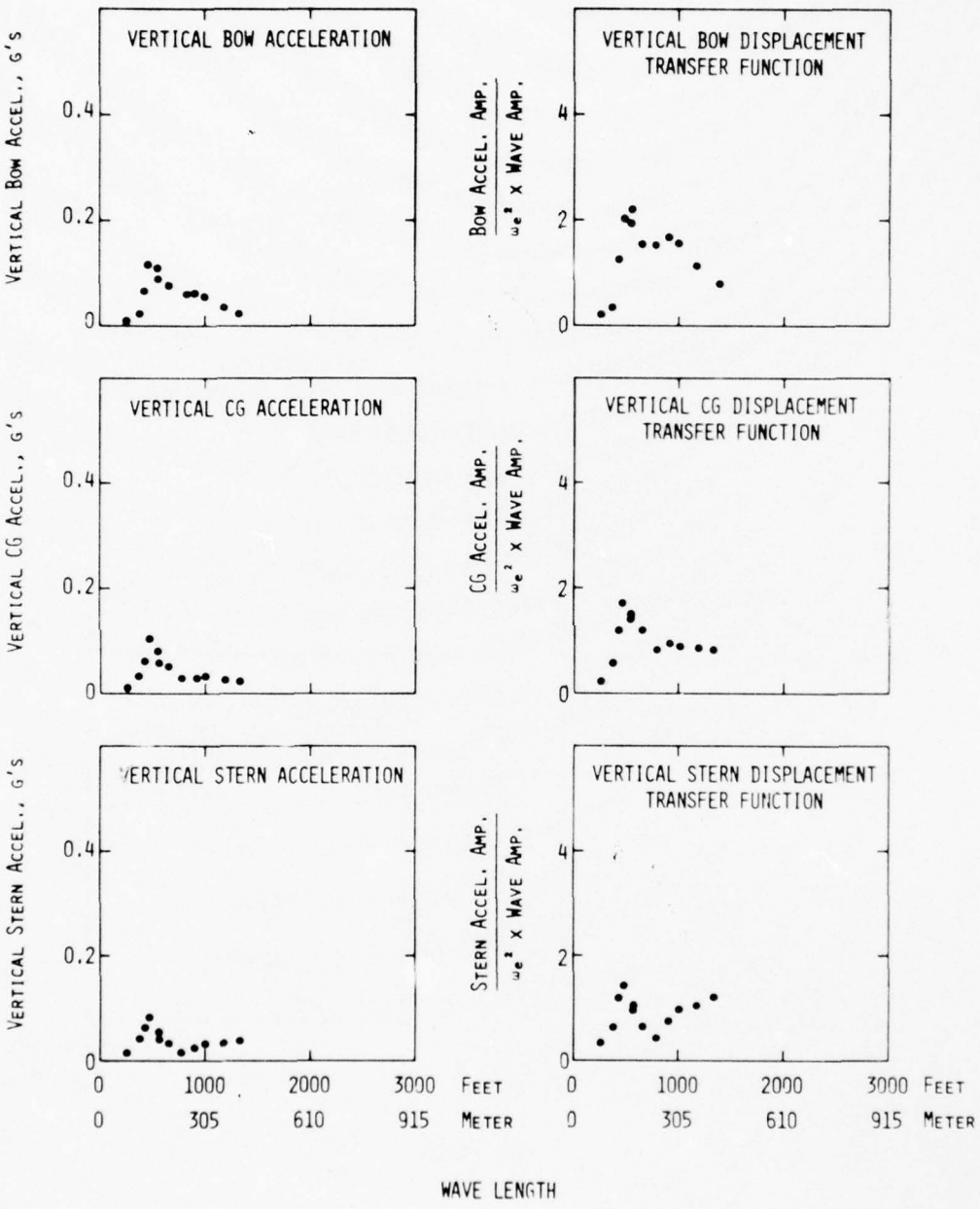

Figure 13 - Vertical Accelerations and Vertical Displacement Transfer Functions in Regular Head Seas for SWATH 6B - 0 Knots

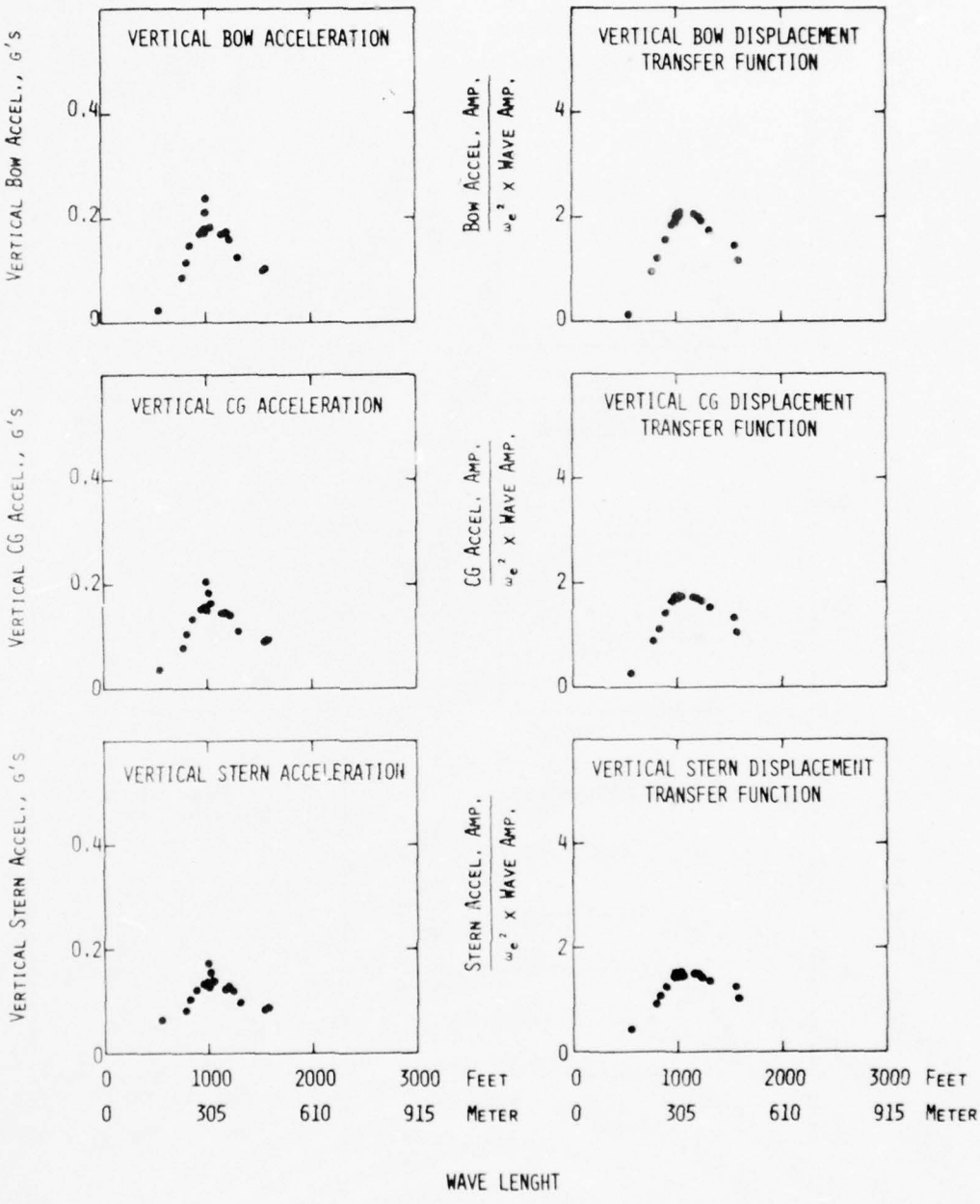

Figure 14 - Vertical Accelerations and Vertical Displacement Transfer Functions in Regular Head Seas for SWATH 6B - 20 Knots

SWATH 6B - REGULAR HEAD SEAS - 28 KNOTS

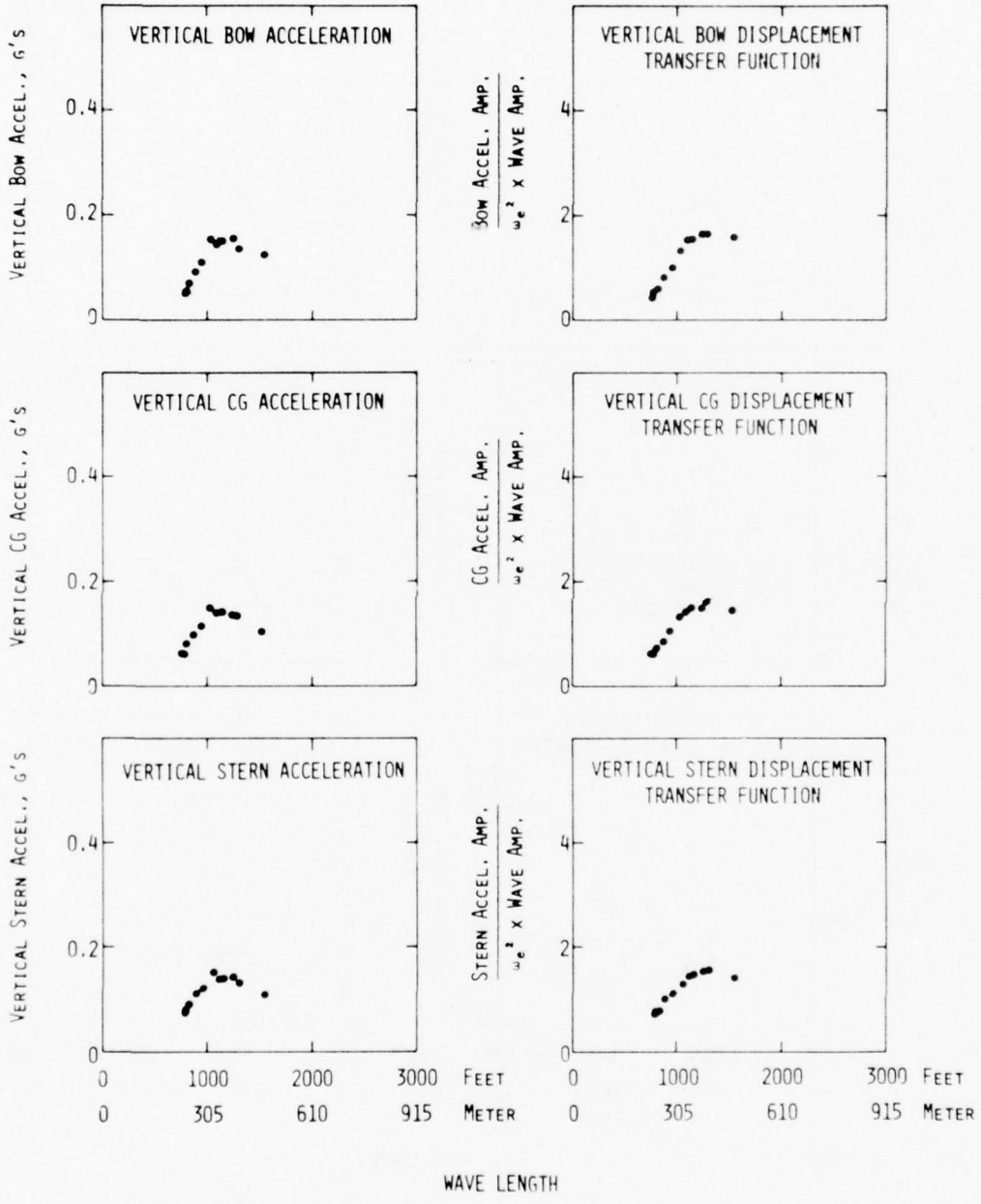

Figure 15 - Vertical Accelerations and Vertical Displacement Transfer Functions in Regular Head Seas for SWATH 6B - 28 Knots

SWATH 6C - REGULAR HEAD SEAS - 0 KNOTS

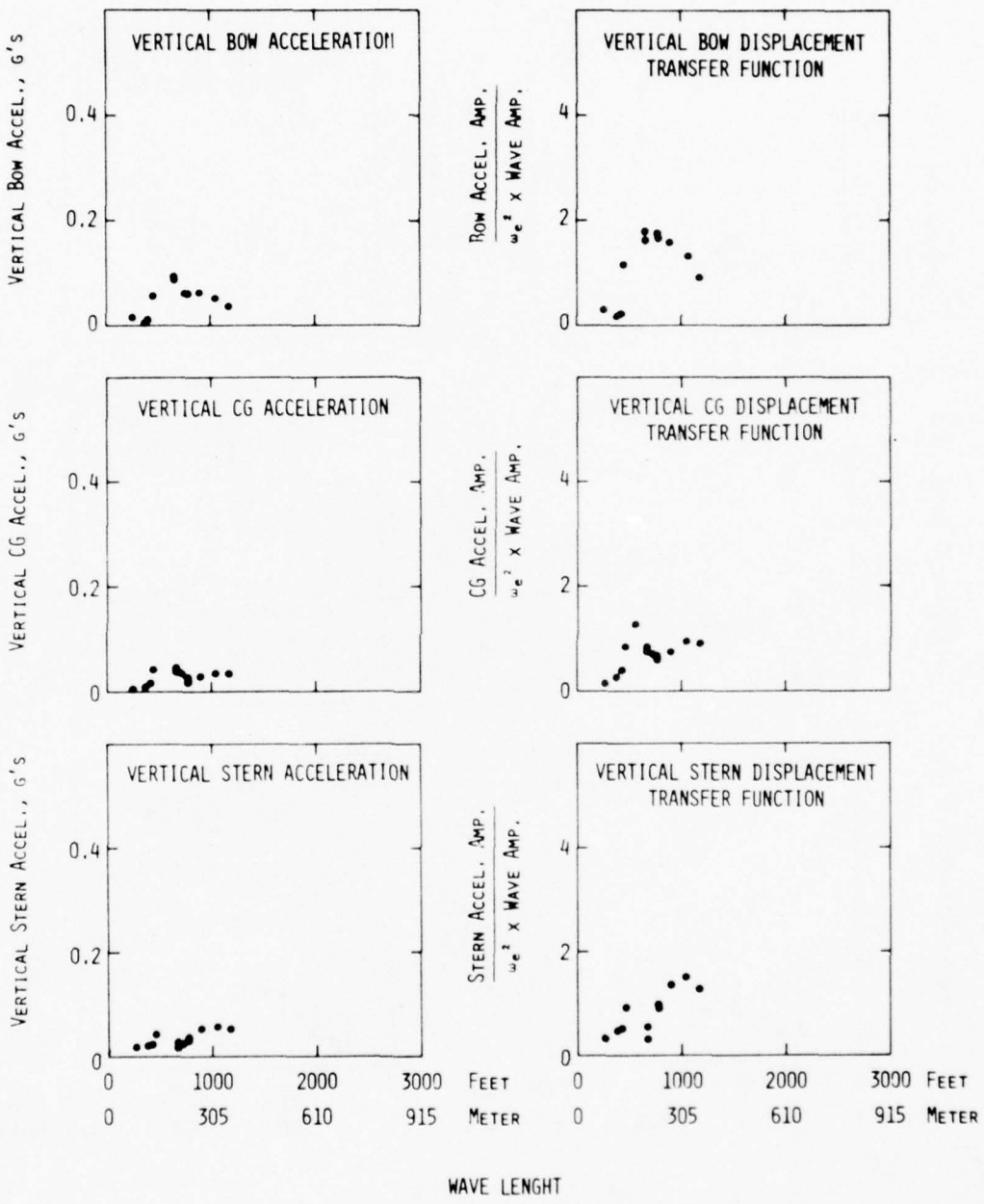

Figure 16 - Vertical Accelerations and Vertical Displacement Transfer Functions in Regular Head Seas for SWATH 6C - 0 Knots

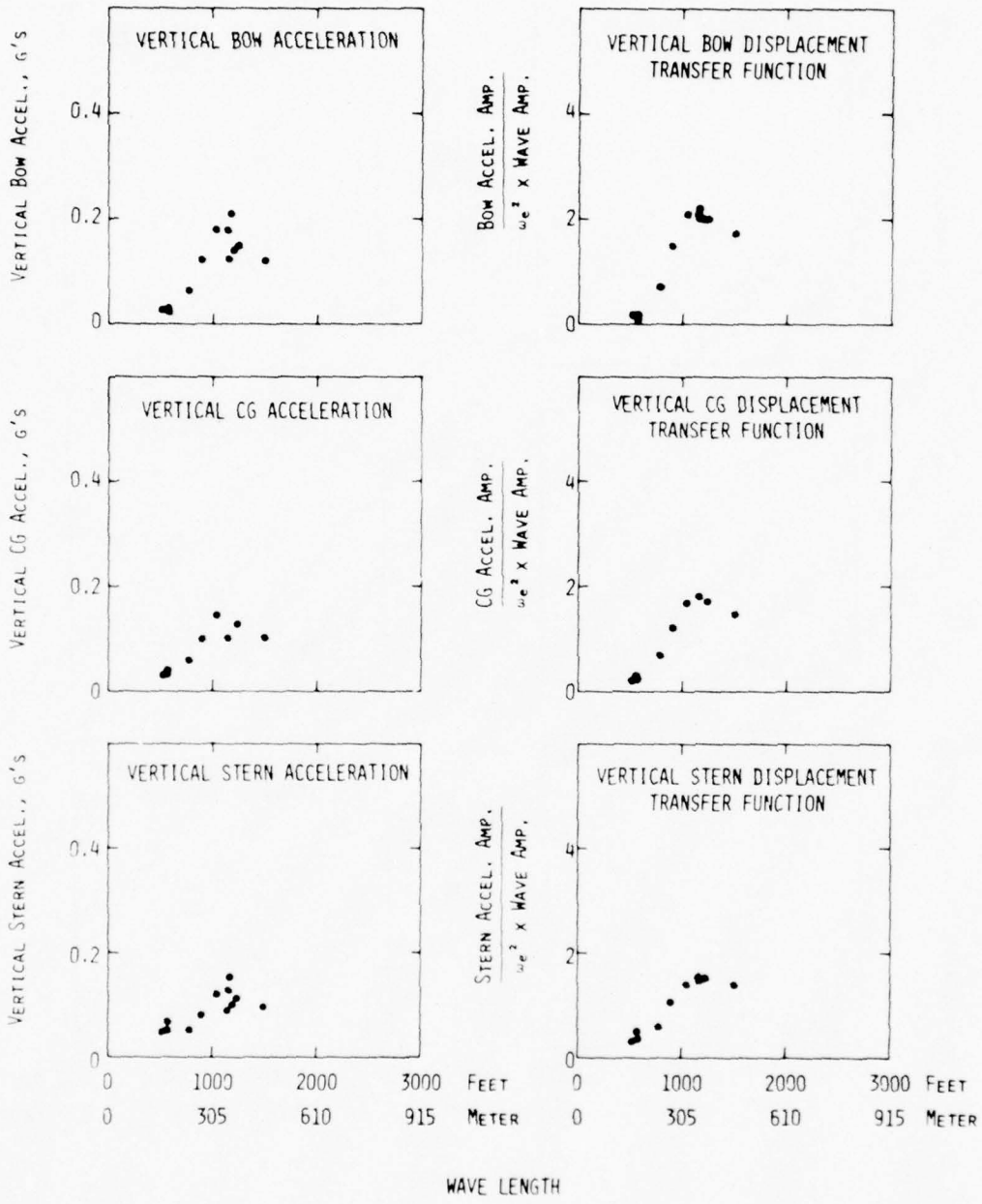

Figure 17 - Vertical Accelerations and Vertical Displacement Transfer Functions in Regualr Head Seas for SWATH 6C - 20 Knots

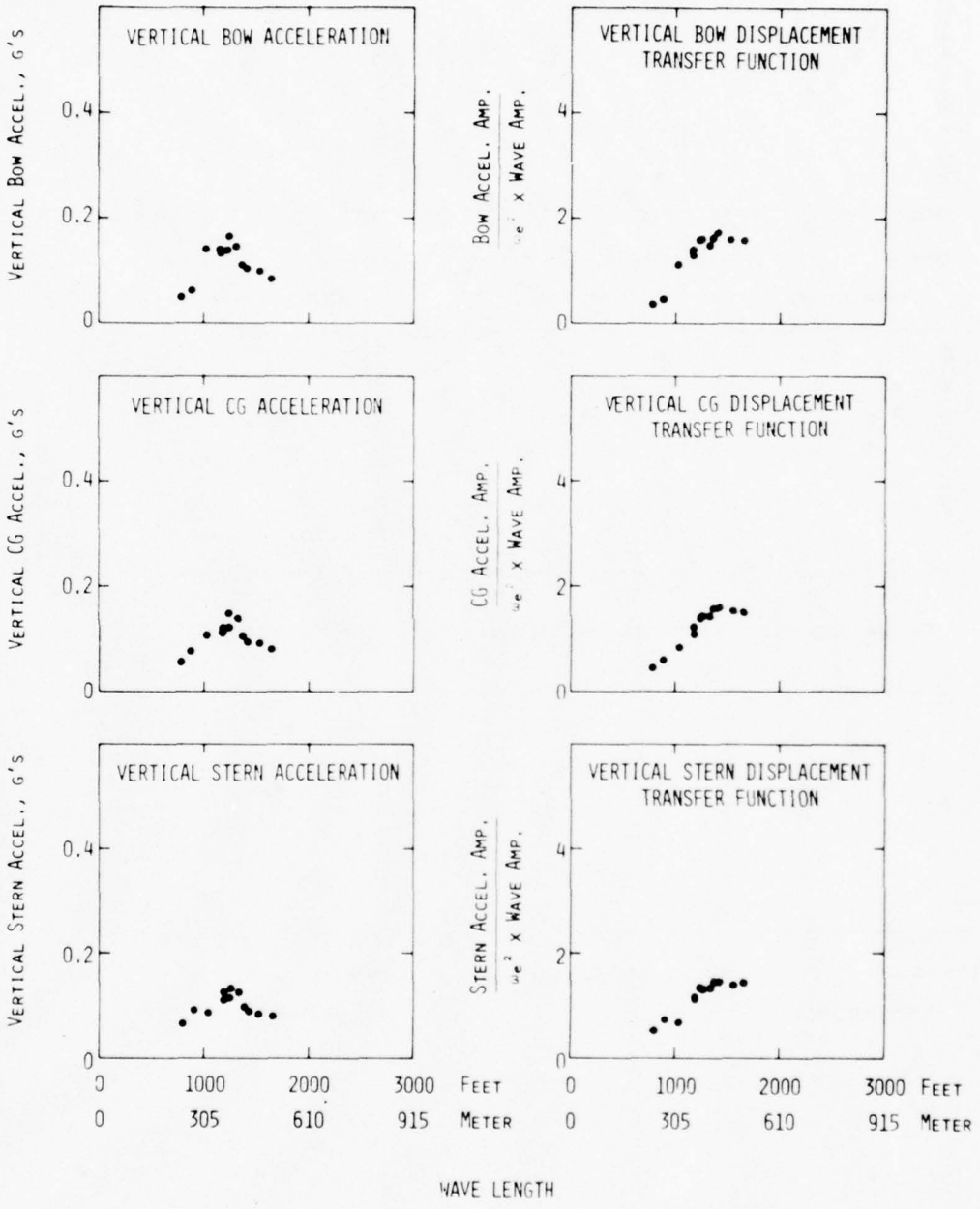

Figure 18 - Vertical Accelerations and Vertical Displacement Transfer Functions in Regular Head Seas for SWATH 6C - 28 Knots

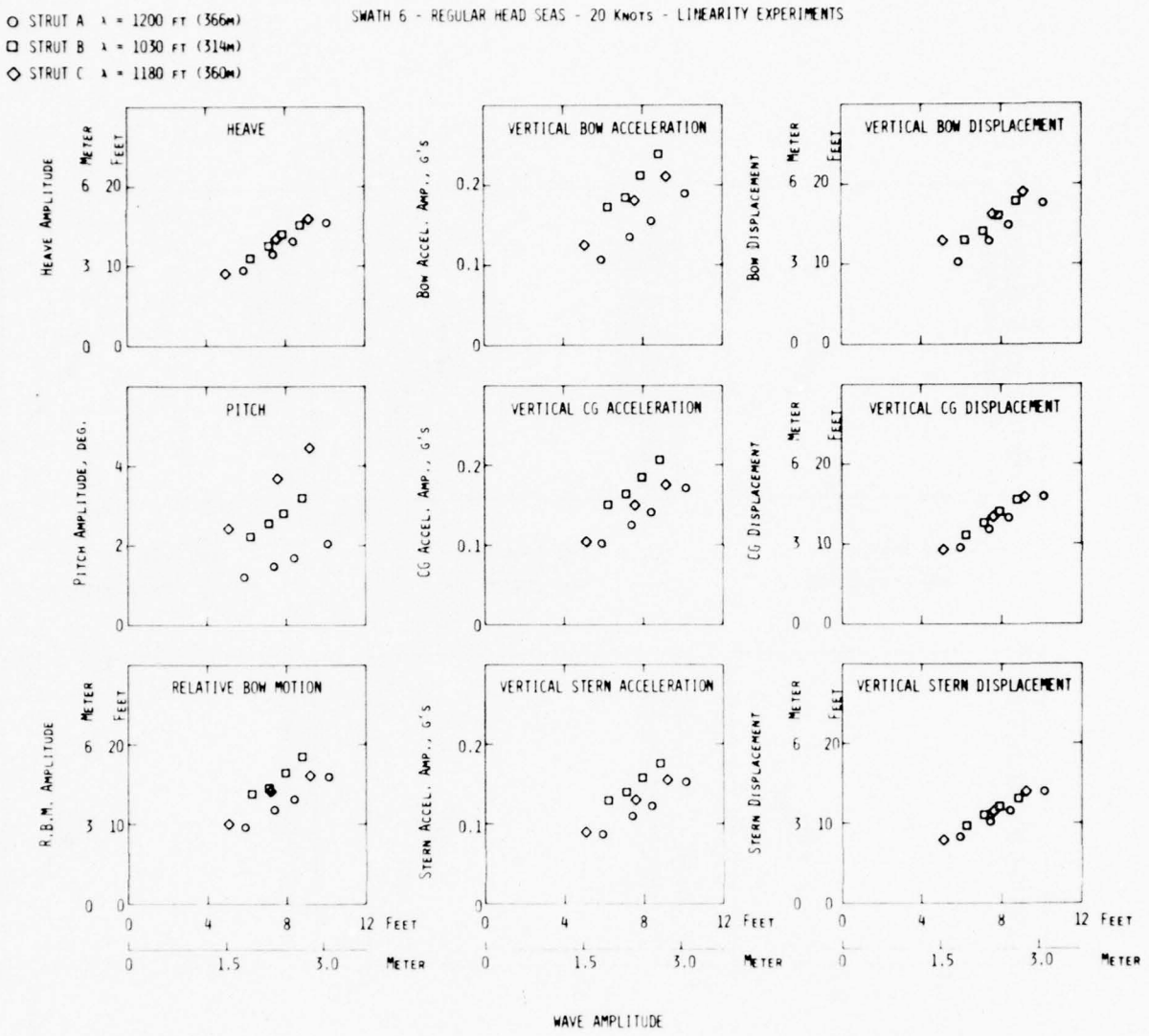

Figure 19 - Results of Linearity Experiments in Regular Head Seas for SWATH 6 - 20 Knots

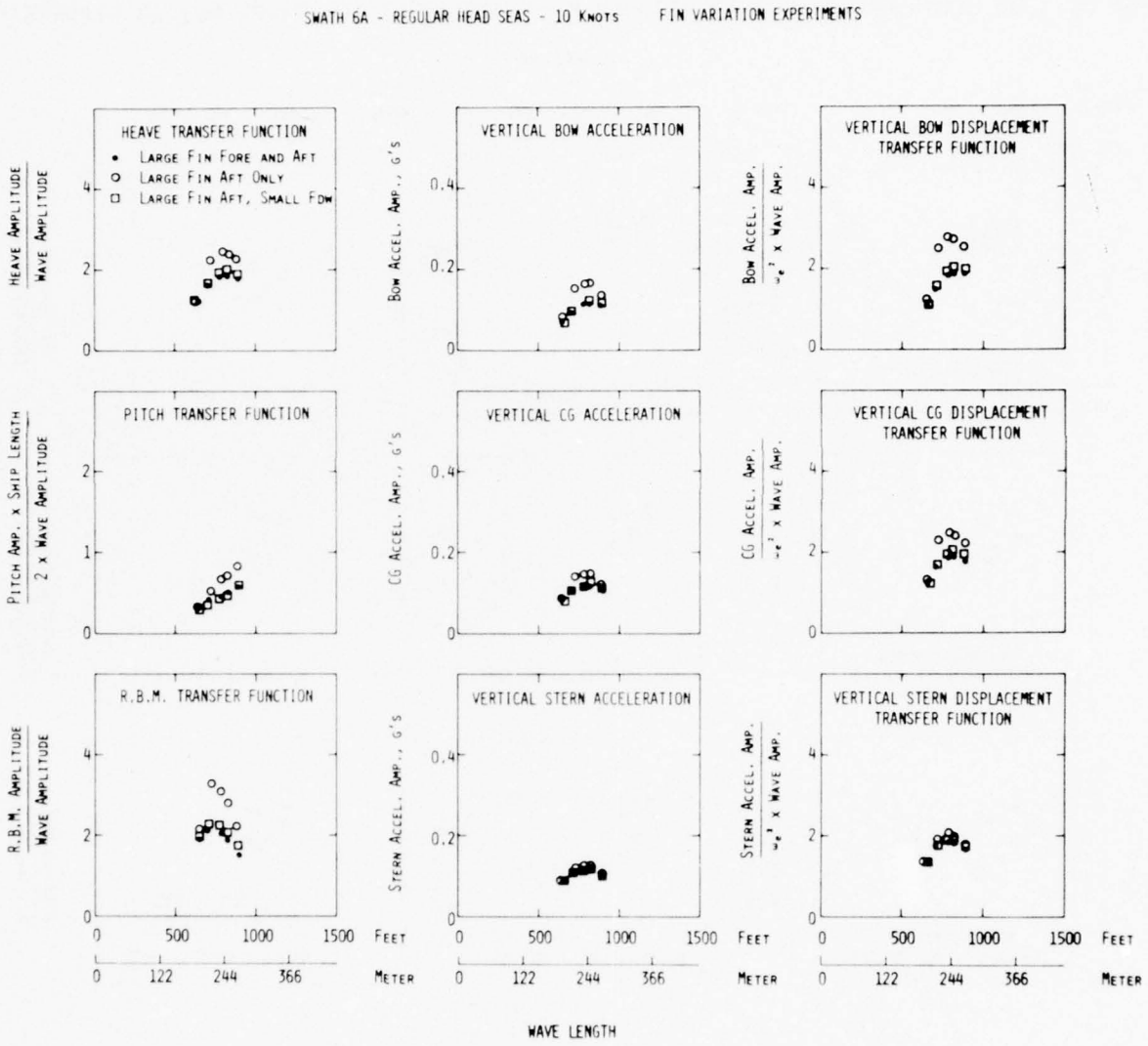

Figure 20 - Results of Fin Variation Experiments in Regular Head Seas for SWATH 6A - 10 Knots

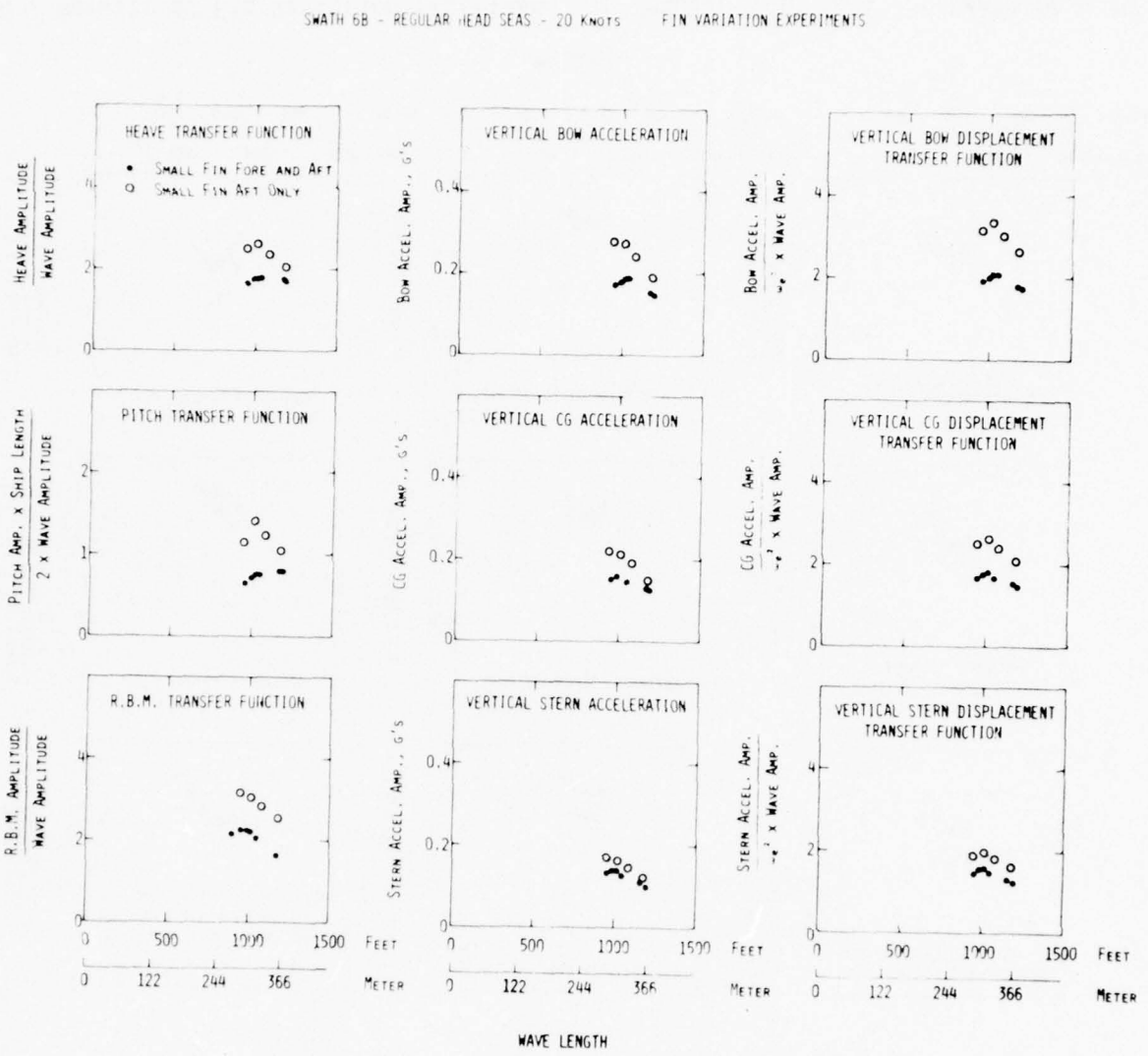

Figure 22 - Results of Fin Variation Experiments in Regular Head Seas for SWATH 6B - 20 Knots

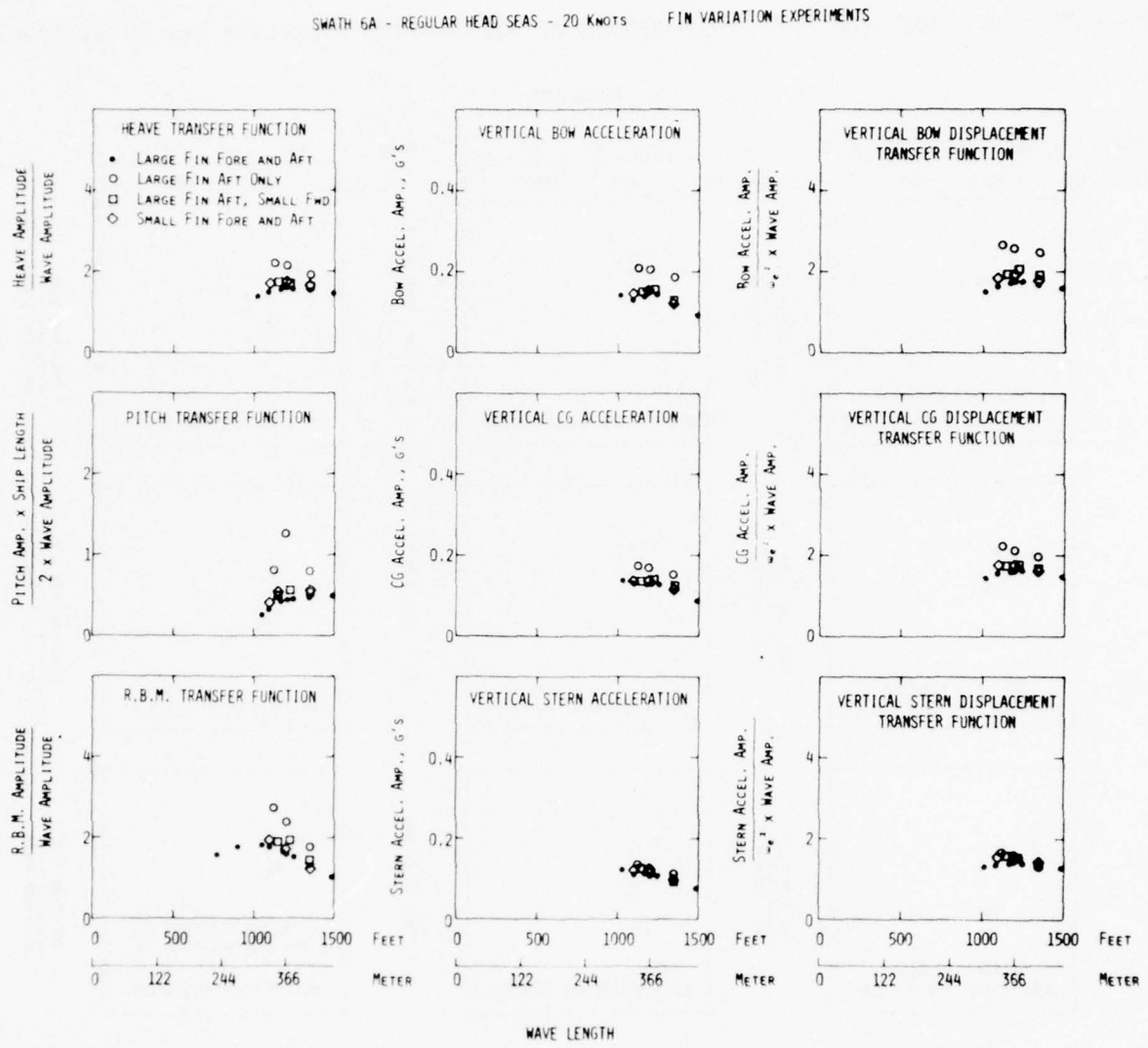

Figure 21 - Results of Fin Variation Experiments in Regular Head Seas for SWATH 6A - 20 Knots

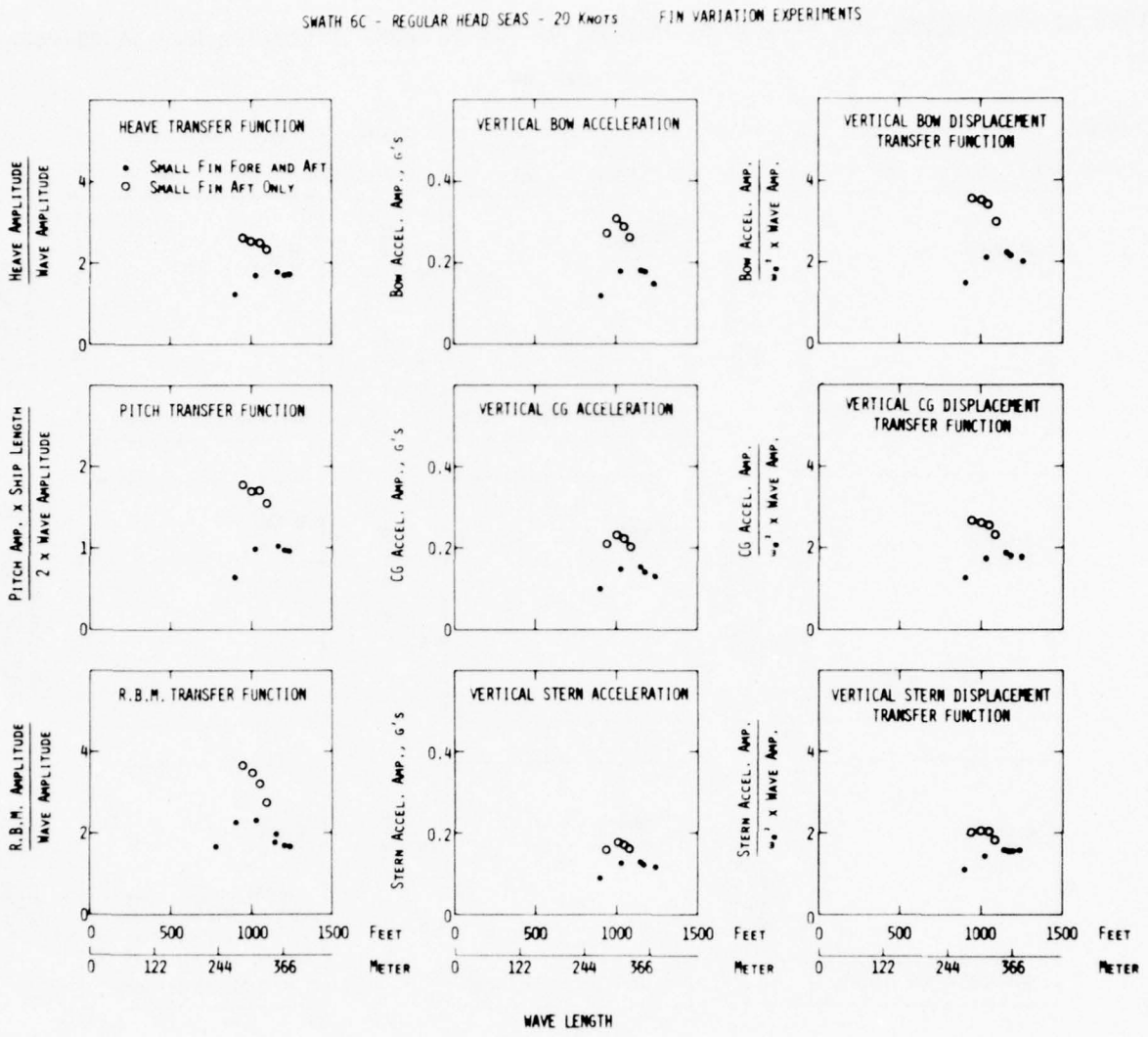

Figure 23 - Results of Fin Variation Experiments in Regular Head Seas for SWATH 6C - 20 Knots

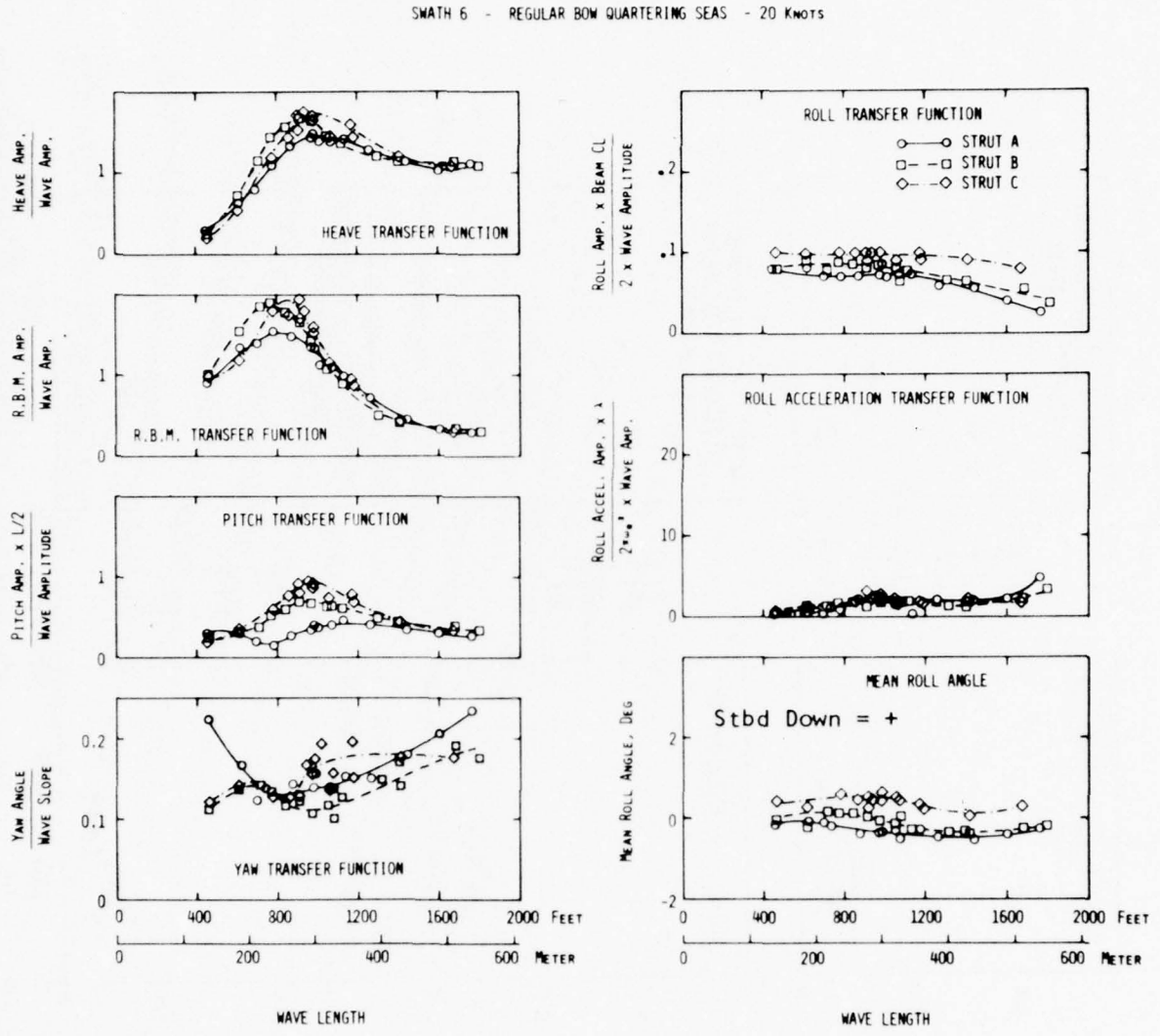

Figure 24 - Motion Transfer Functions in Regular Bow Quartering Seas for SWATH 6 - 20 Knots

SWATH 6A - REGULAR BOW QUARTERING SEAS - 20 KNOTS

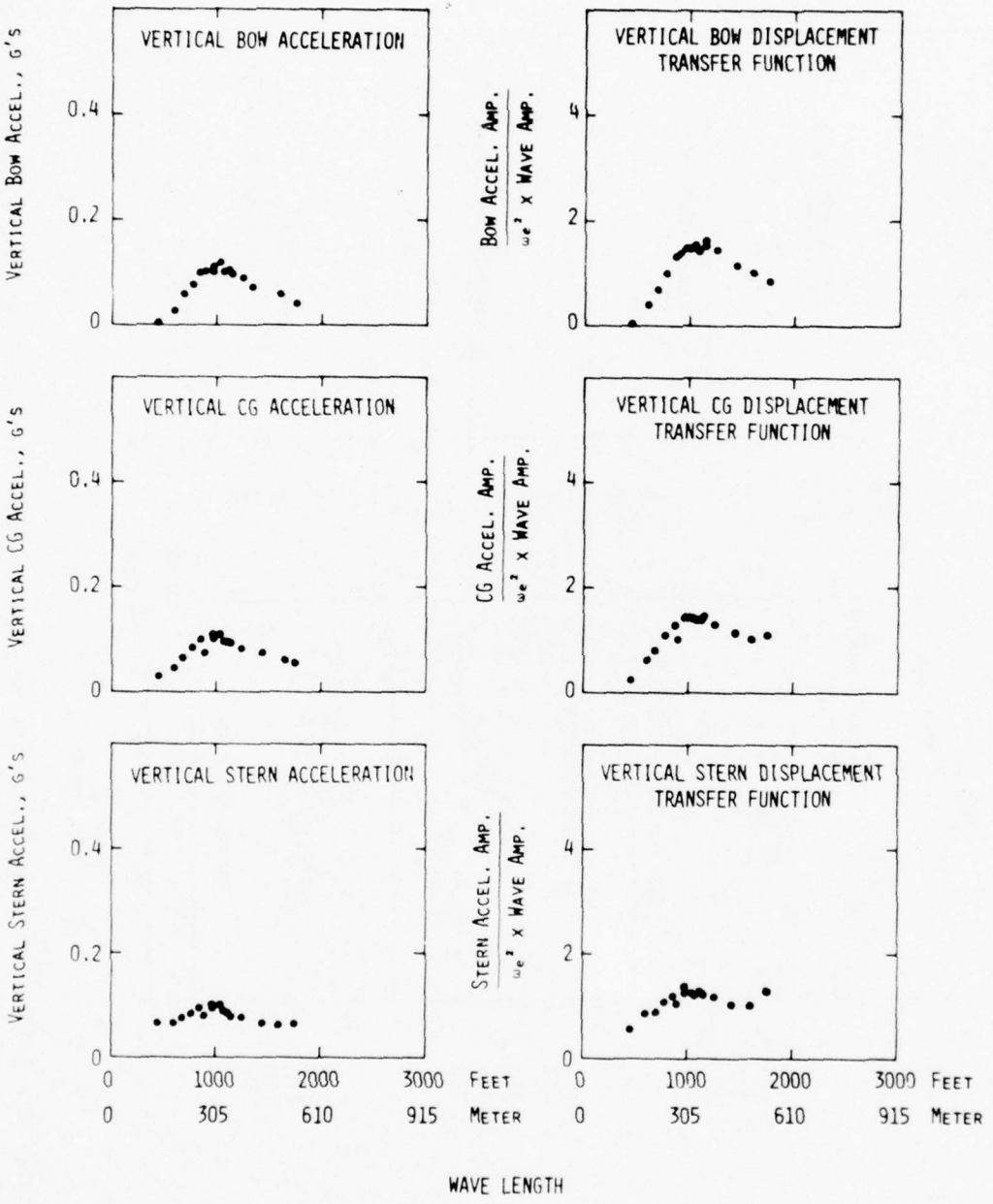

Figure 25 - Vertical Accelerations and Vertical Displacement Transfer Functions in Regular Bow Quartering Seas for SWATH 6A - 20 Knots

SWATH 6B - REGULAR BOW QUARTERING SEAS - 20 KNOTS

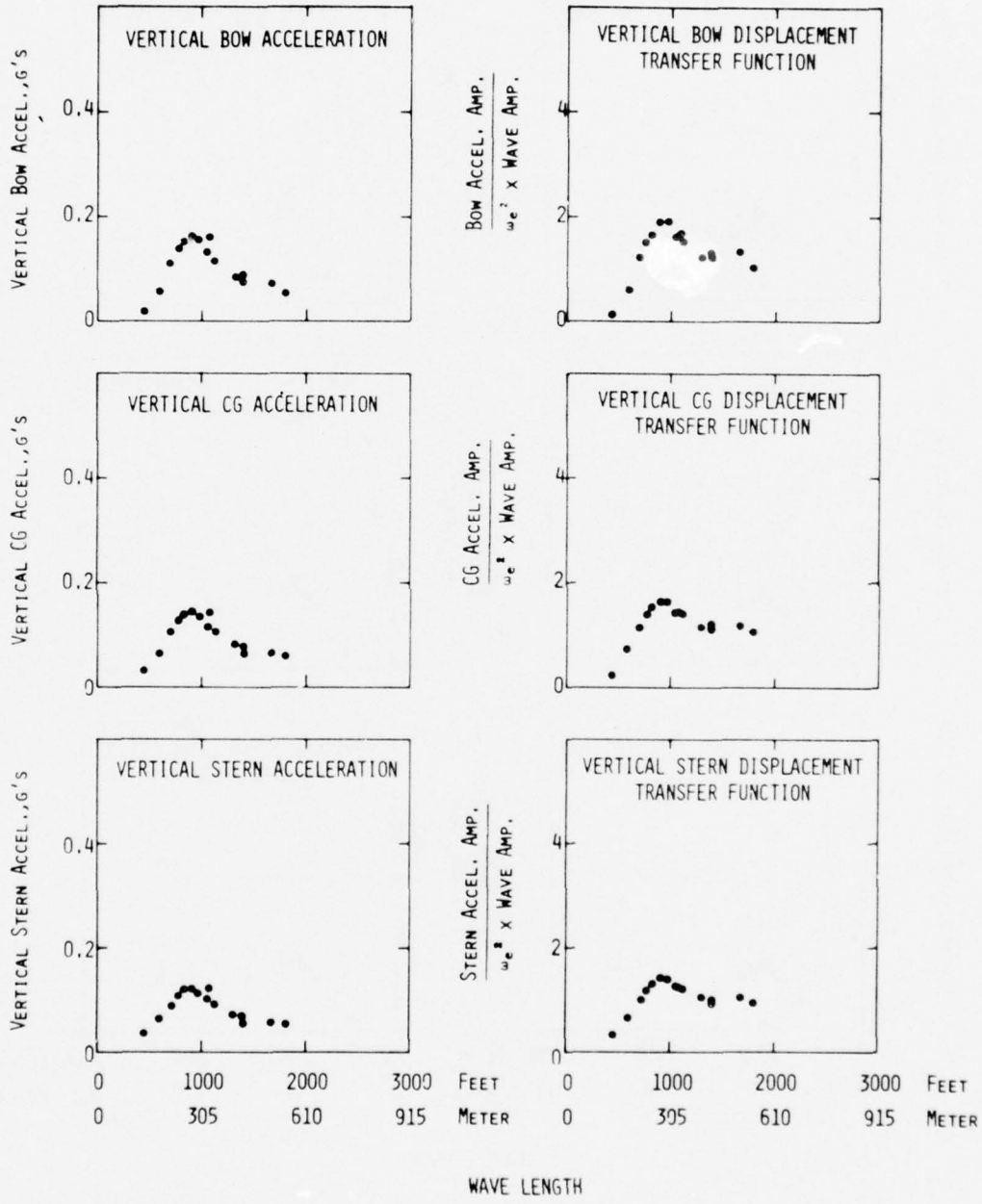

Figure 26 - Vertical Accelerations and Vertical Displacement Transfer Functions in Regular Bow Quartering Seas for SWATH 6B - 20 Knots

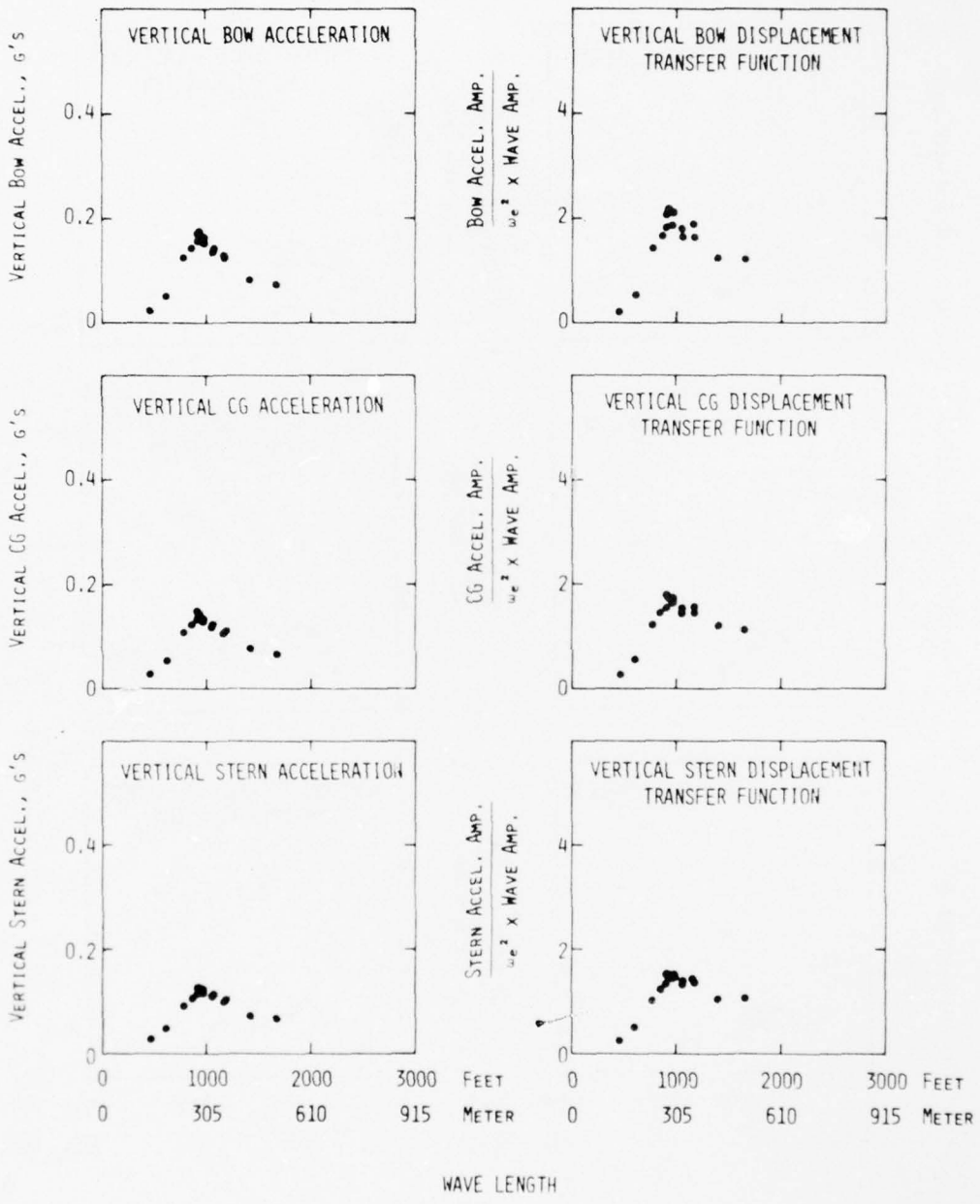

Figure 27 - Vertical Accelerations and Vertical Displacement Transfer Functions in Regular Bow Quartering Seas for SWATH 6C - 20 Knots

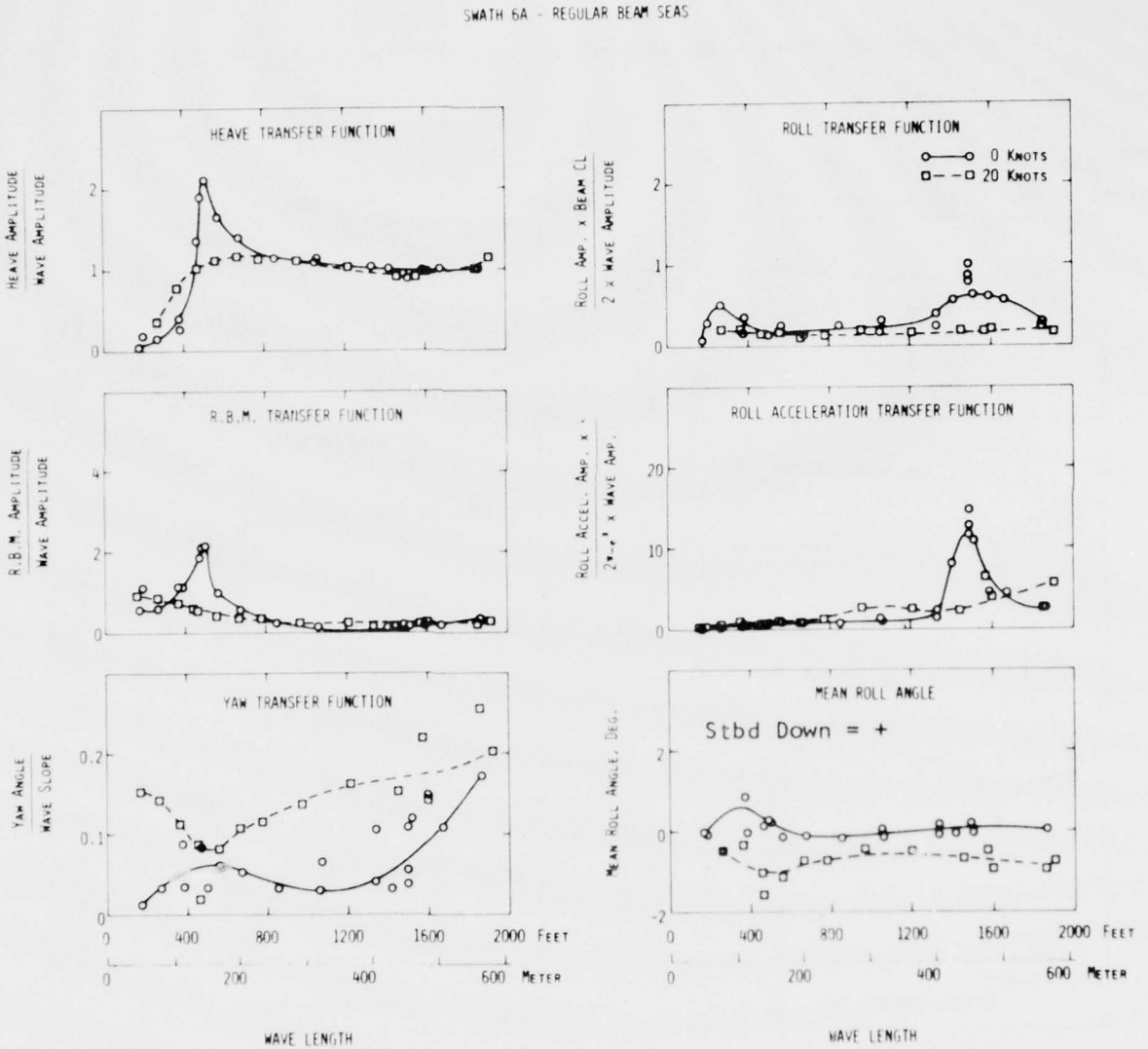

Figure 28 - Motion Transfer Functions in Regular Beam Seas for SWATH 6A

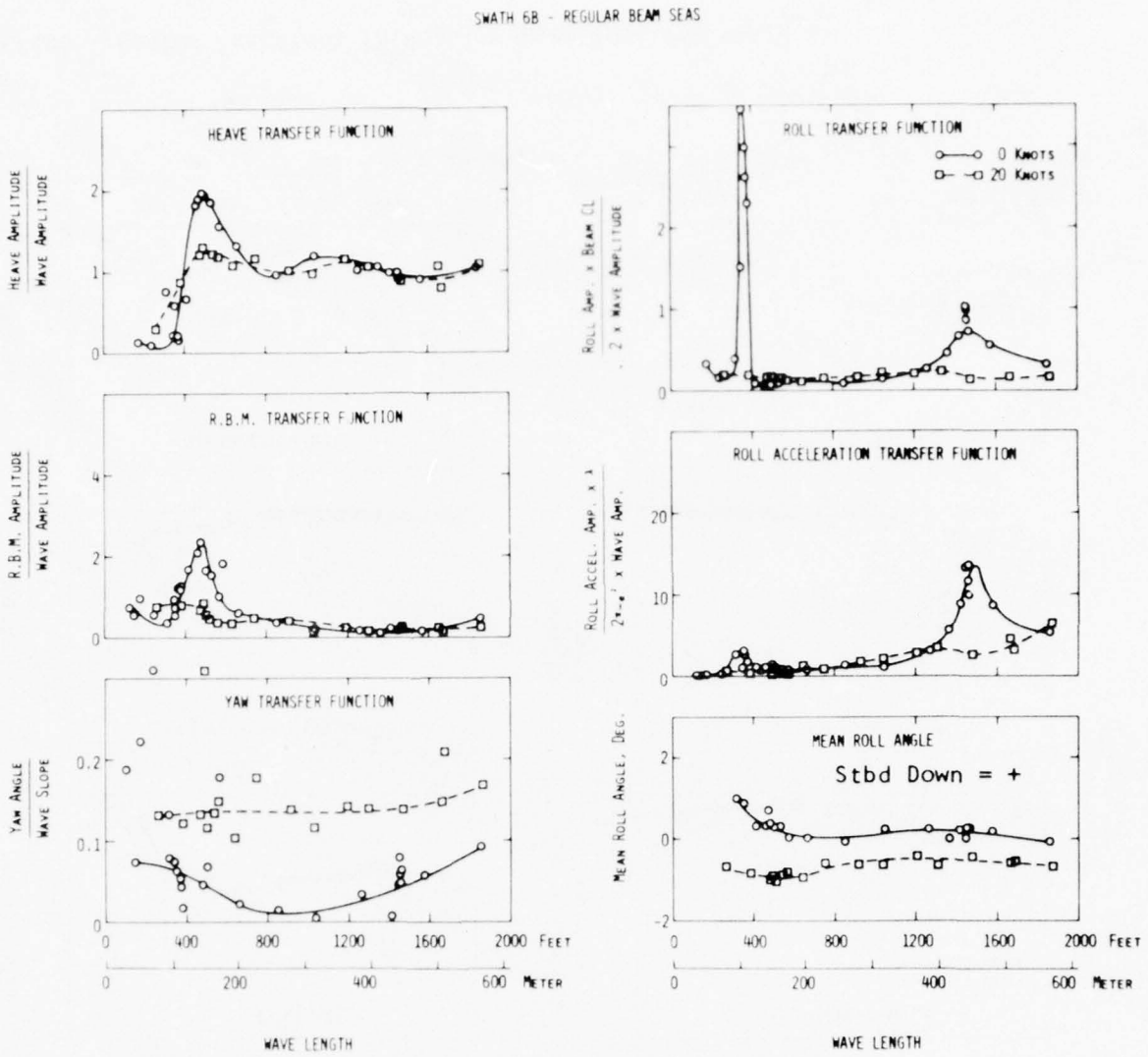

Figure 29 - Motion Transfer Functions in Regular Beam Seas for SWATH 6B

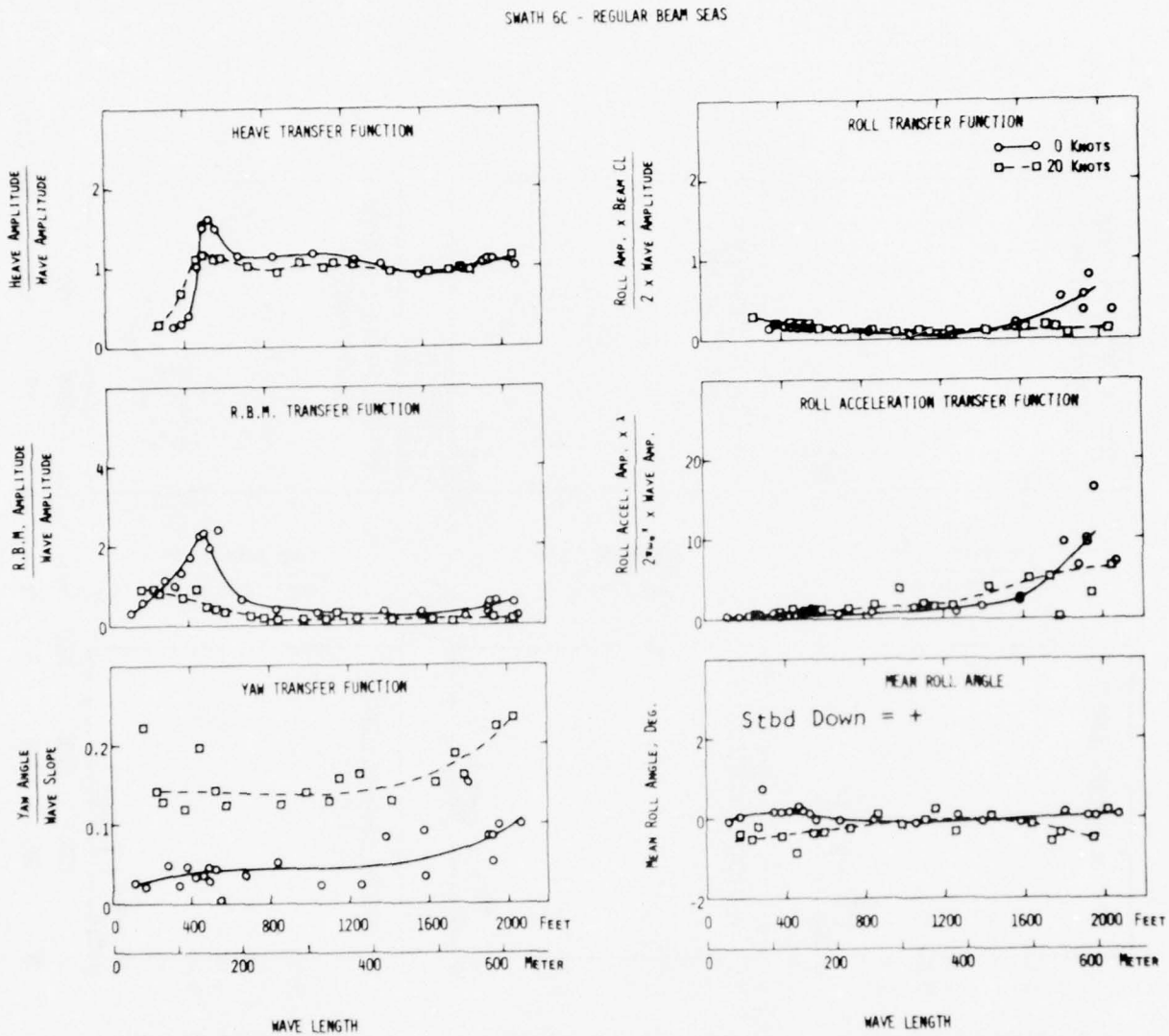

Figure 30 - Motion Transfer Functions in Regular Beam Seas for SWATH 6C

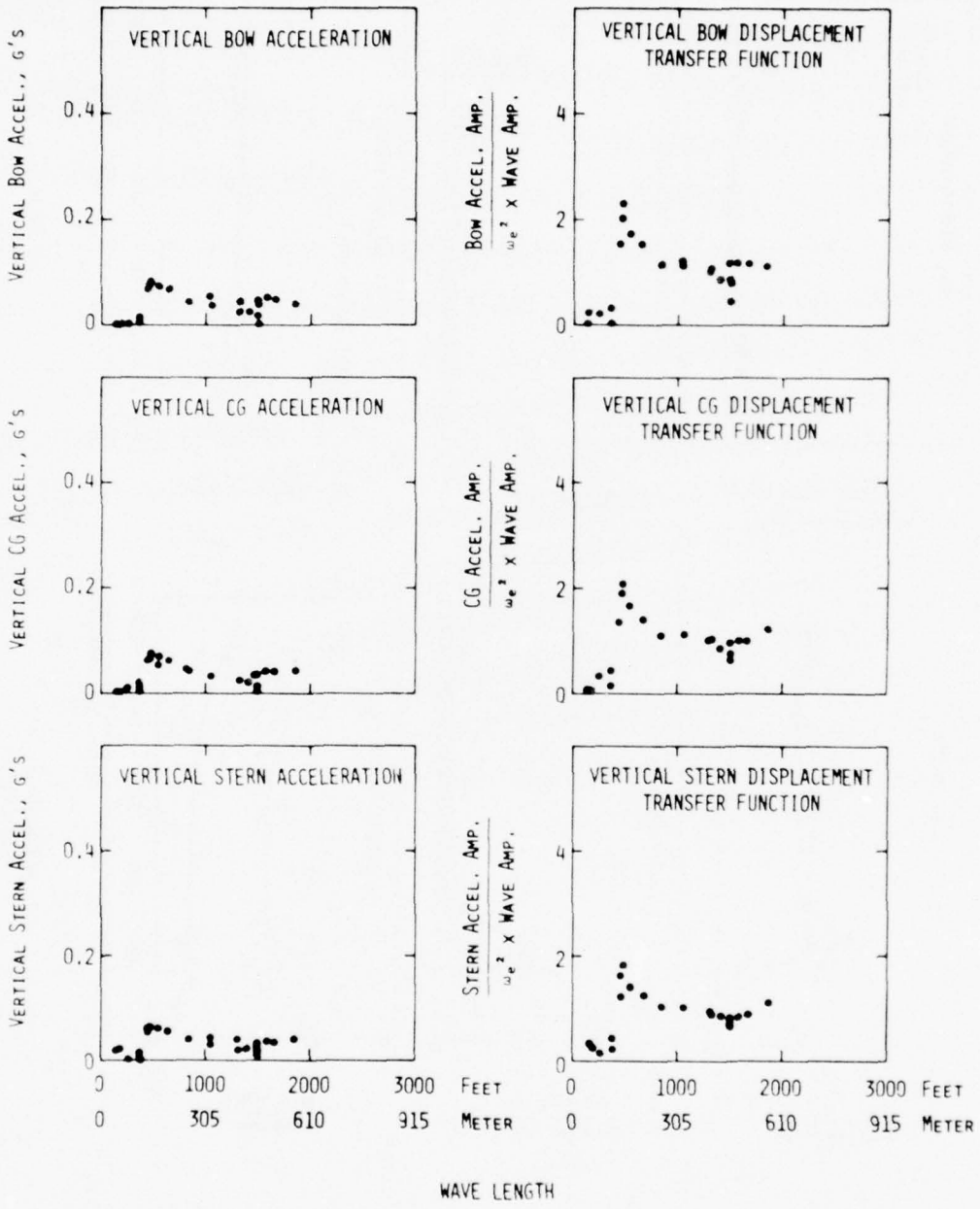

Figure 31 - Vertical Accelerations and Vertical Displacement Transfer Functions in Regular Beam Seas for SWATH 6A - 0 Knots

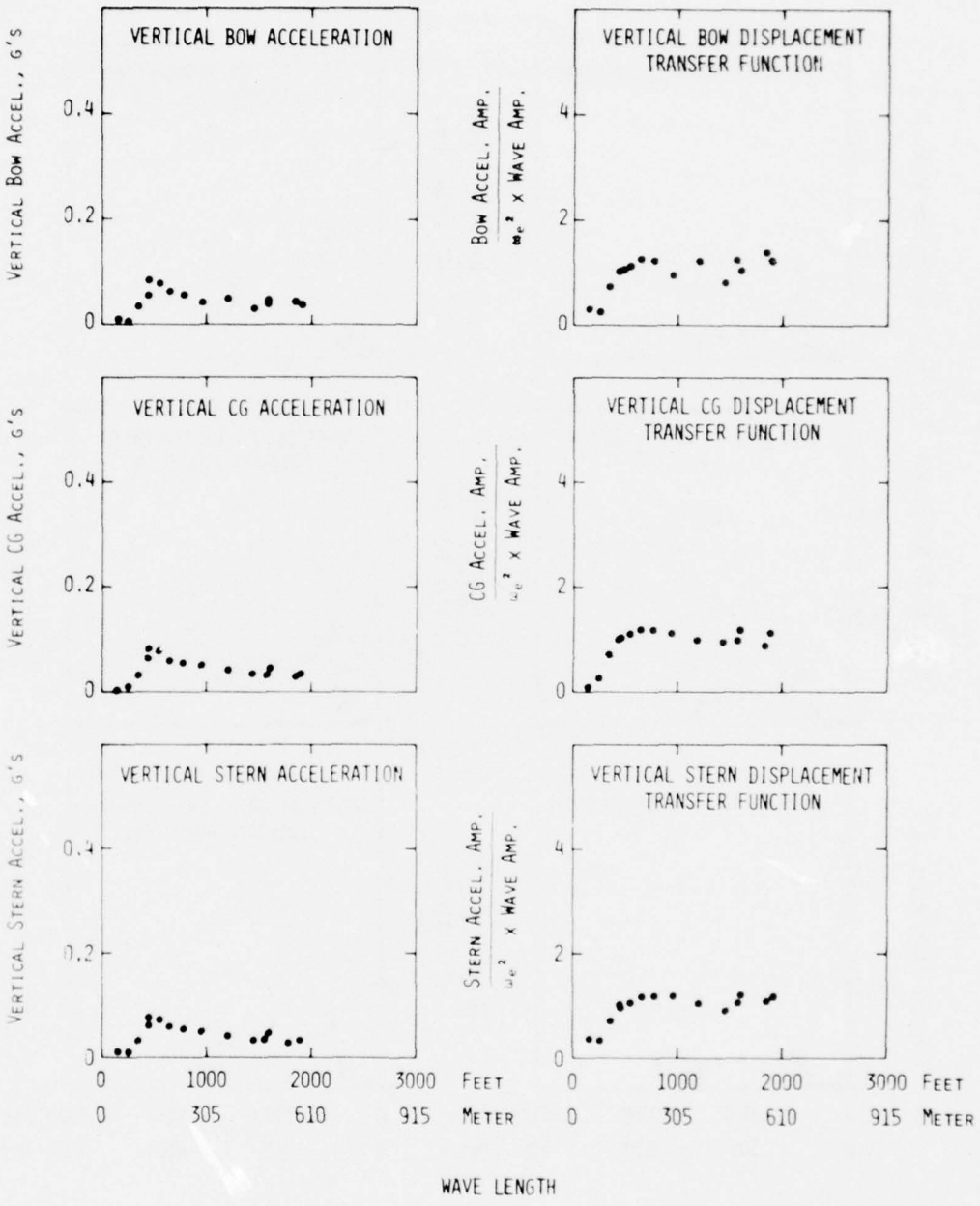

Figure 32 - Vertical Accelerations and Vertical Displacement Transfer Functions in Regular Beam Seas for SWATH 6A - 20 Knots

SWATH 6B - REGULAR BEAM SEAS - 0 KNOTS

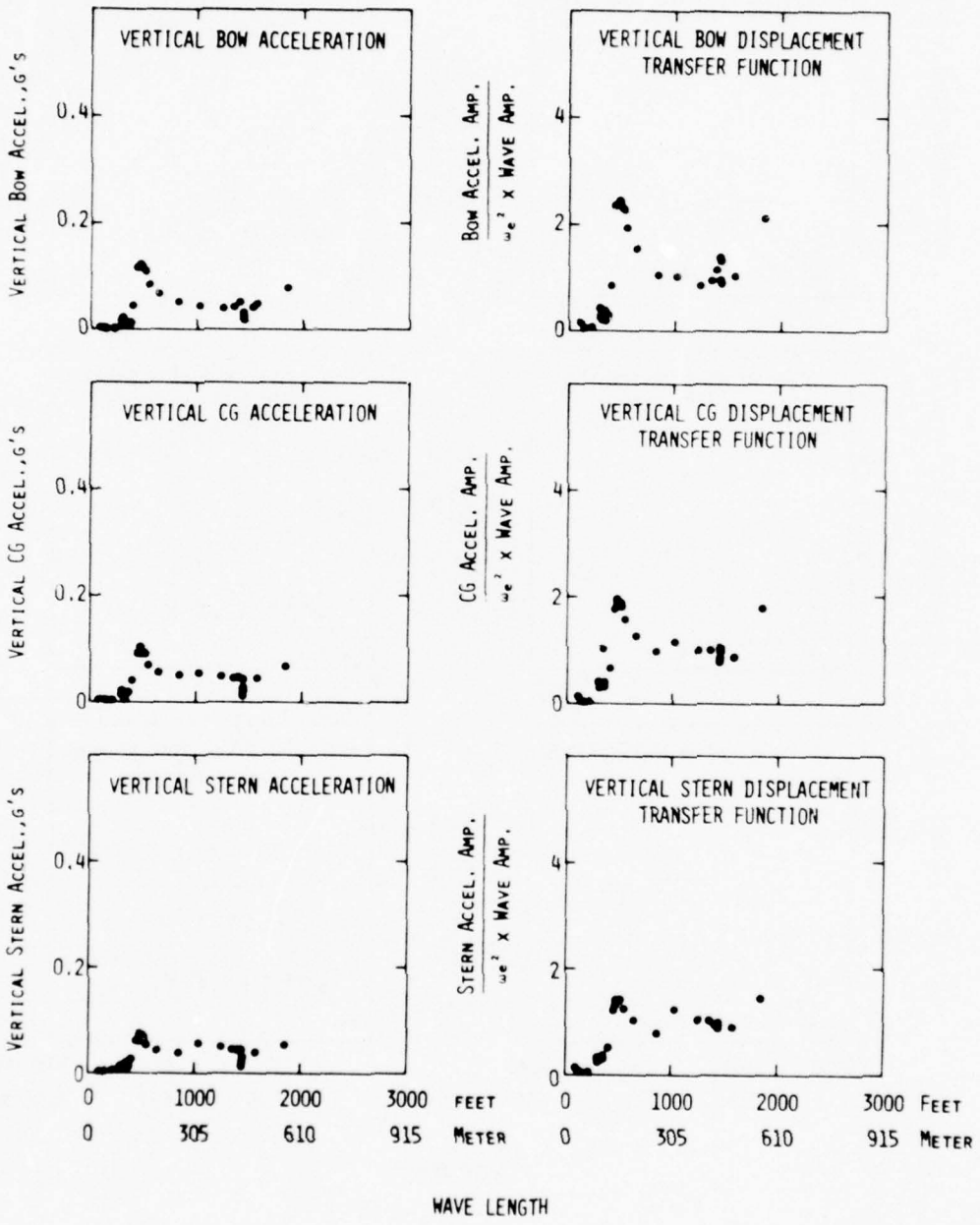

Figure 33 - Vertical Accelerations and Vertical Displacement Transfer Functions in Regular Beam Seas for SWATH 6B - 0 Knots

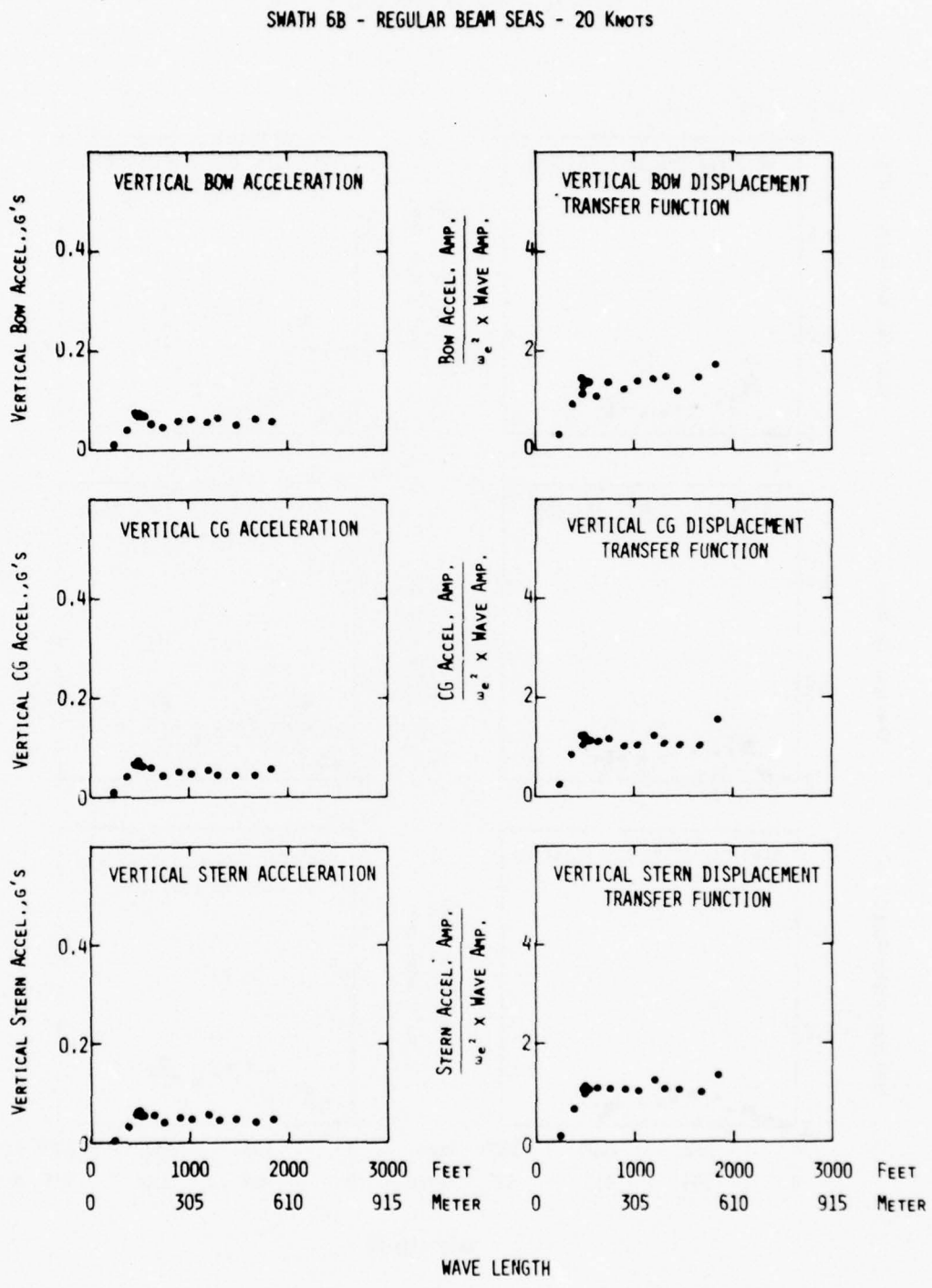

Figure 34 - Vertical Accelerations and Vertical Displacement Transfer Functions in Regular Beam Seas for SWATH 6B - 20 Knots

SWATH 6C - REGULAR BEAM SEAS - 0 KNOTS

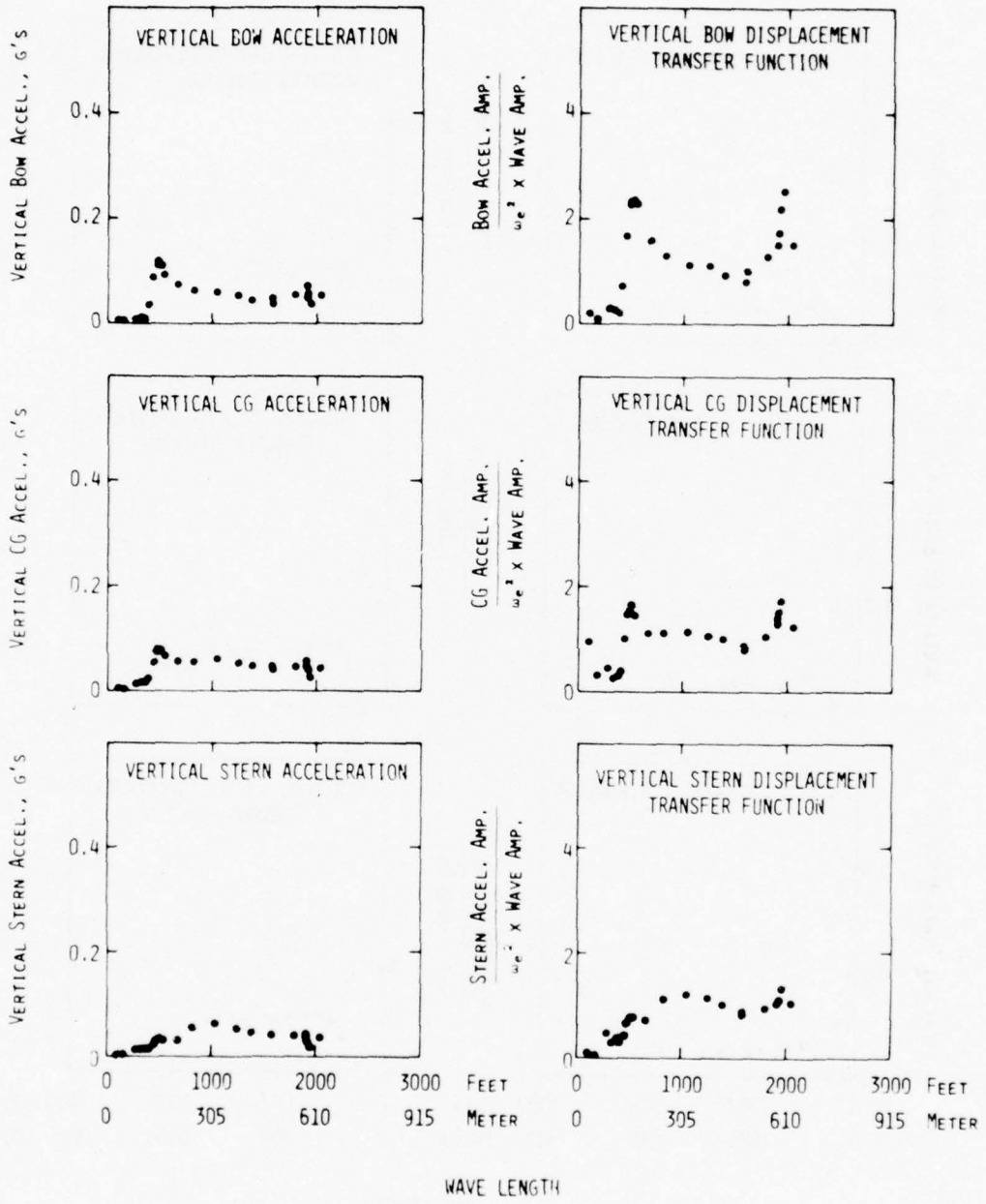

Figure 35 - Vertical Accelerations and Vertical Displacement Transfer Functions in Regular Beam Seas for SWATH 6C - 0 Knots

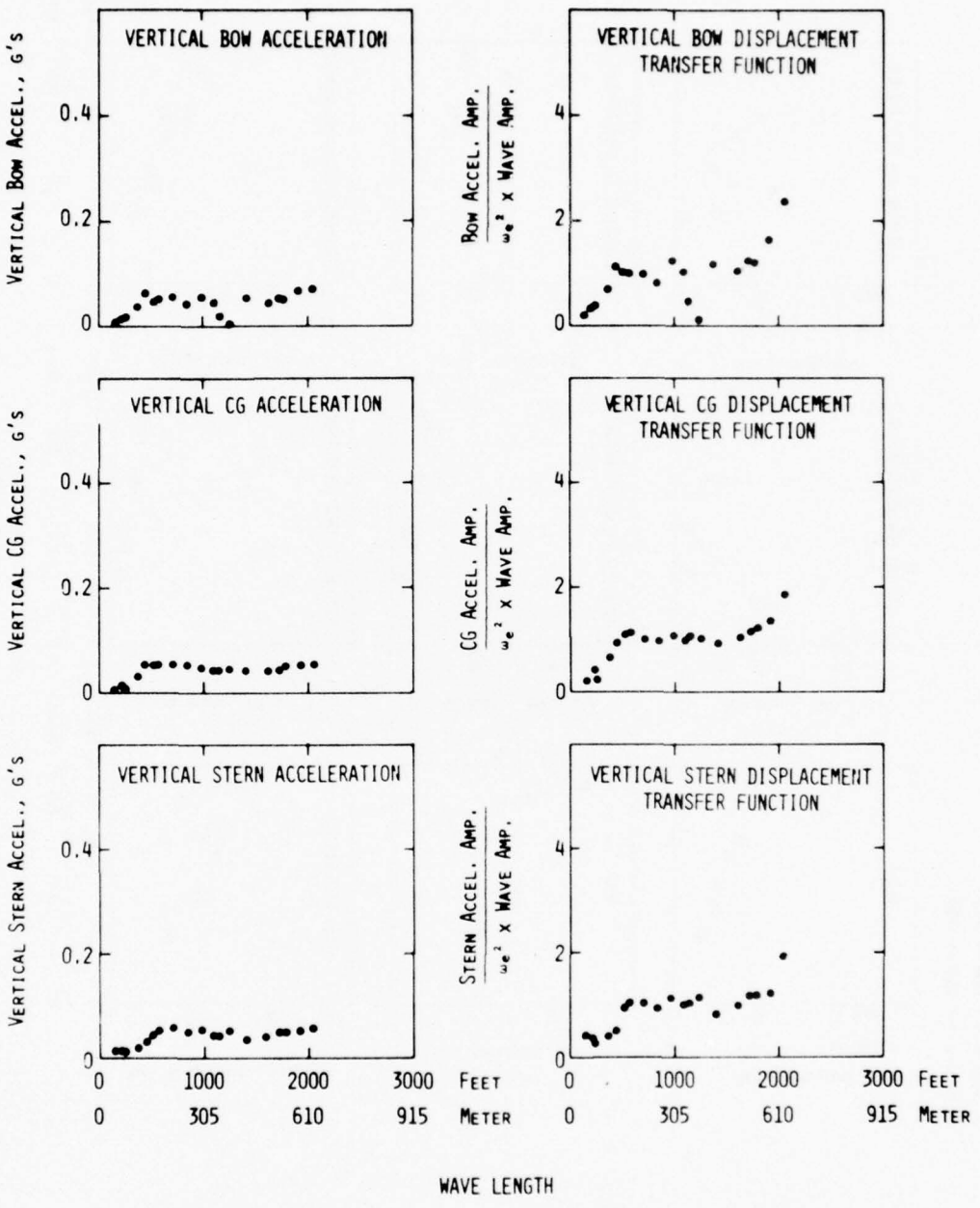

Figure 36 - Vertical Accelerations and Vertical Displacement Transfer Functions in Regular Beam Seas for SWATH 6C - 20 Knots

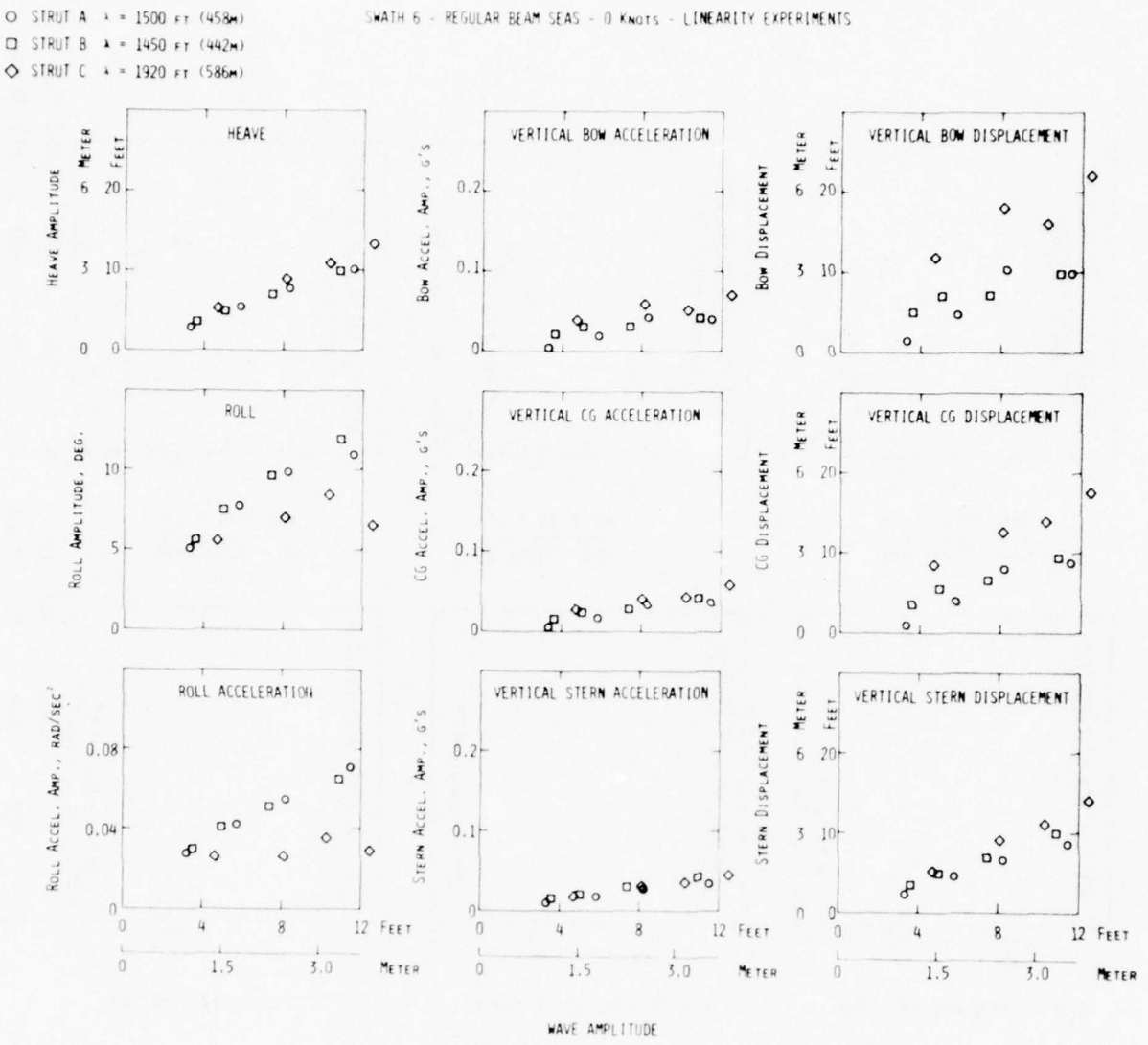

Figure 37 - Results of Linearity Experiments in Regular Beam Seas for SWATH 6 - 0 Knots

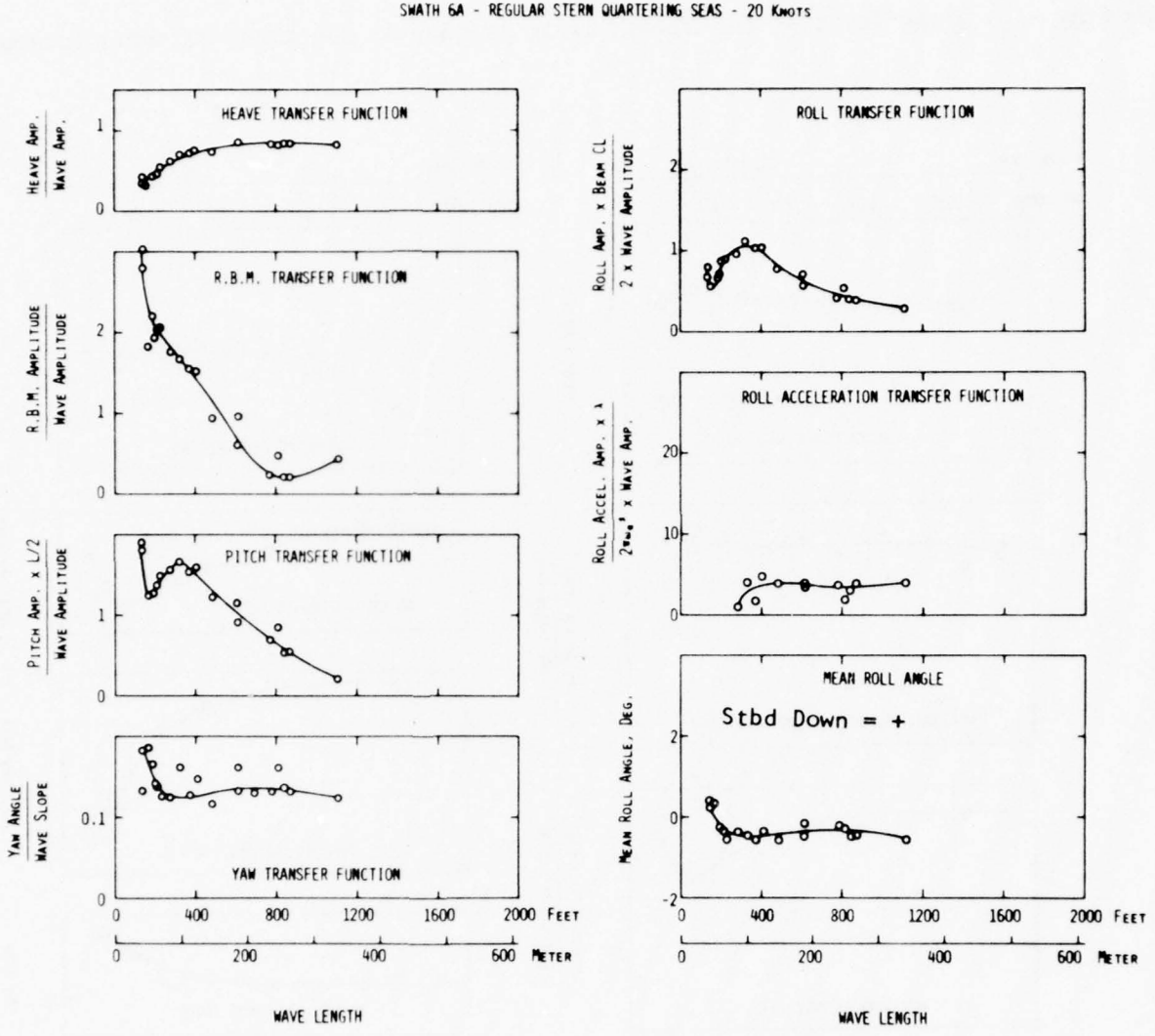

Figure 38 - Motion Transfer Functions in Regular Stern Quartering Seas for SWATH 6A - 20 Knots

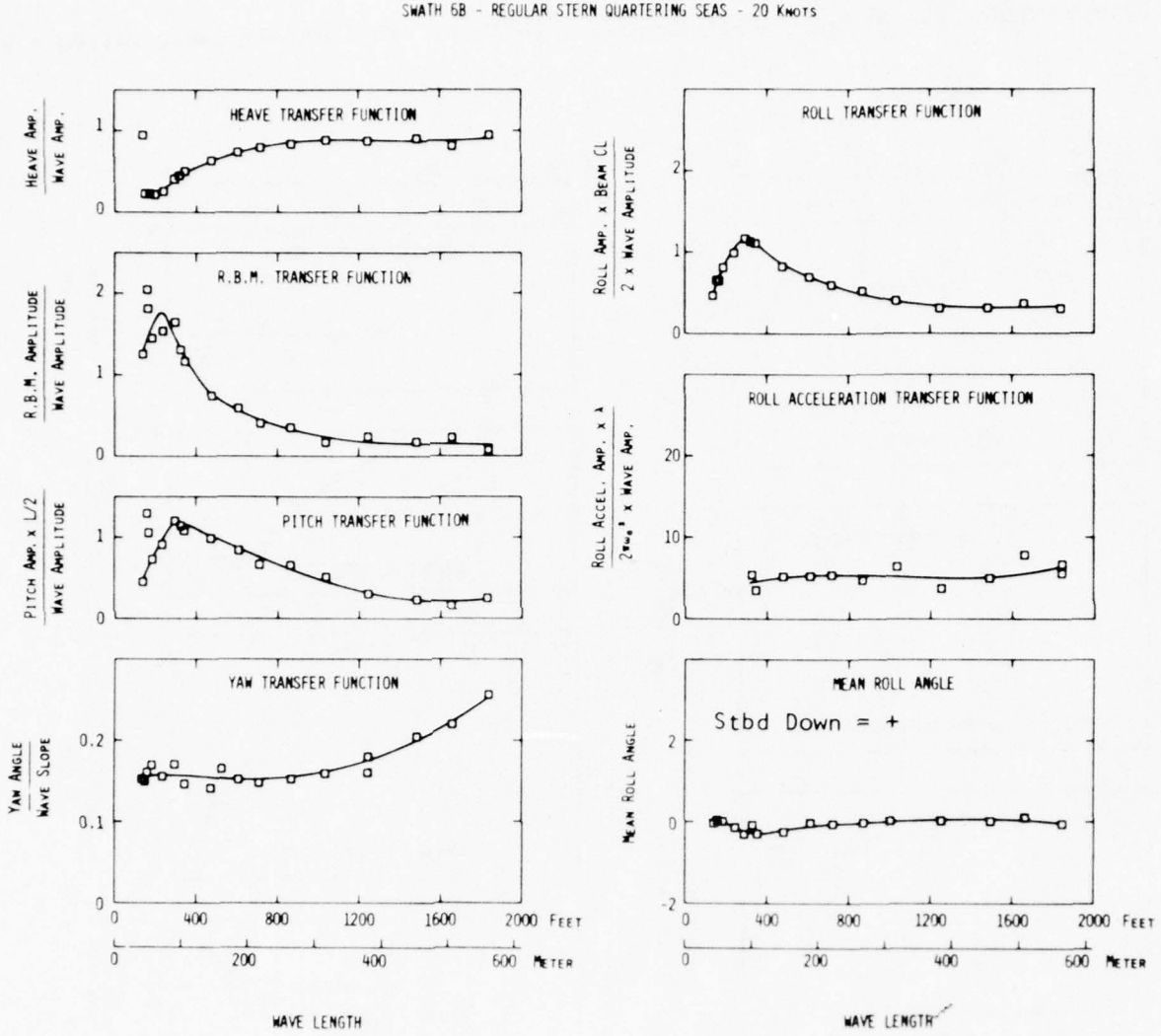

Figure 39 - Motion Transfer Functions in Regular Stern Quartering Seas for SWATH 6B - 20 Knots

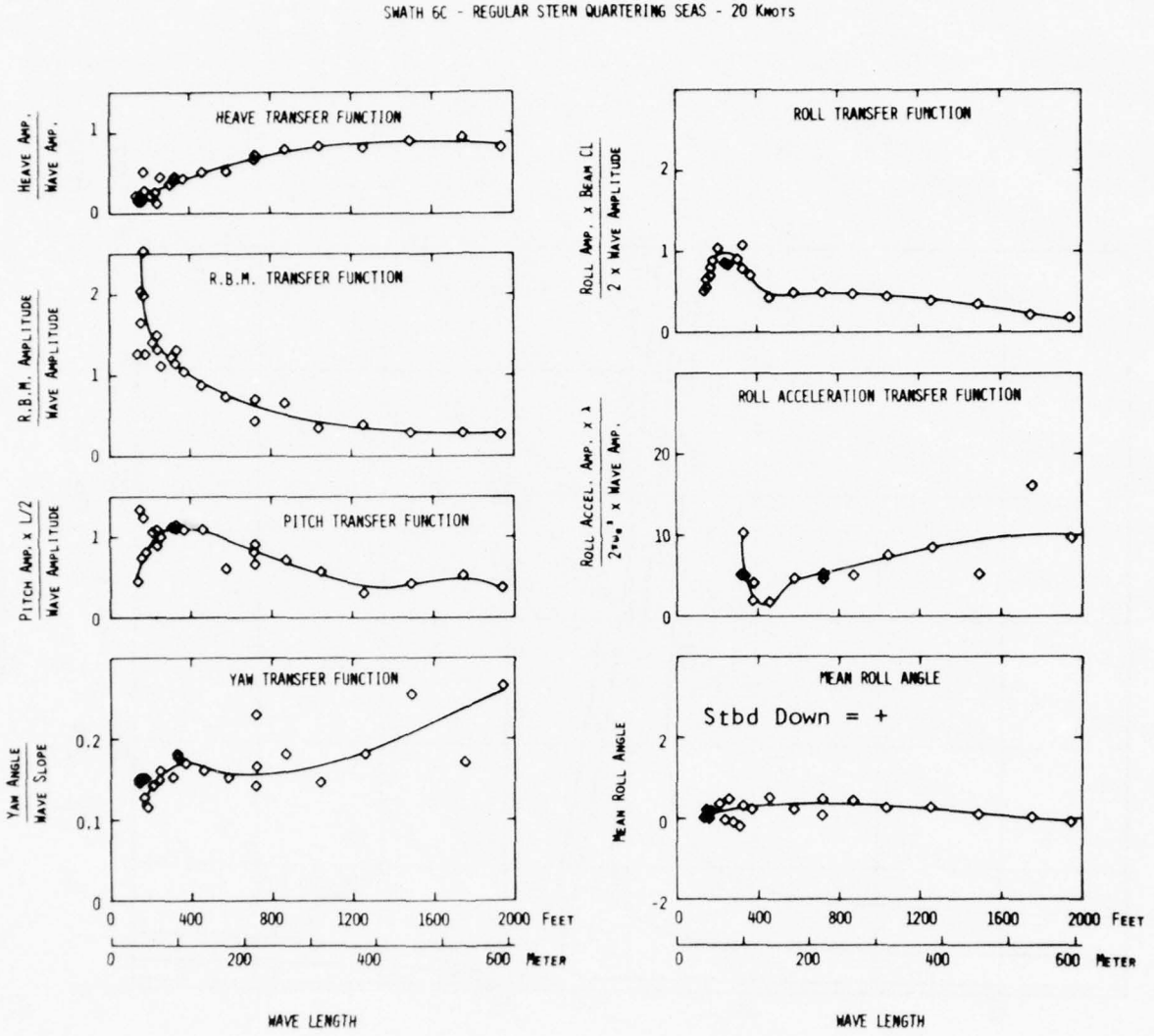

Figure 40 - Motion Transfer Functions in Regular Stern Quartering Seas for SWATH 6C - 20 Knots

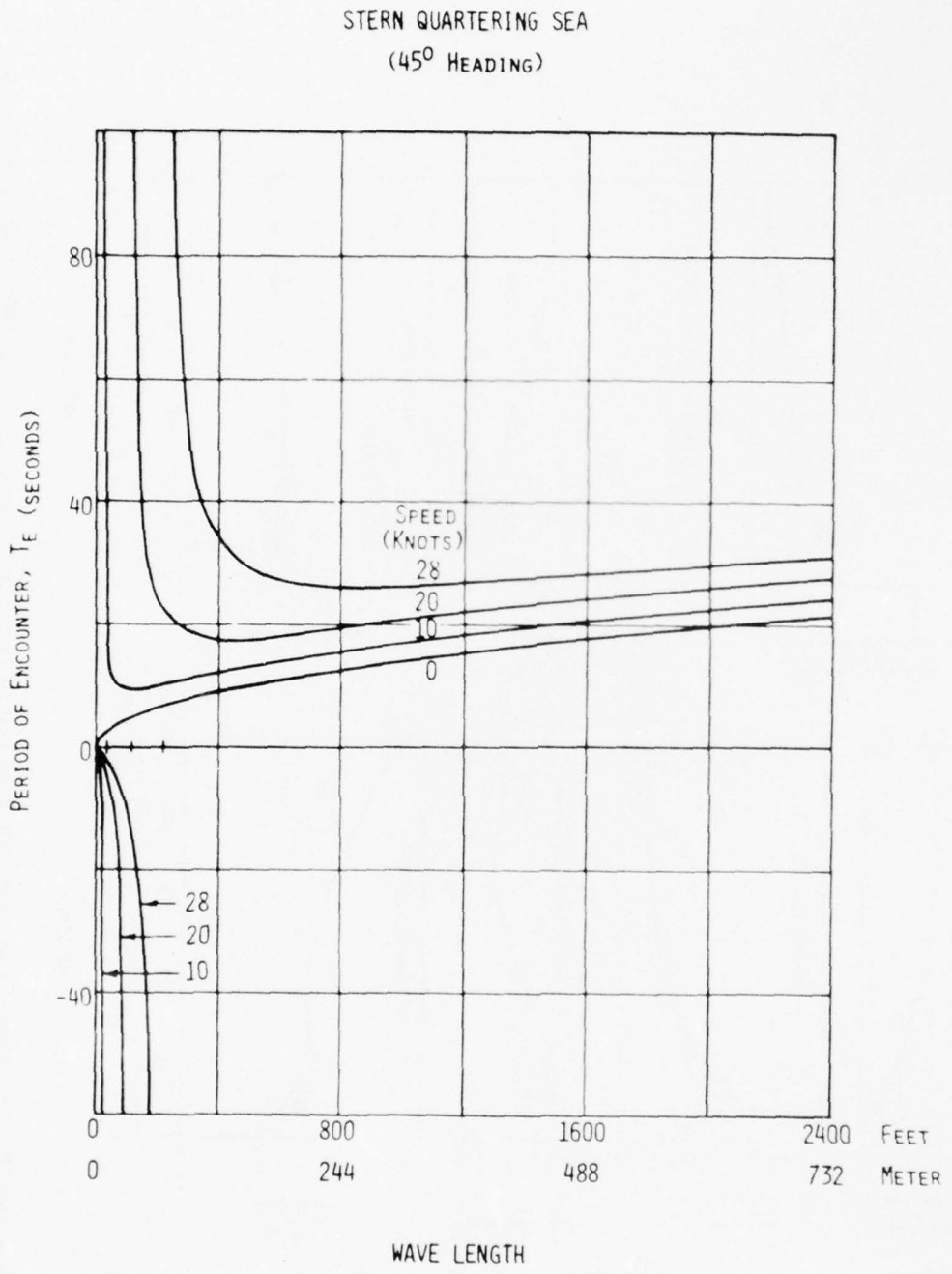

Figure 41 - Encounter Period for a Craft Traveling at Various Speeds in Regular Stern Quartering Seas

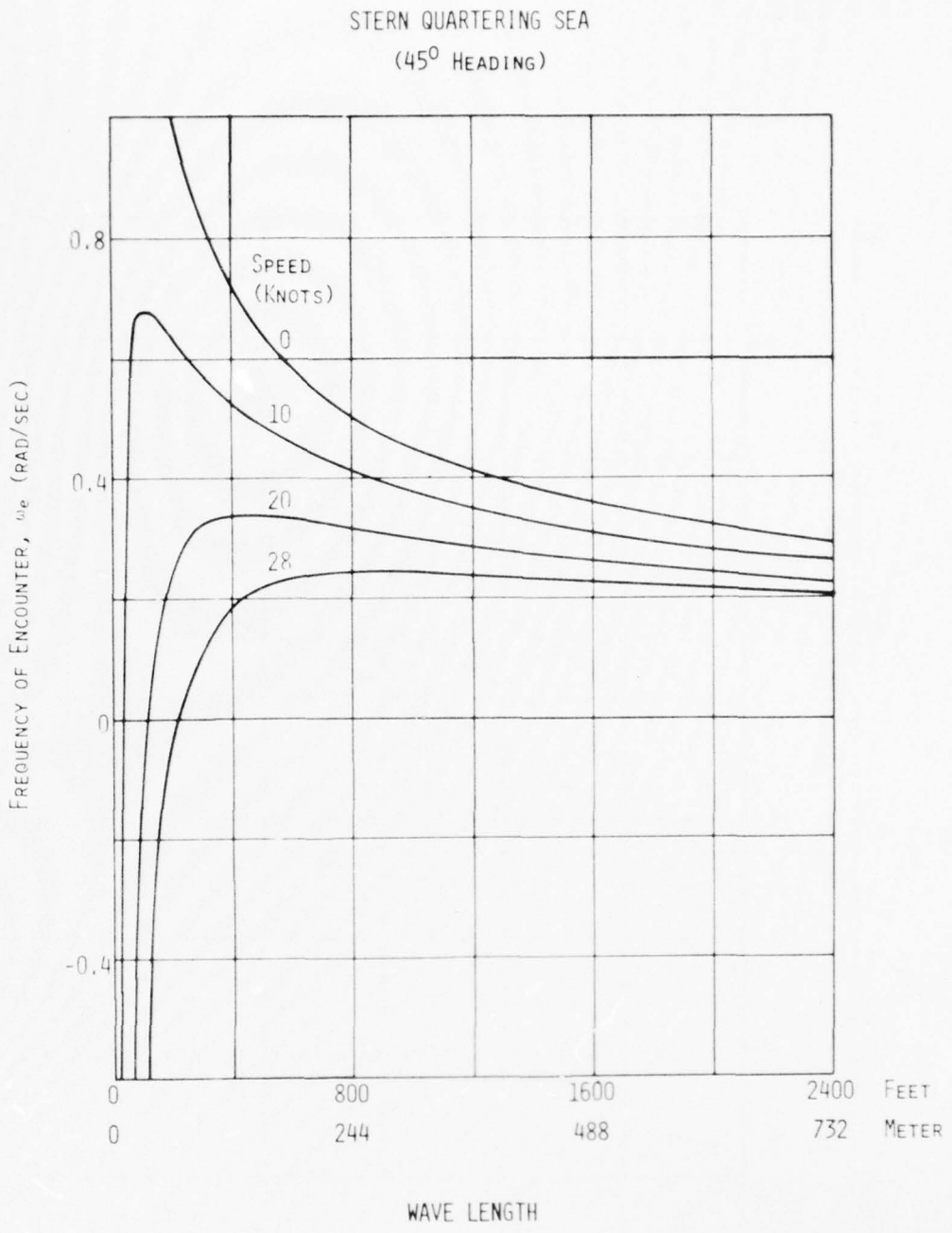

Figure 42 - Encounter Frequency for a Craft Traveling at Various Speeds in Regular Stern Quartering Seas

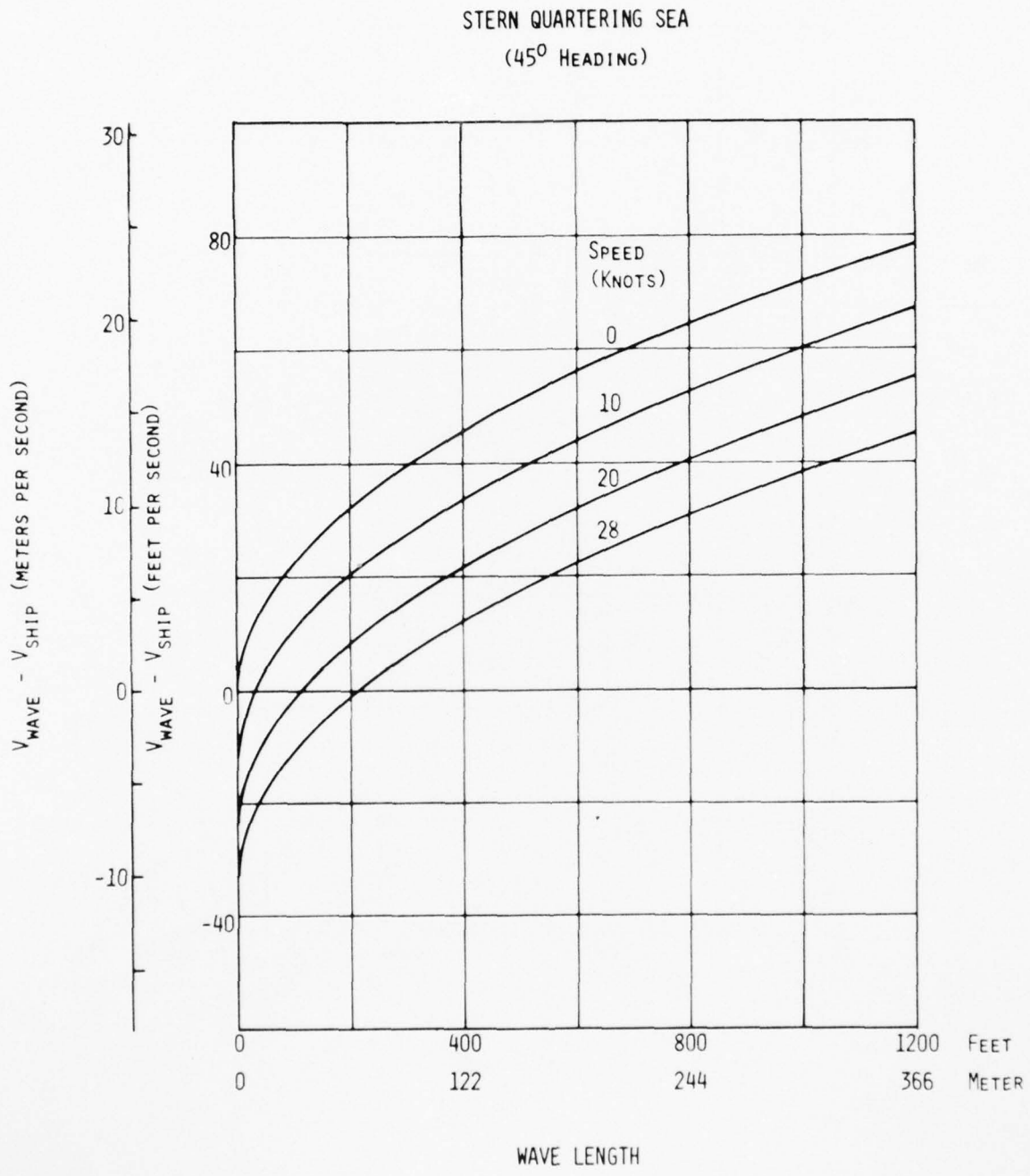

Figure 43 - Relative Velocity Between Craft and Wave for Various Speeds in Regular Stern Quartering Seas

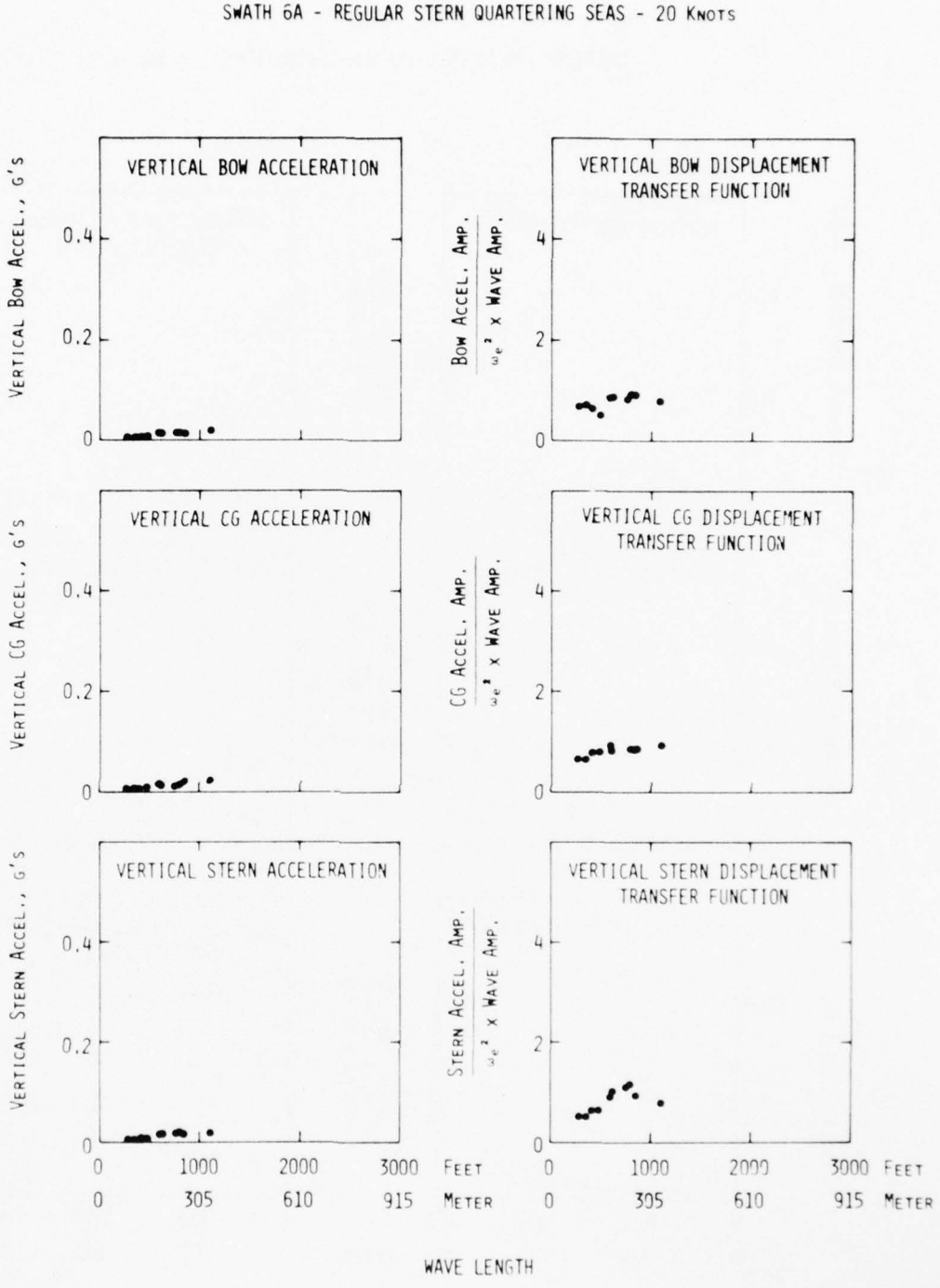

Figure 44 - Vertical Accelerations and Vertical Displacement Transfer Functions in Regular Stern Quartering Seas for SWATH 6A - 20 Knots

SWATH 6B - REGULAR STERN QUARTERING SEAS - 20 KNOTS

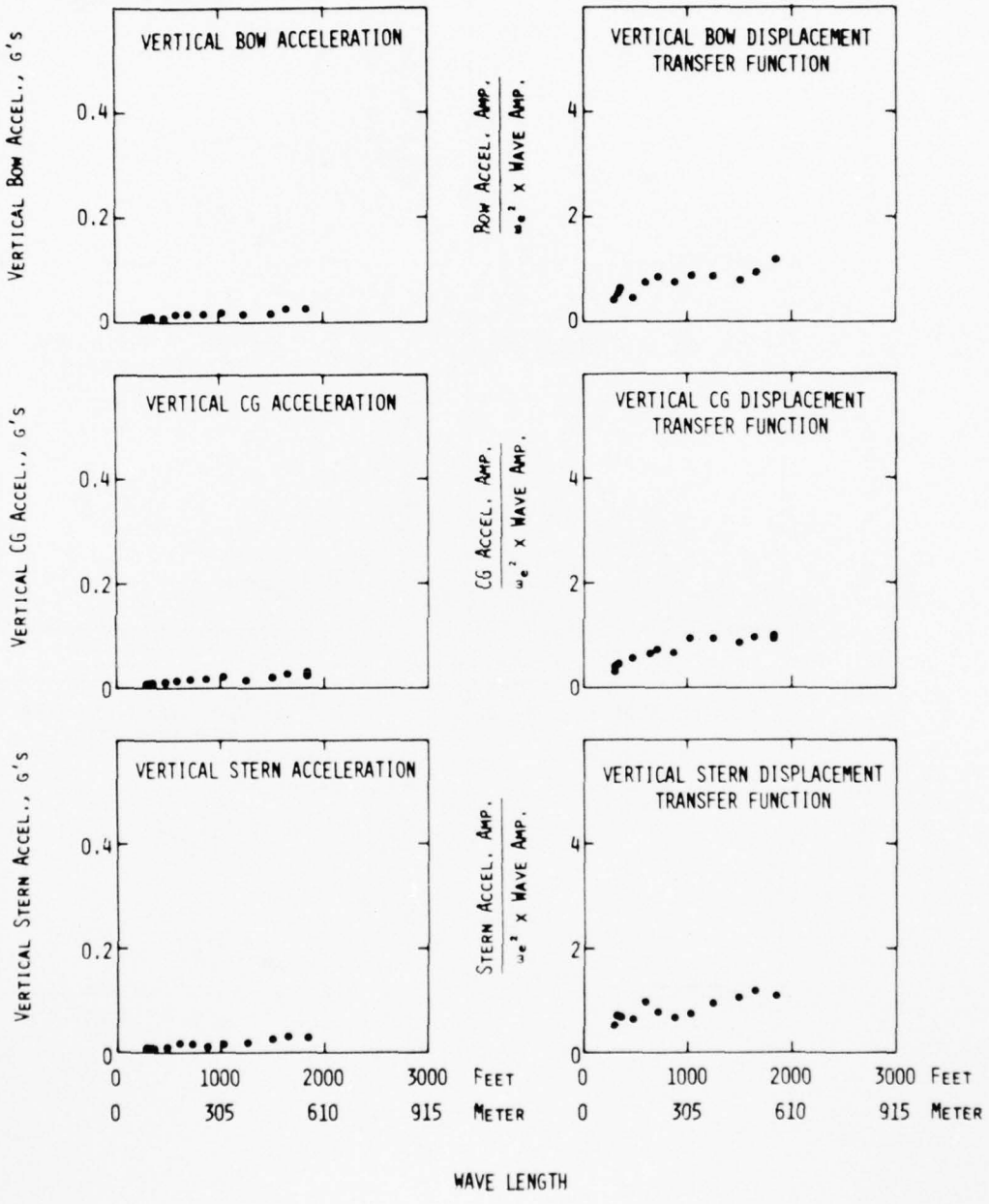

Figure 45 - Vertical Accelerations and Vertical Displacement Transfer Functions in Regular Stern Quartering Seas for SWATH 6B - 20 Knots

SWATH 6C - REGULAR STERN QUARTERING SEAS - 20 KNOTS

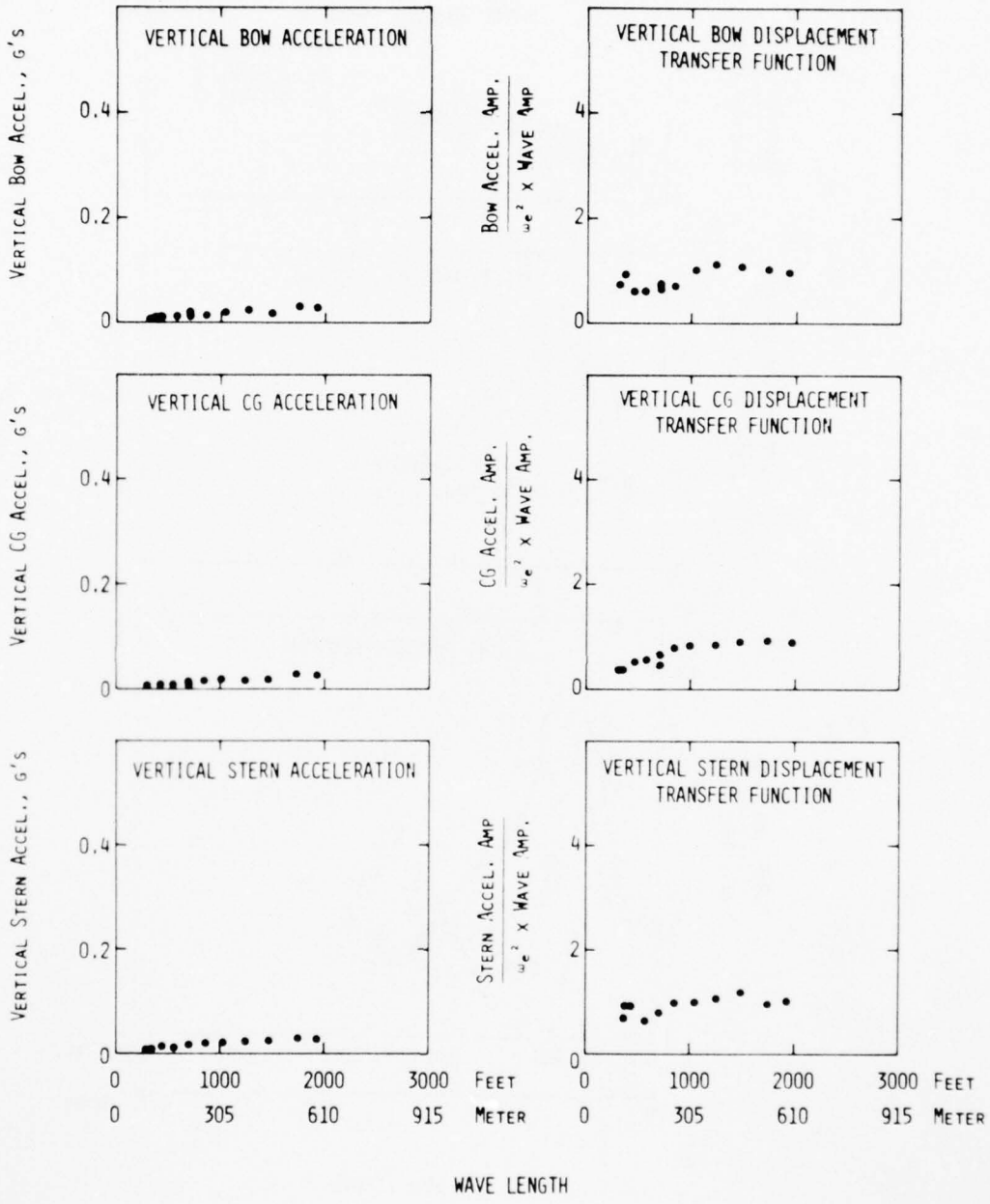

Figure 46 - Vertical Accelerations and Vertical Displacement Transfer Functions in Regular Stern Quartering Seas for SWATH 6C - 20 Knots

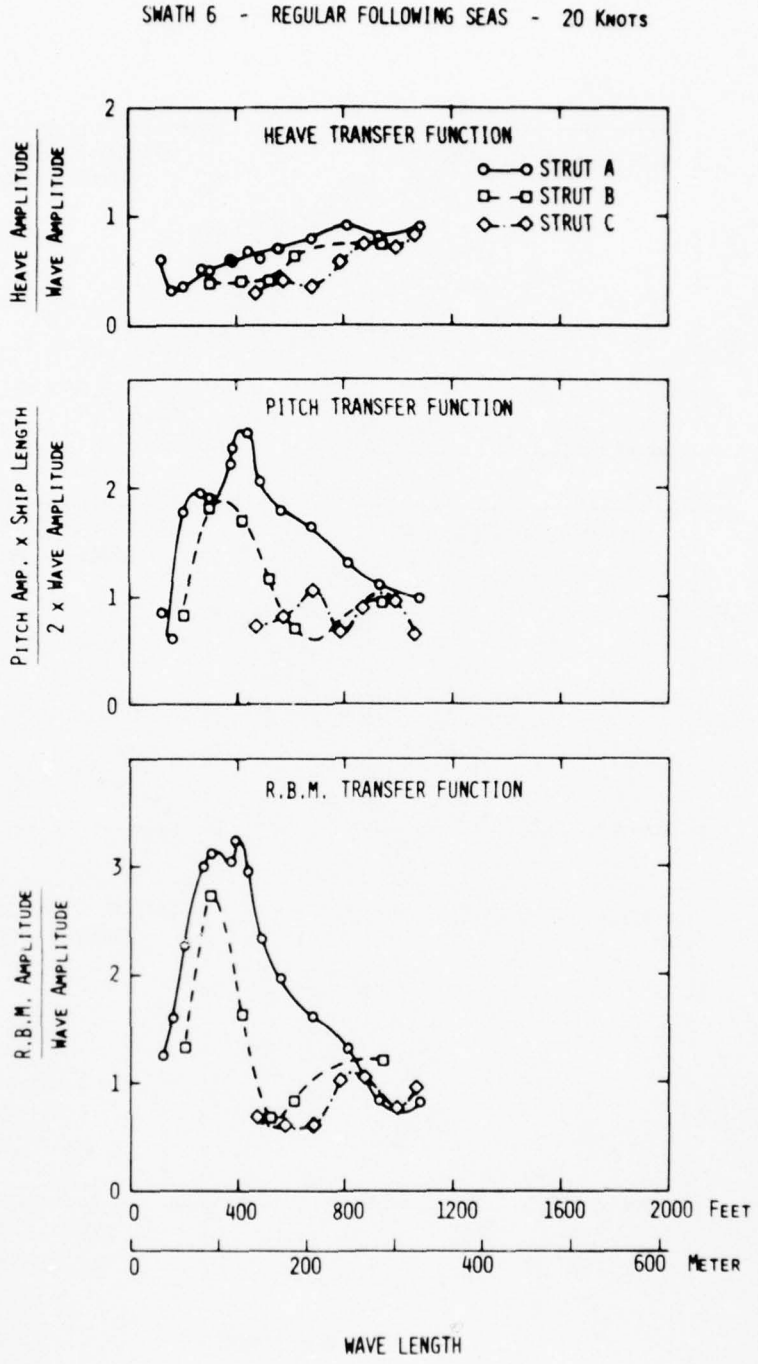

Figure 47 - Motion Transfer Functions in Regular Following Seas for SWATH 6 - 20 Knots

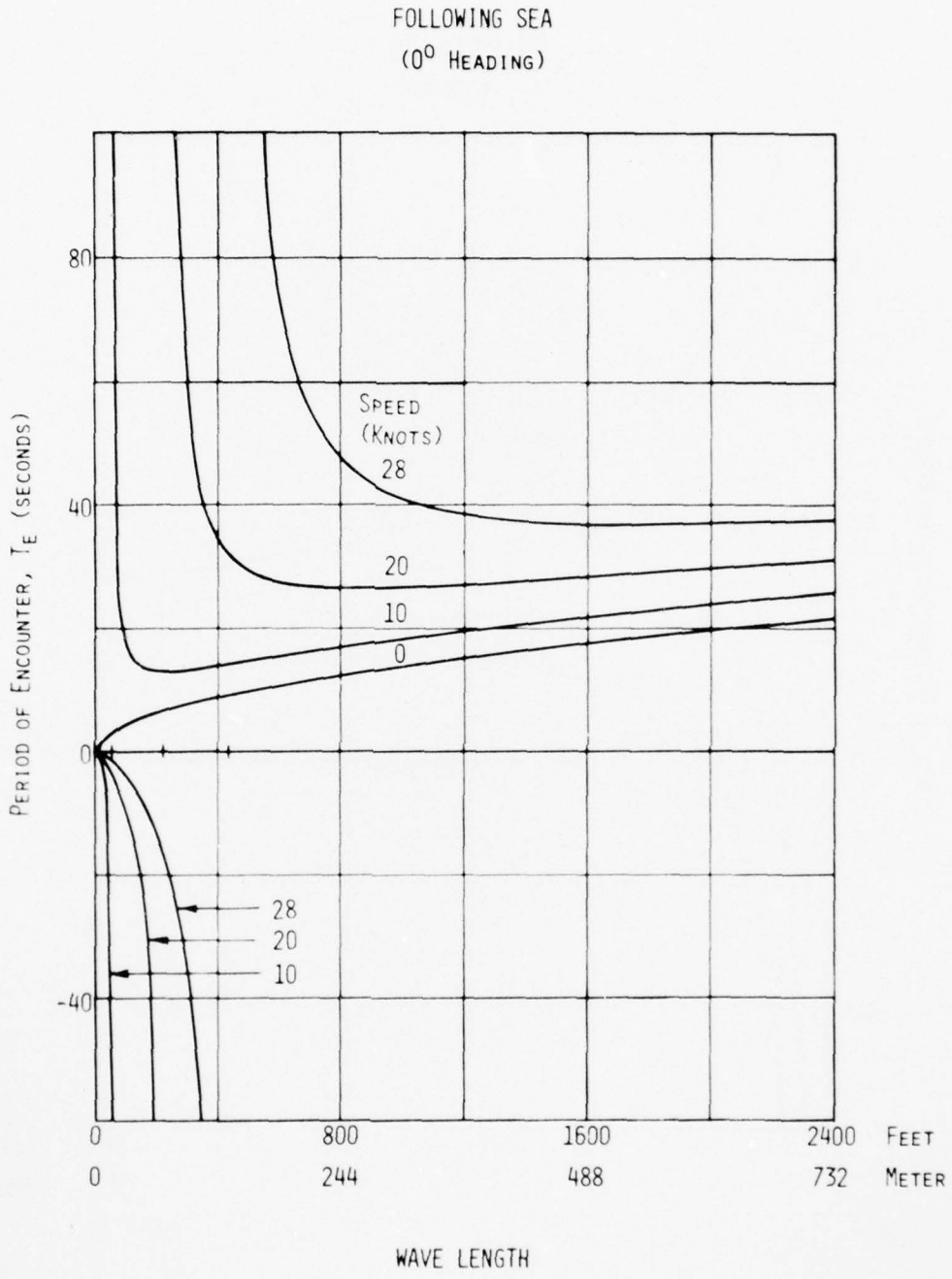

Figure 48 - Encounter Period for a Craft Traveling at Various Speeds in Regular Following Seas

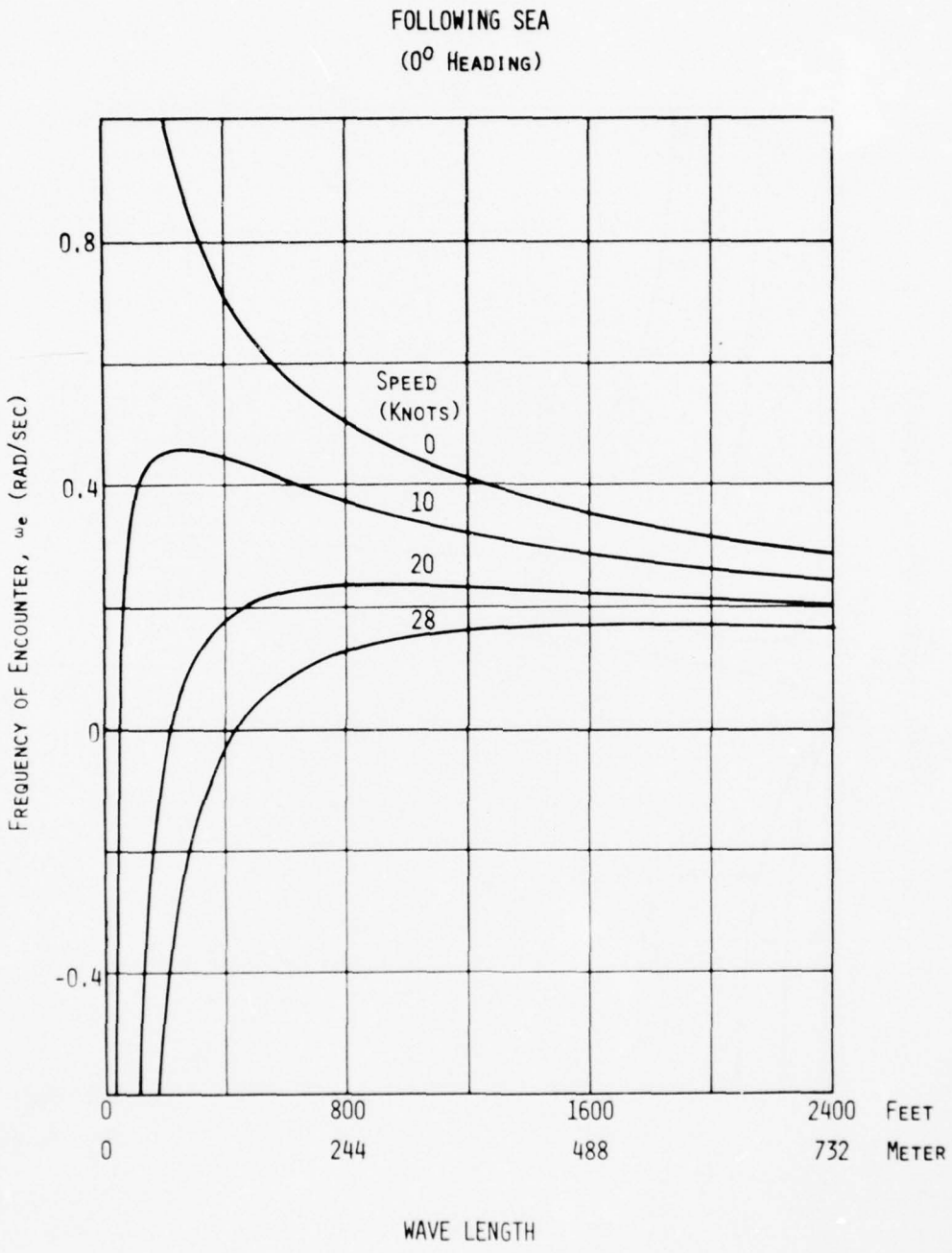

Figure 49 - Encounter Frequency for a Craft Traveling at Various Speeds in Regular Following Seas

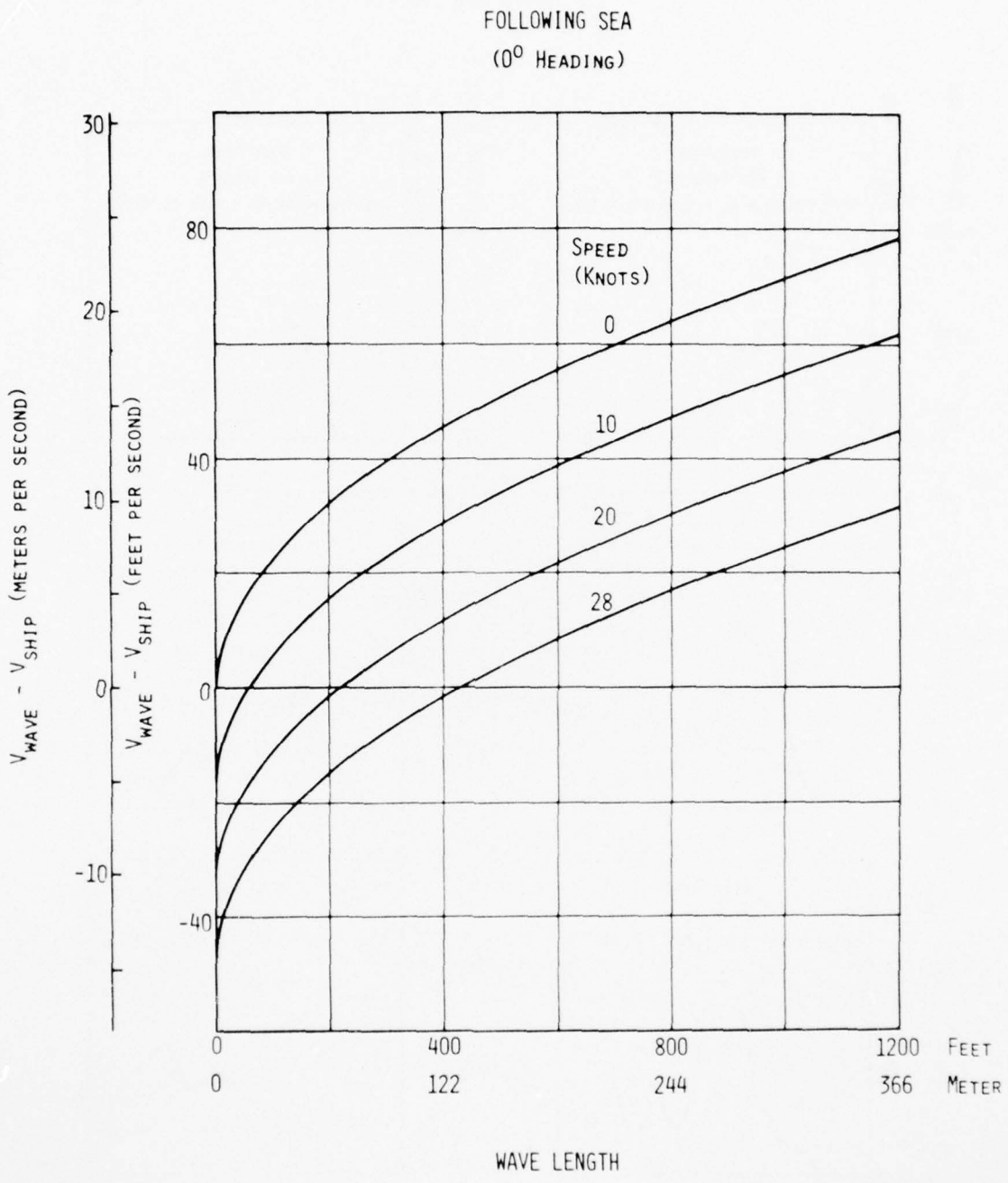

Figure 50 - Relative Velocity Between Craft and Wave for Various Speeds in Regular Following Seas

SWATH 6

ZERO SPEED WAVE SPECTRA

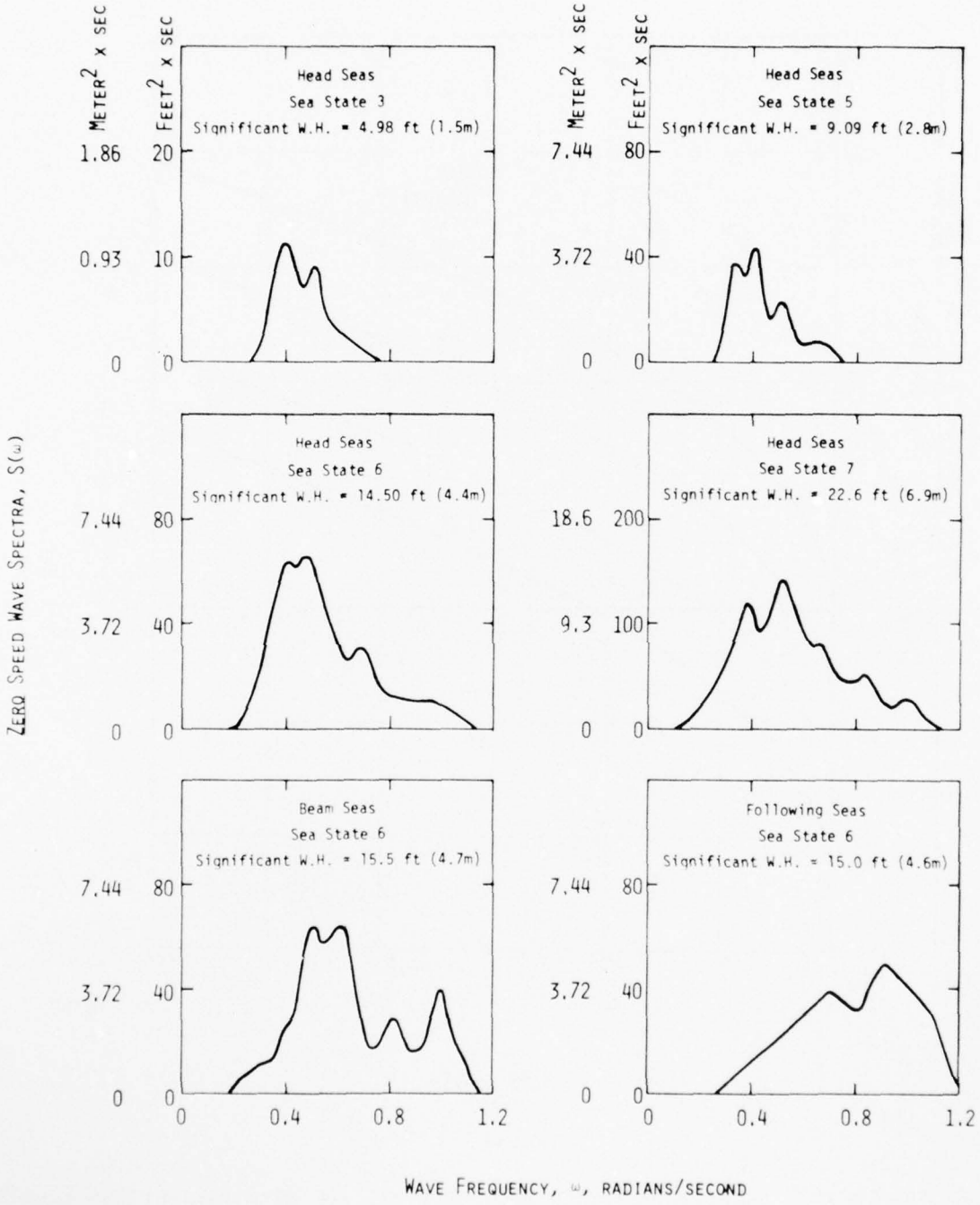

Figure 51 - Zero Speed Experimental Wave Spectra

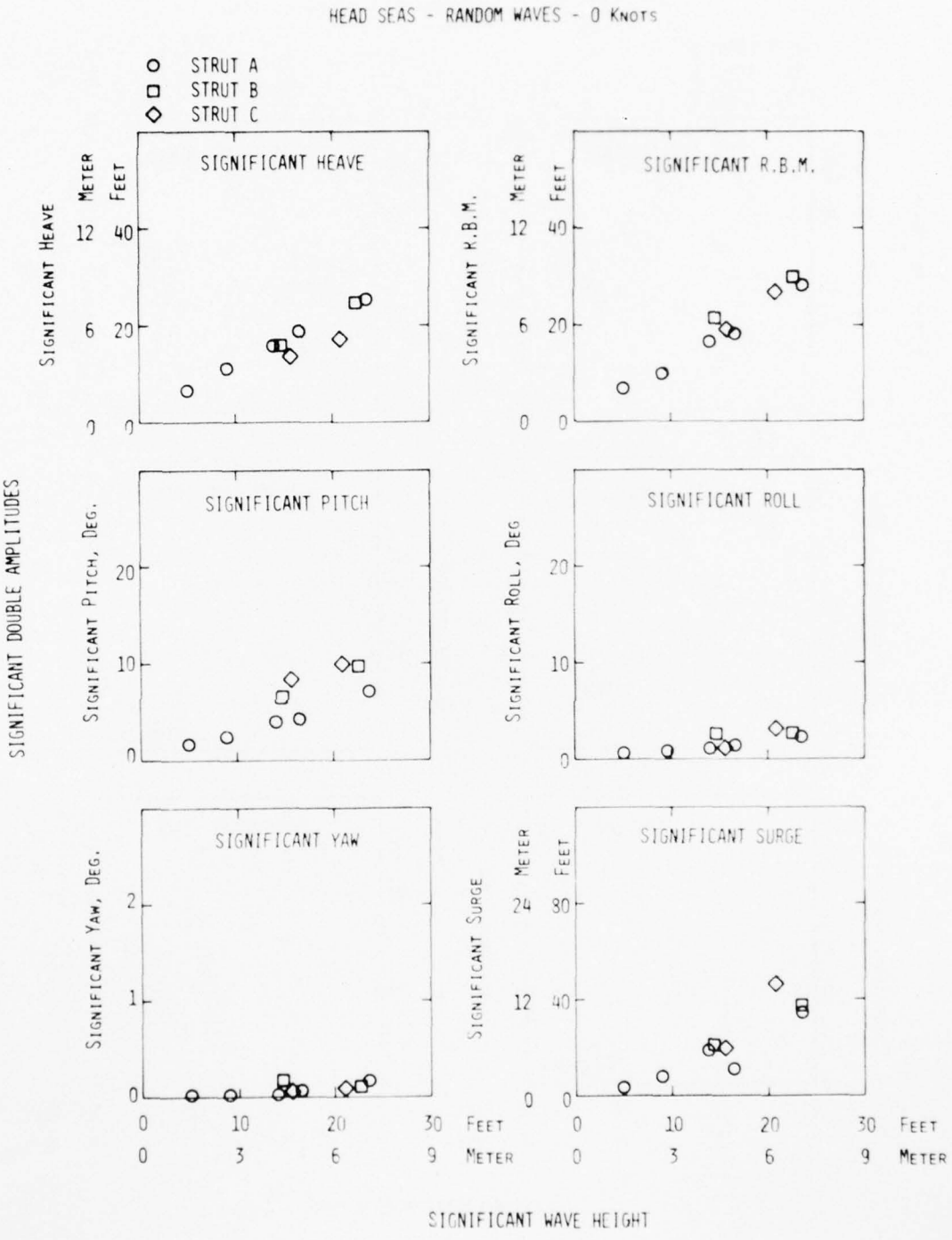

Figure 52 - Significant Double Amplitudes of Motions in Random Head Seas for SWATH 6 - 0 Knots

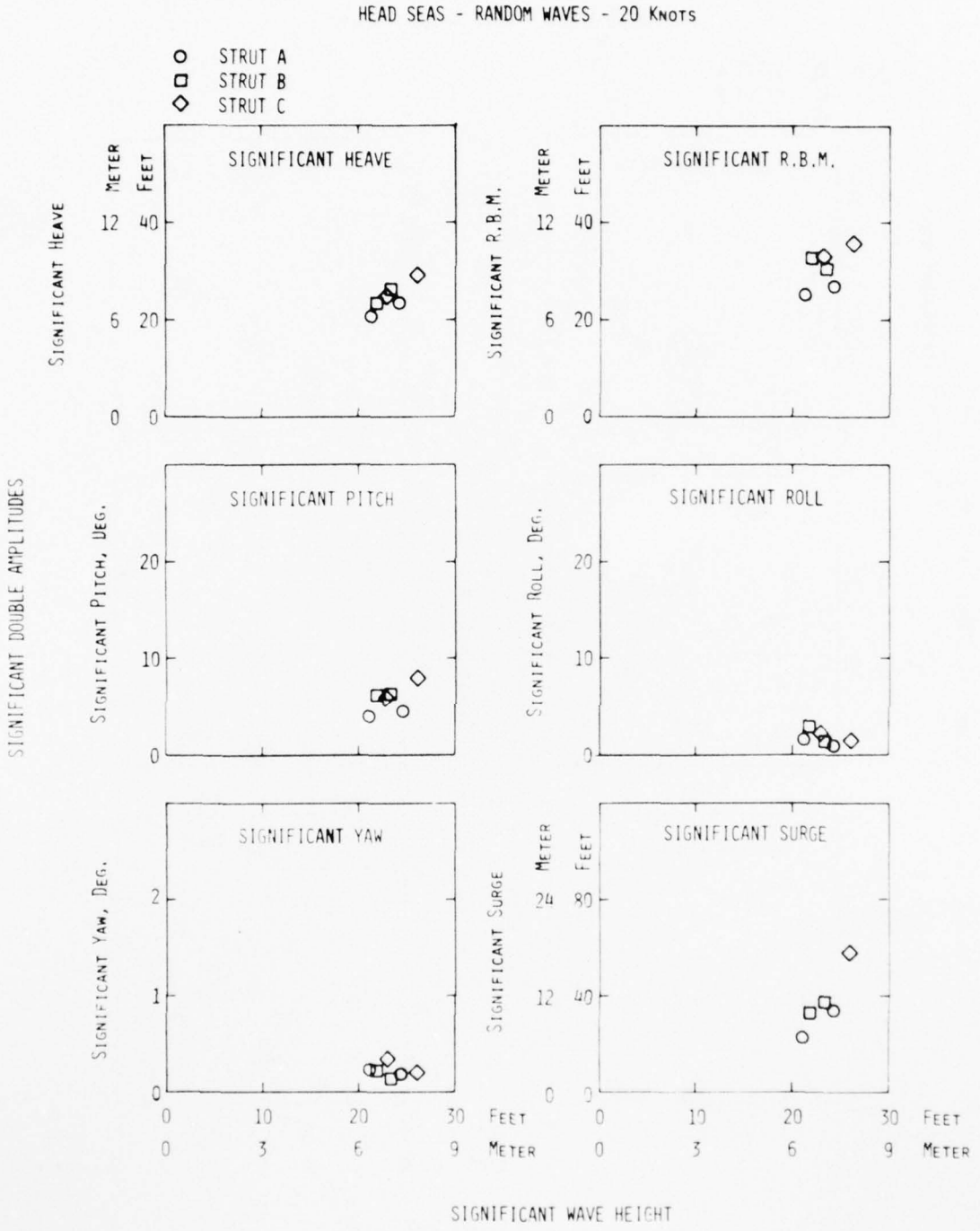

Figure 53 - Significant Double Amplitudes of Motions in Random Head Seas for SWATH 6 - 20 Knots

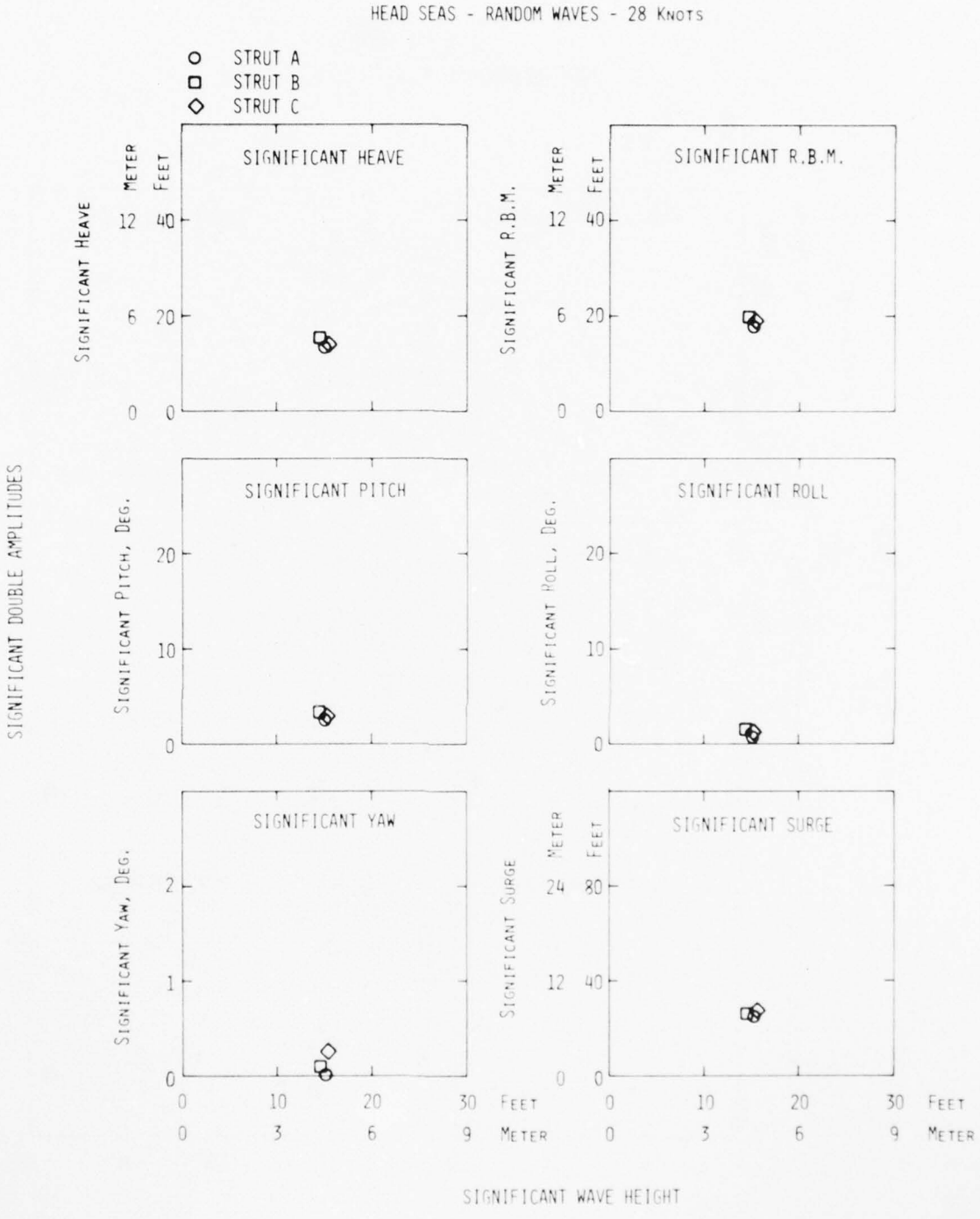

Figure 54 - Significant Double Amplitudes of Motions in Random Head Seas for SWATH 6 - 28 Knots

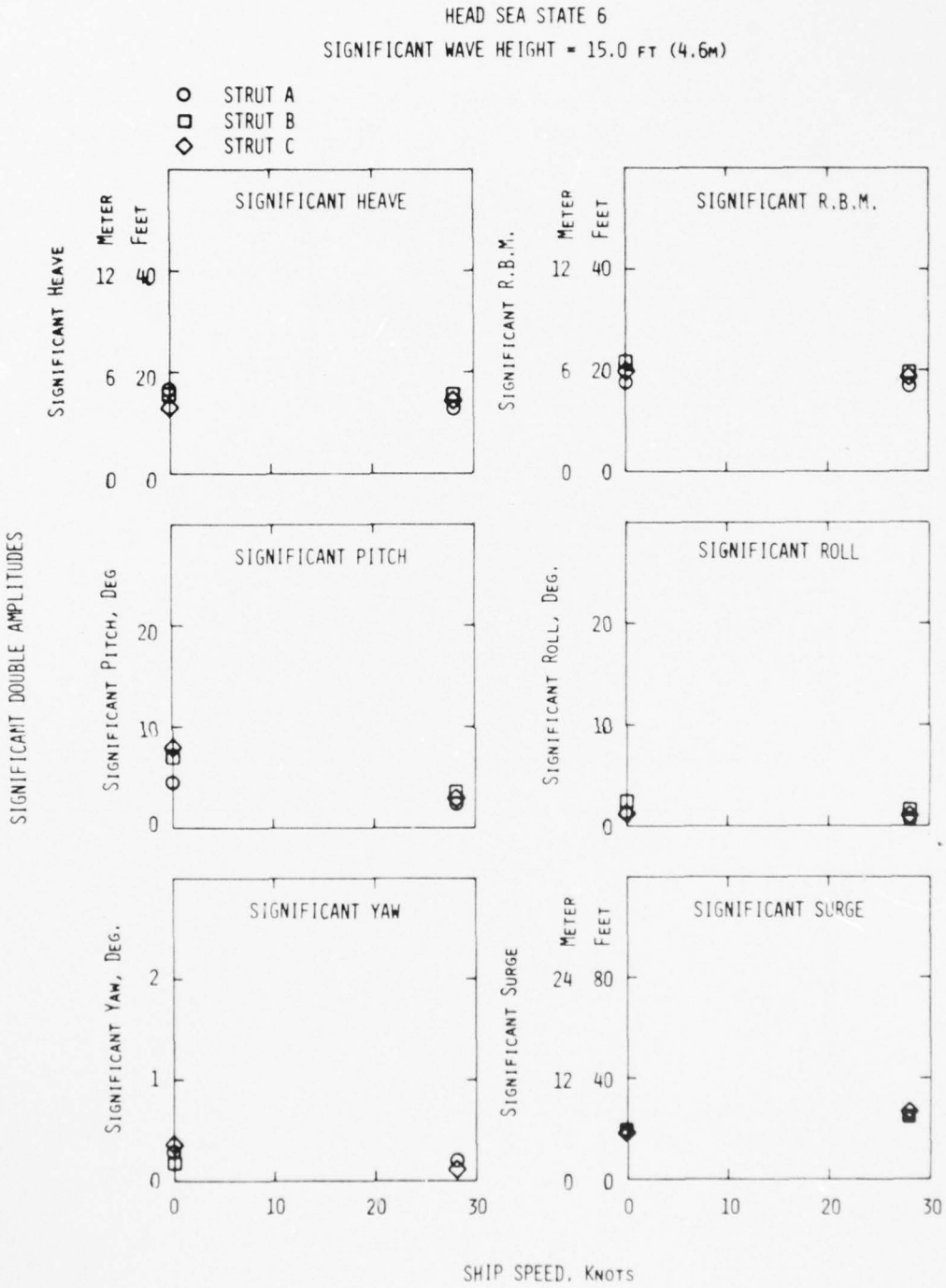

Figure 55 - Significant Double Amplitudes of Motions in Head Sea State 6 for SWATH 6

AD-A044 261 DAVID W TAYLOR NAVAL SHIP RESEARCH AND DEVELOPMENT CE--ETC F/G 1/3
SEAWORTHINESS CHARACTERISTICS OF A 2900 TON SMALL WATERPLANE AR--ETC(U)
SEP 76 J A KALLIO

UNCLASSIFIED SPD-620-03 NL

2 OF 2
ADA
044261

END
DATE
FILMED
10-77
DDC

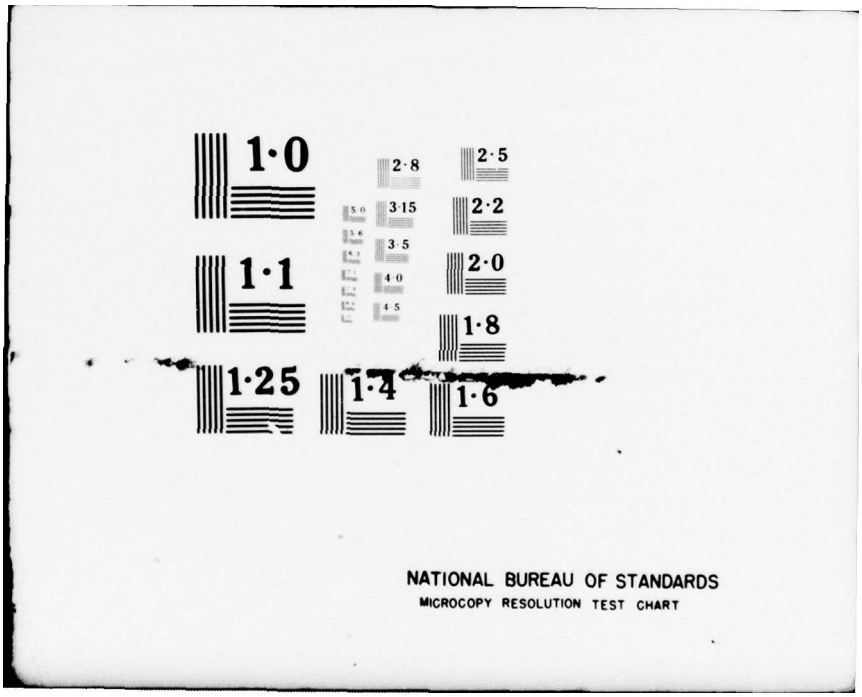
1·0
1·1
1·25
1·4
1·6
1·8
2·0
2·2
2·5
2·8
3·15
3·5
4·0
4·5
5·0
5·6
NATIONAL BUREAU OF STANDARDS
MICROCOPY RESOLUTION TEST CHART

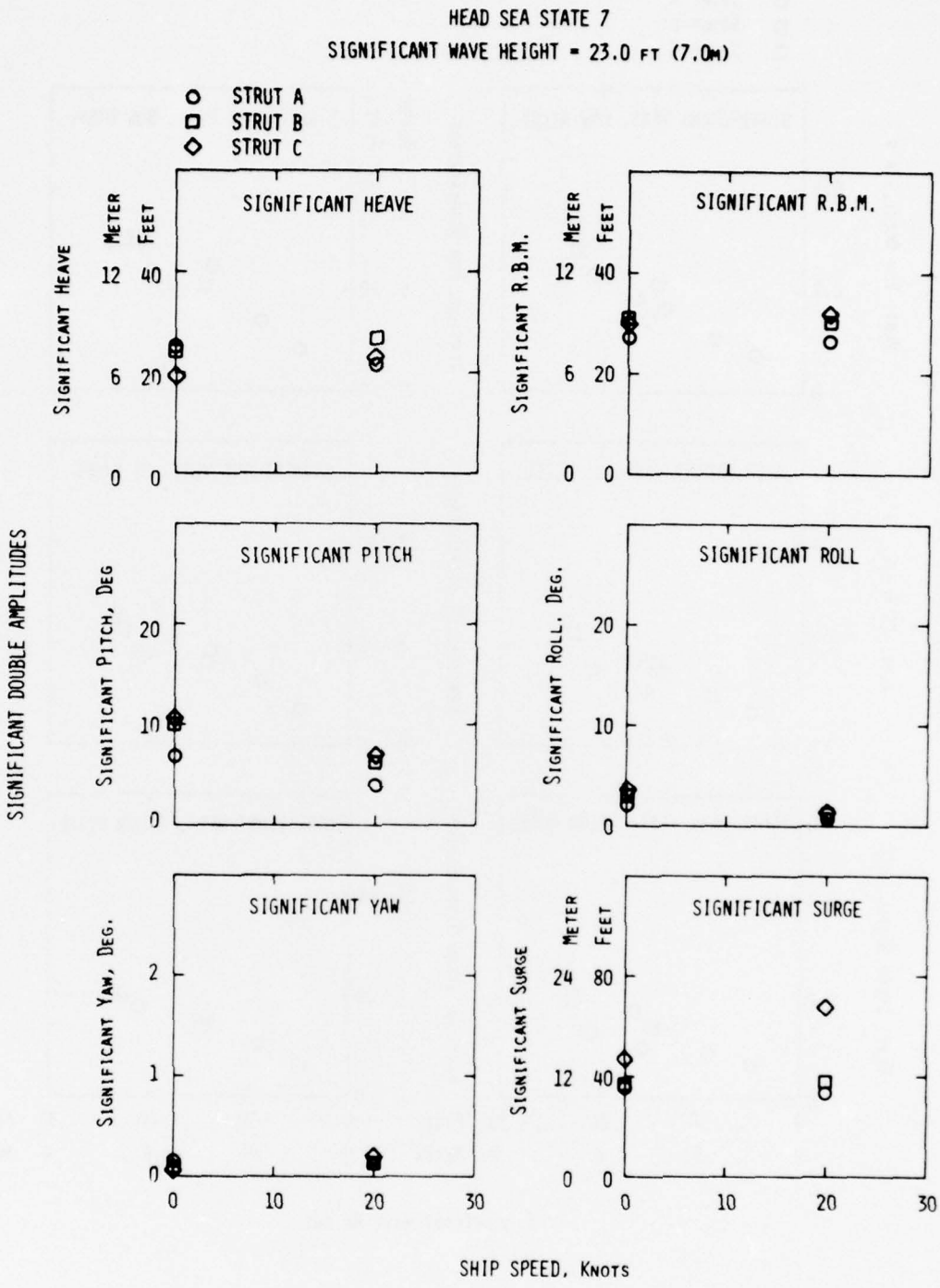

Figure 56 - Significant Double Amplitudes of Motions in Head Sea State 7 for SWATH 6

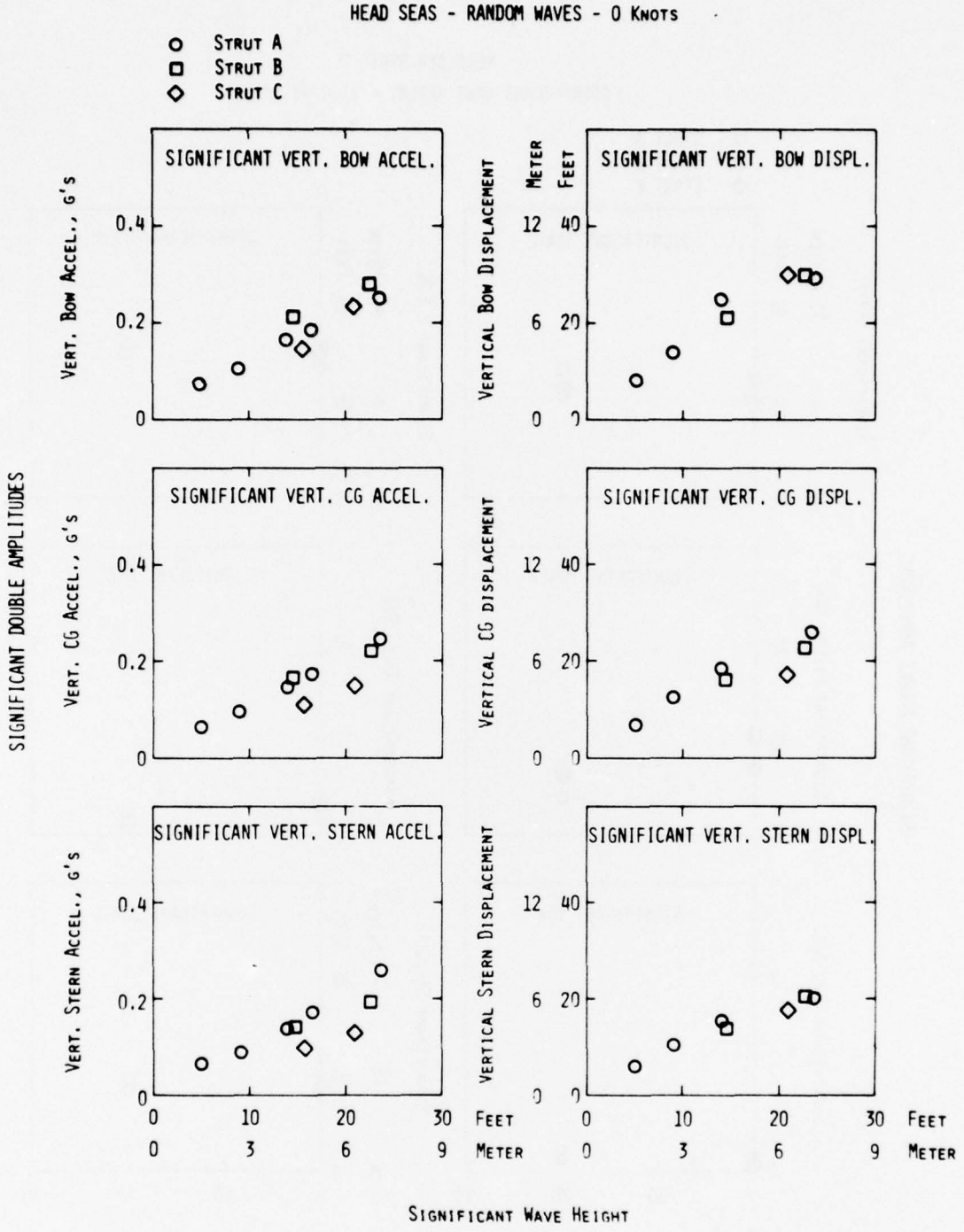

Figure 57 - Significant Double Amplitudes of Vertical Accelerations and Vertical Motions in Random Head Seas for SWATH 6 - 0 Knots

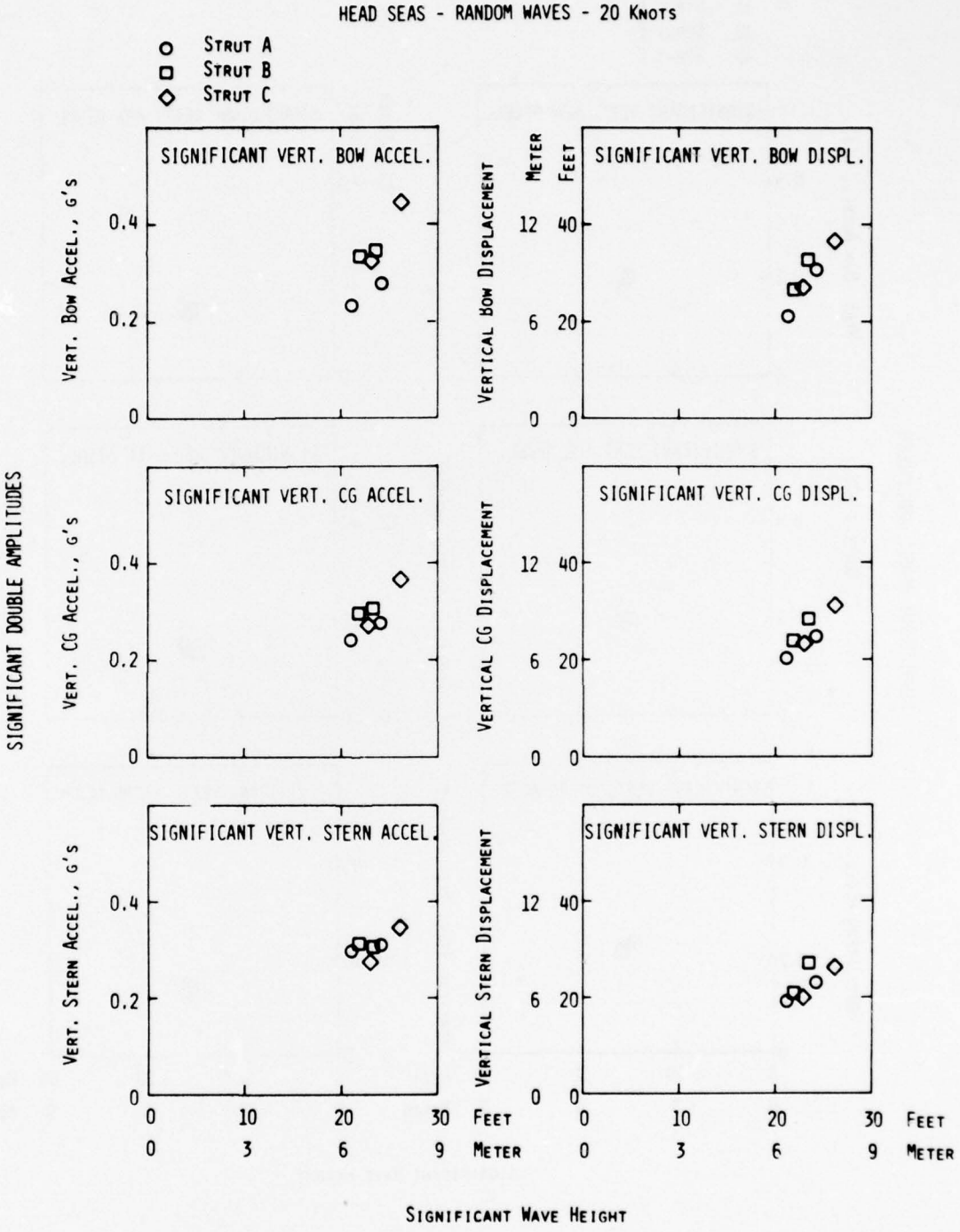

Figure 58 - Significant Double Amplitudes of Vertical Accelerations and Vertical Motions in Random Head Seas for SWATH 6 - 20 Knots

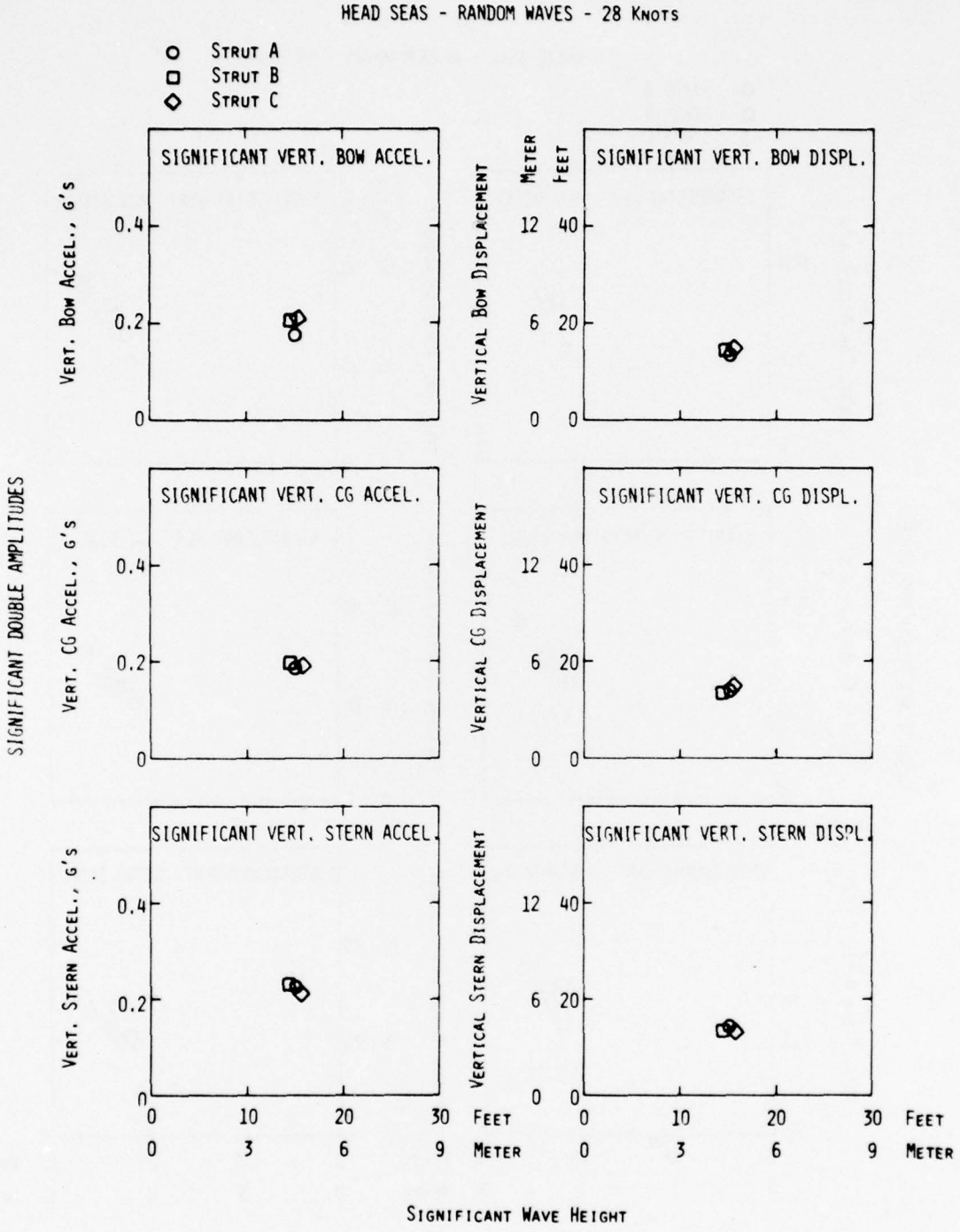

Figure 59 - Significant Double Amplitudes of Vertical Accelerations and Vertical Motions in Random Head Seas for SWATH 6 - 28 Knots

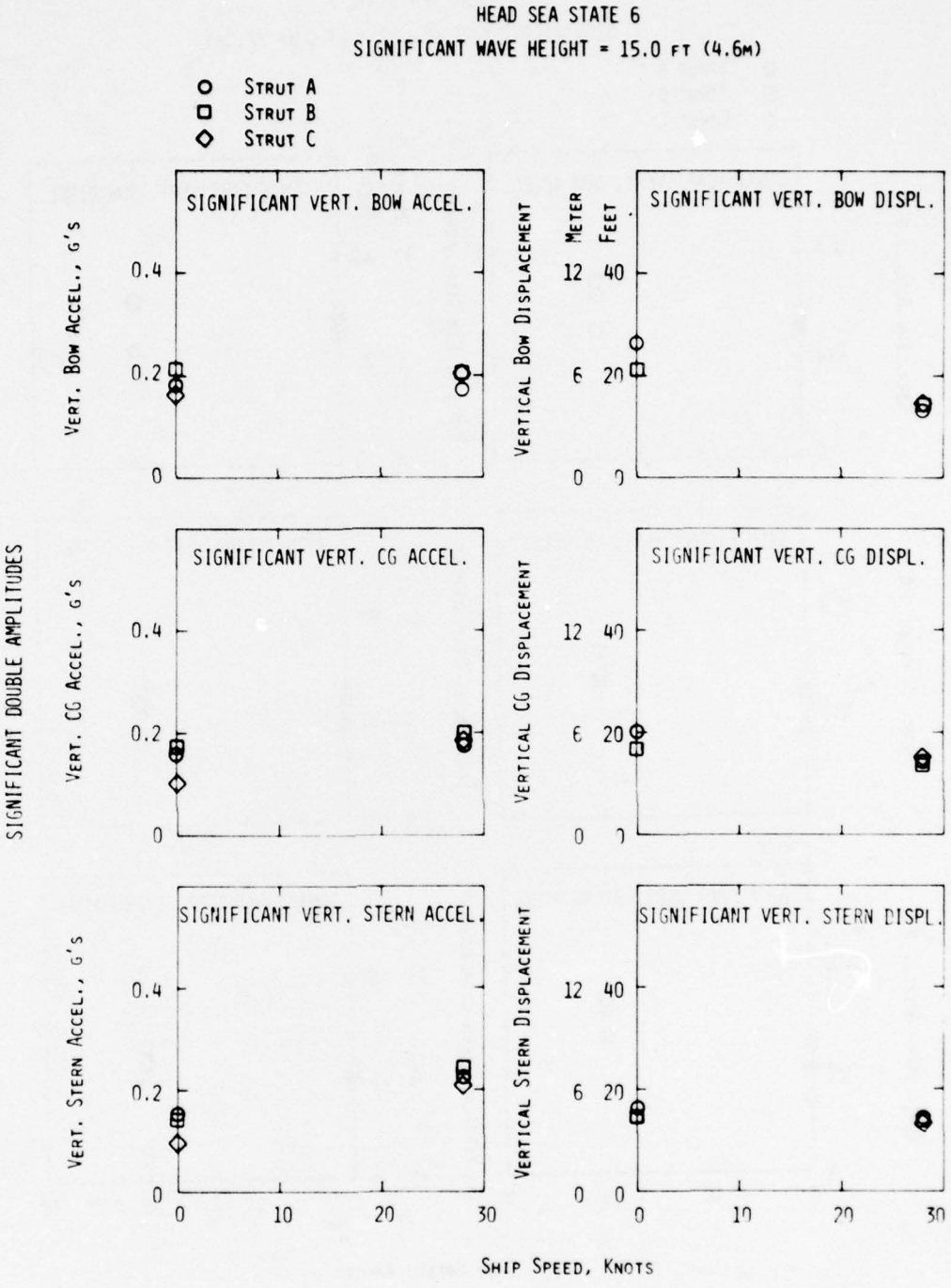

Figure 60 - Significant Double Amplitudes of Vertical Accelerations and Vertical Motions in Head Sea State 6 for SWATH 6

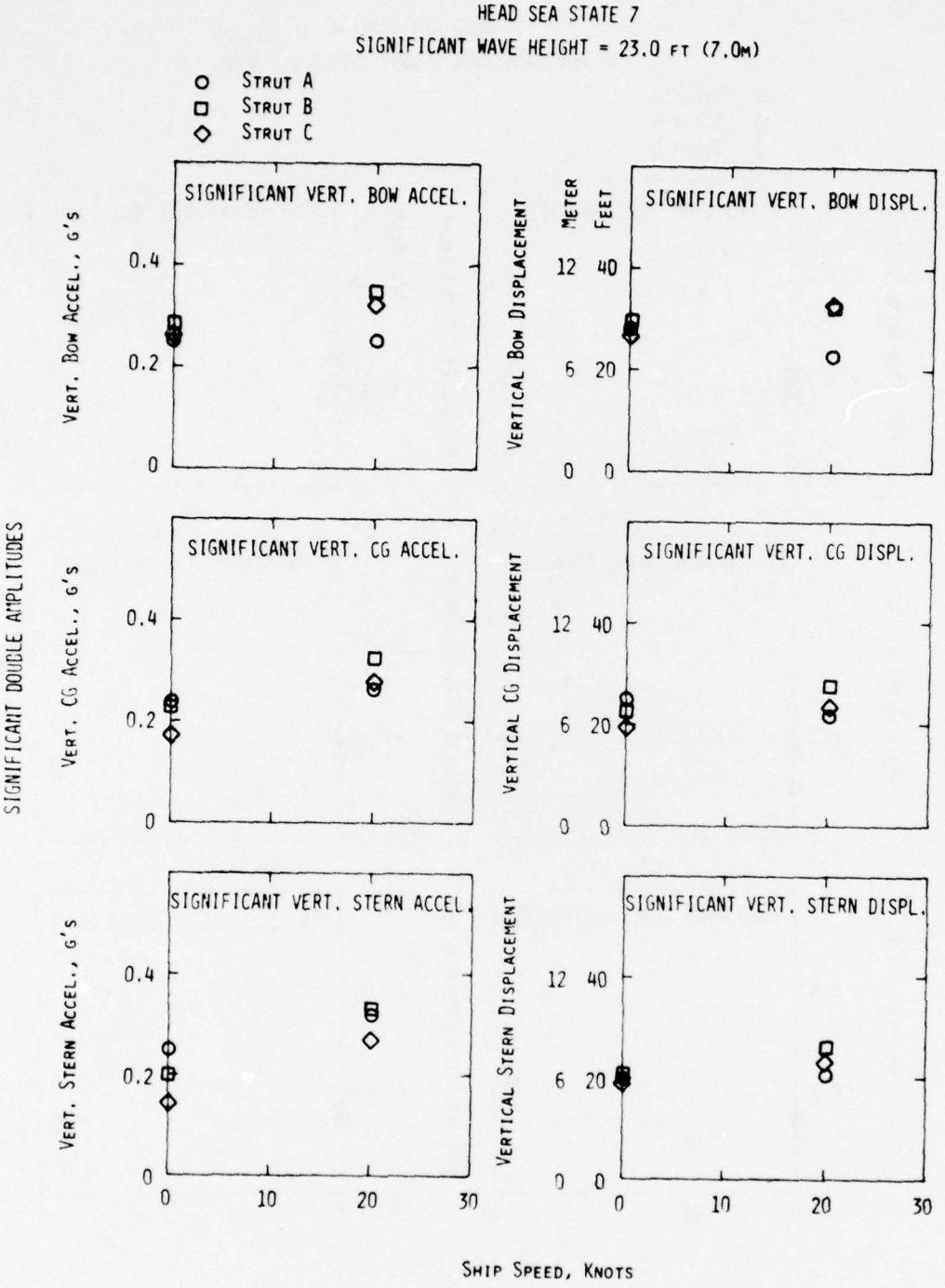

Figure 61 - Significant Double Amplitudes of Vertical Accelerations and Vertical Motions in Head Sea State 7 for SWATH 6

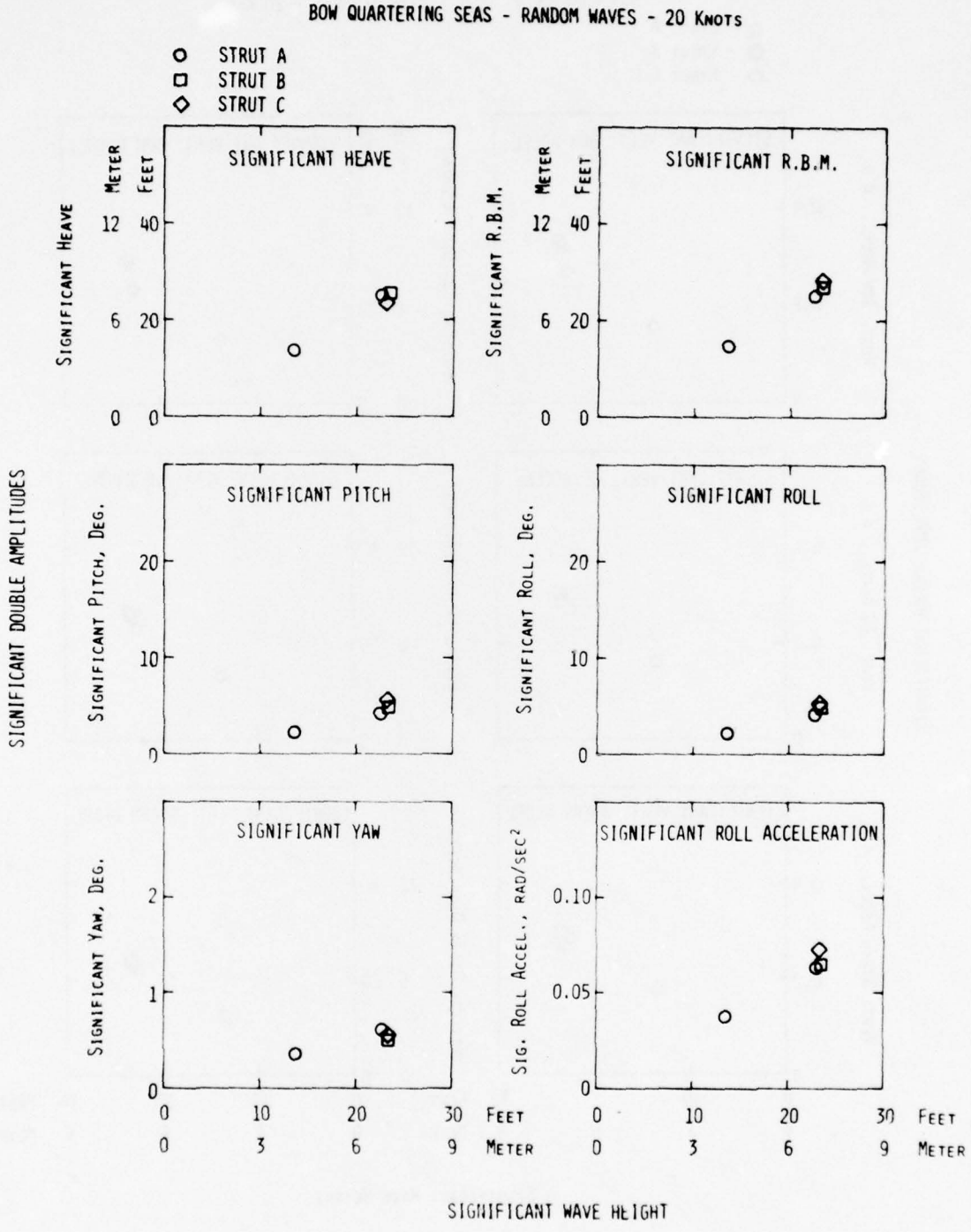

Figure 71 - Significant Double Amplitudes of Motions in Random Bow Quartering Seas for SWATH 6 - 20 Knots

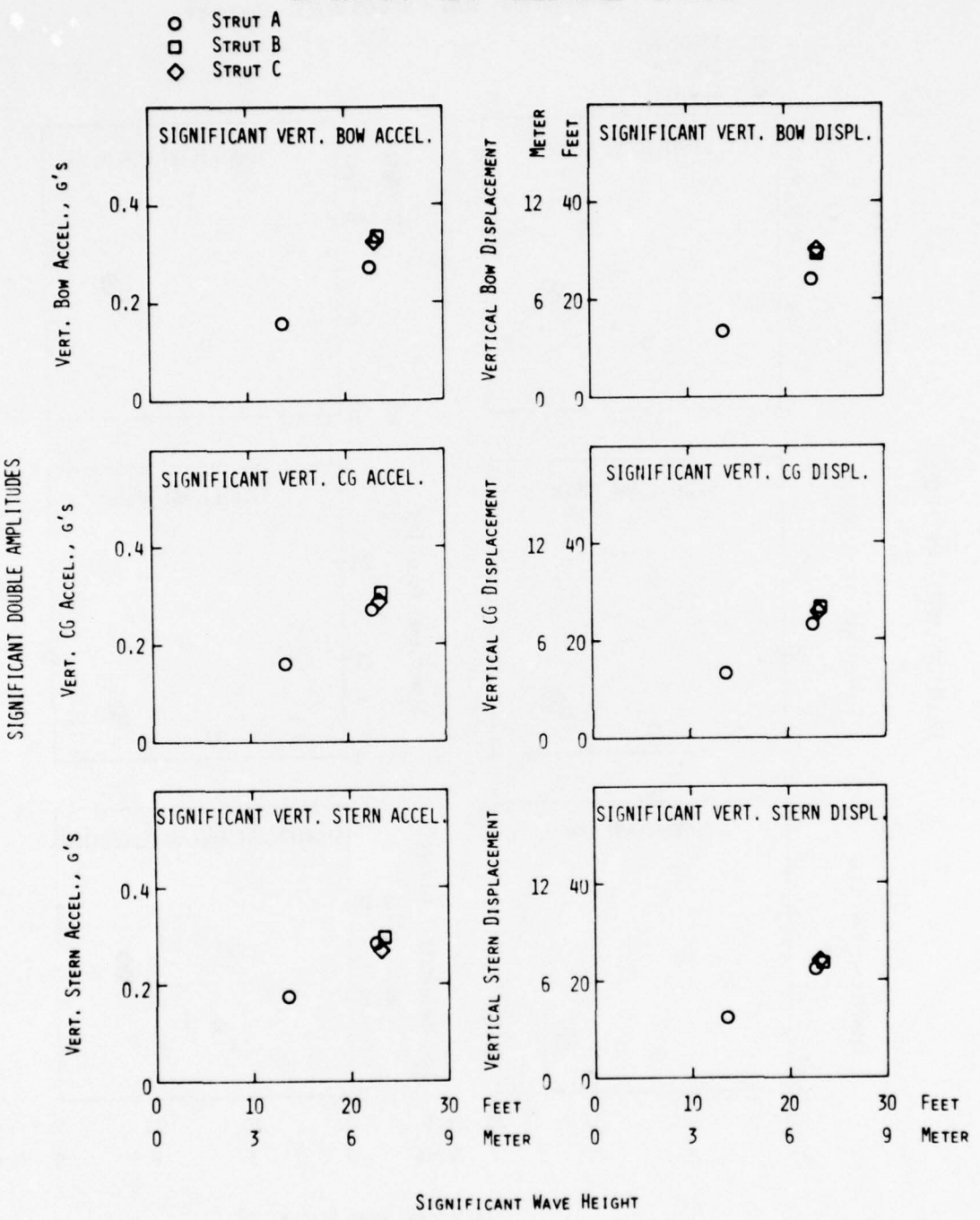

Figure 72 - Significant Double Amplitudes of Vertical Accelerations and Vertical Motions in Random Bow Quartering Seas for SWATH 6 - 20 Knots

HEAD SEAS - RANDOM WAVES - 20 KNOTS

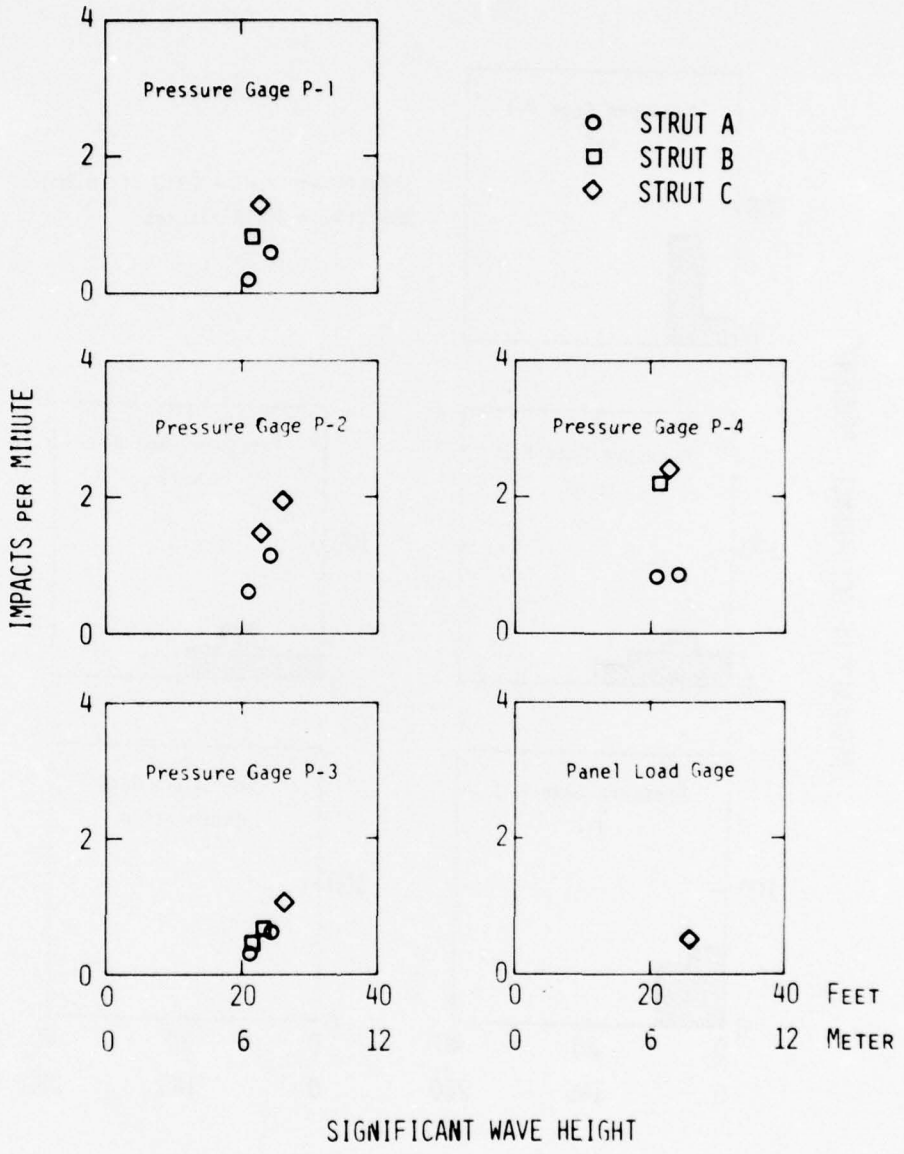

Figure 62 - Frequency of Impacting in Random Head Seas for SWATH 6
20 Knots

SWATH 6A - HEAD SEA STATE 7 - 20 KNOTS

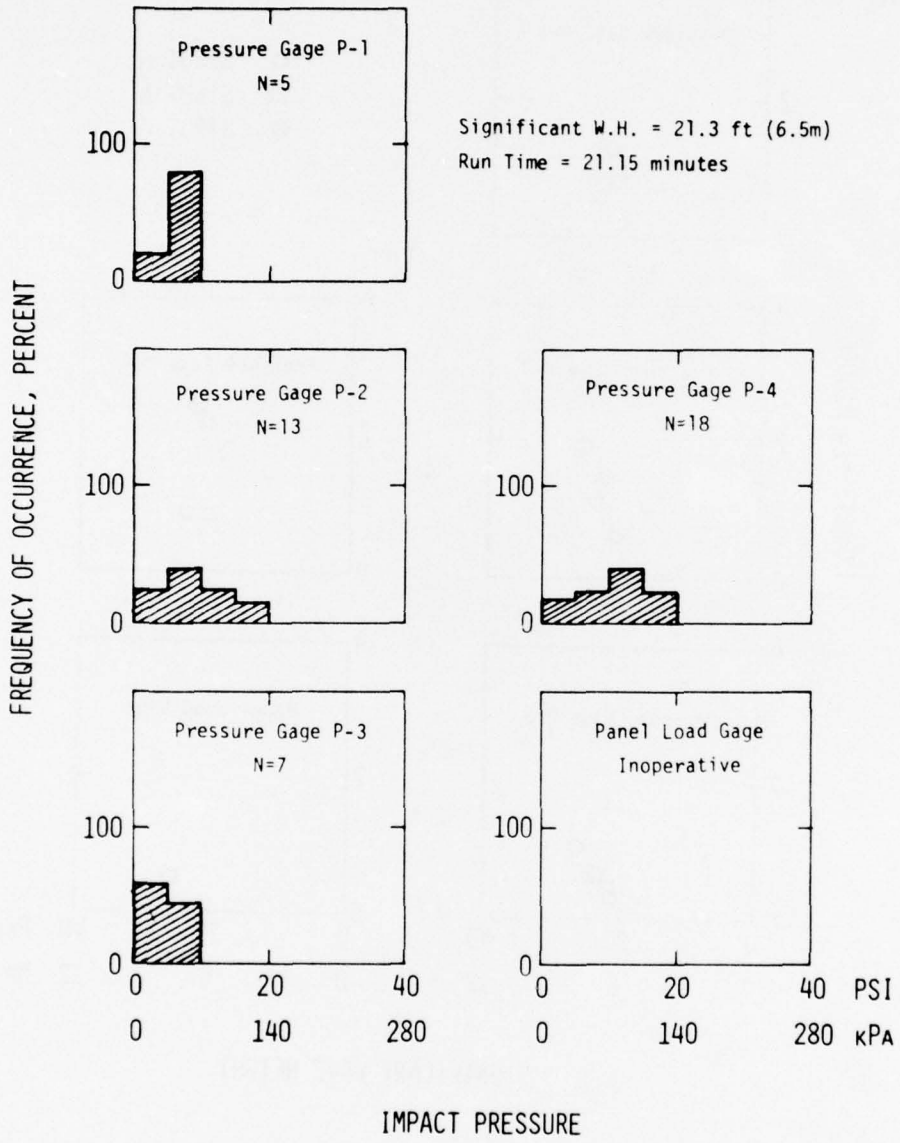

Figure 63 - Impact Pressure Histograms for SWATH 6A in Head Sea State 7 - 20 Knots

SWATH 6B - HEAD SEA STATE 7 - 20 KNOTS

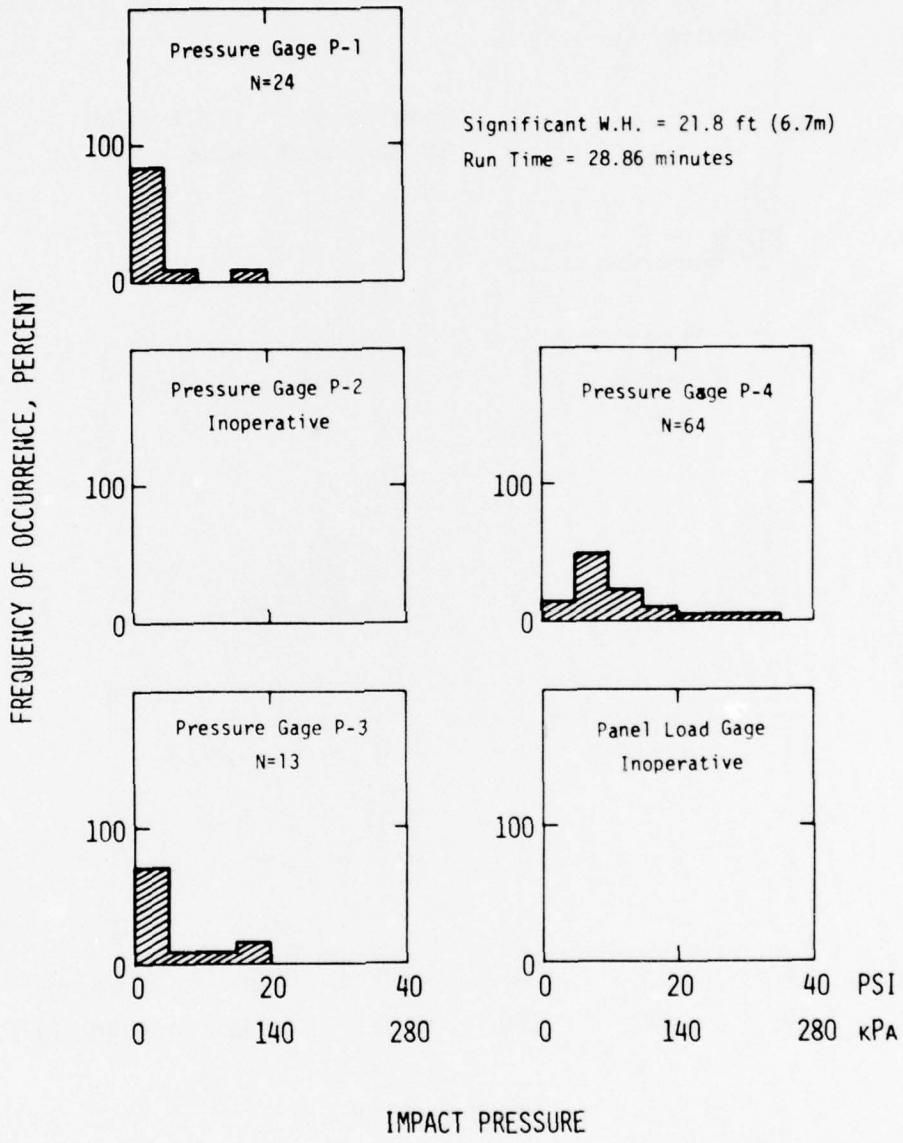

Figure 64 - Impact Pressure Histograms for SWATH 6B in Head Sea State 7 - 20 Knots

SWATH 6C - HEAD SEA STATE 7 - 20 KNOTS

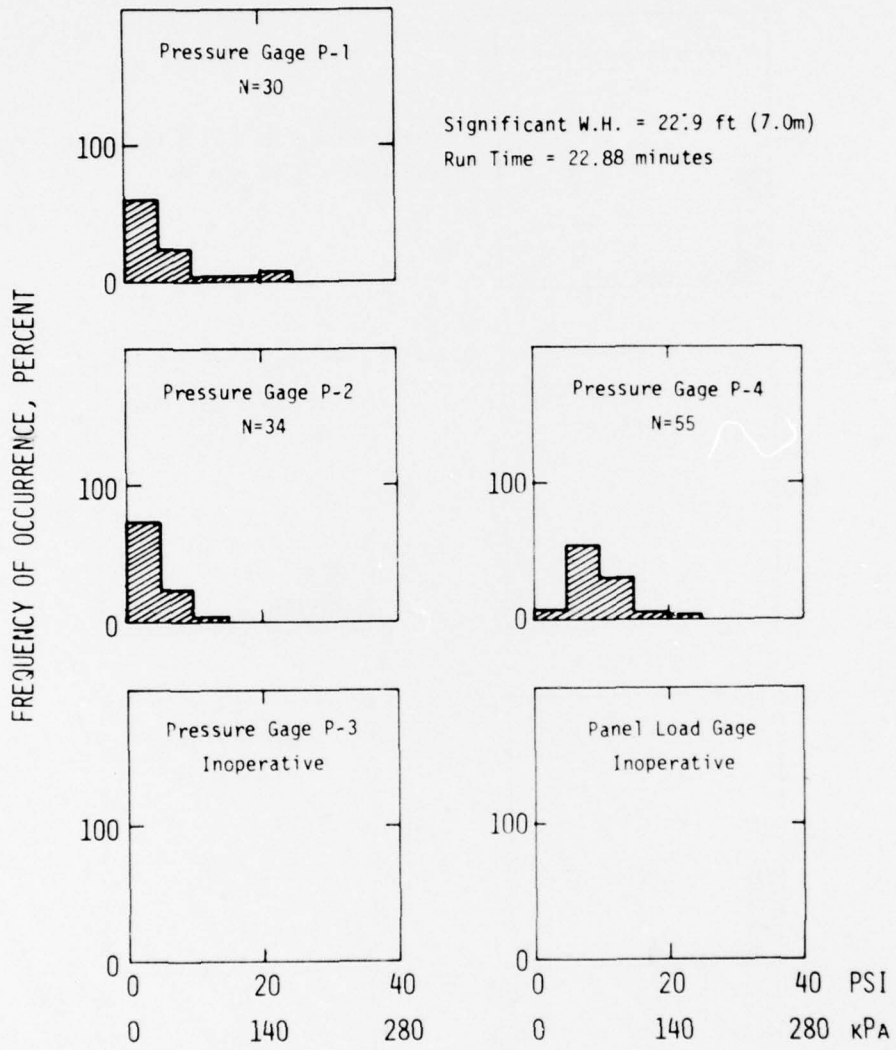

Figure 65 - Impact Pressure Histograms for SWATH 6C in Head Sea State 7 - 20 Knots

SWATH 6C - HEAD SEA STATE 7 - 20 KNOTS

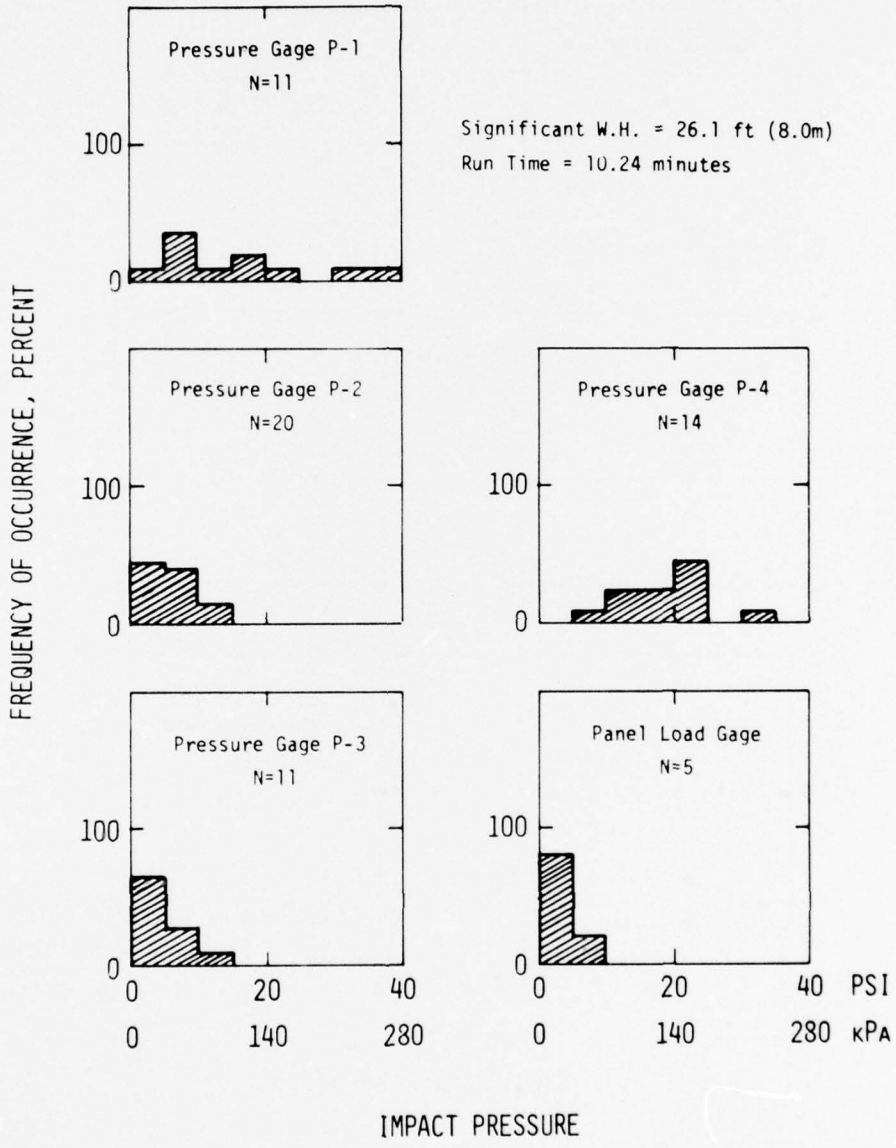

Figure 66 - Impact Pressure Histograms for SWATH 6C in Head Sea State 7 - 20 Knots

HEAD SEAS - RANDOM WAVES - 28 KNOTS

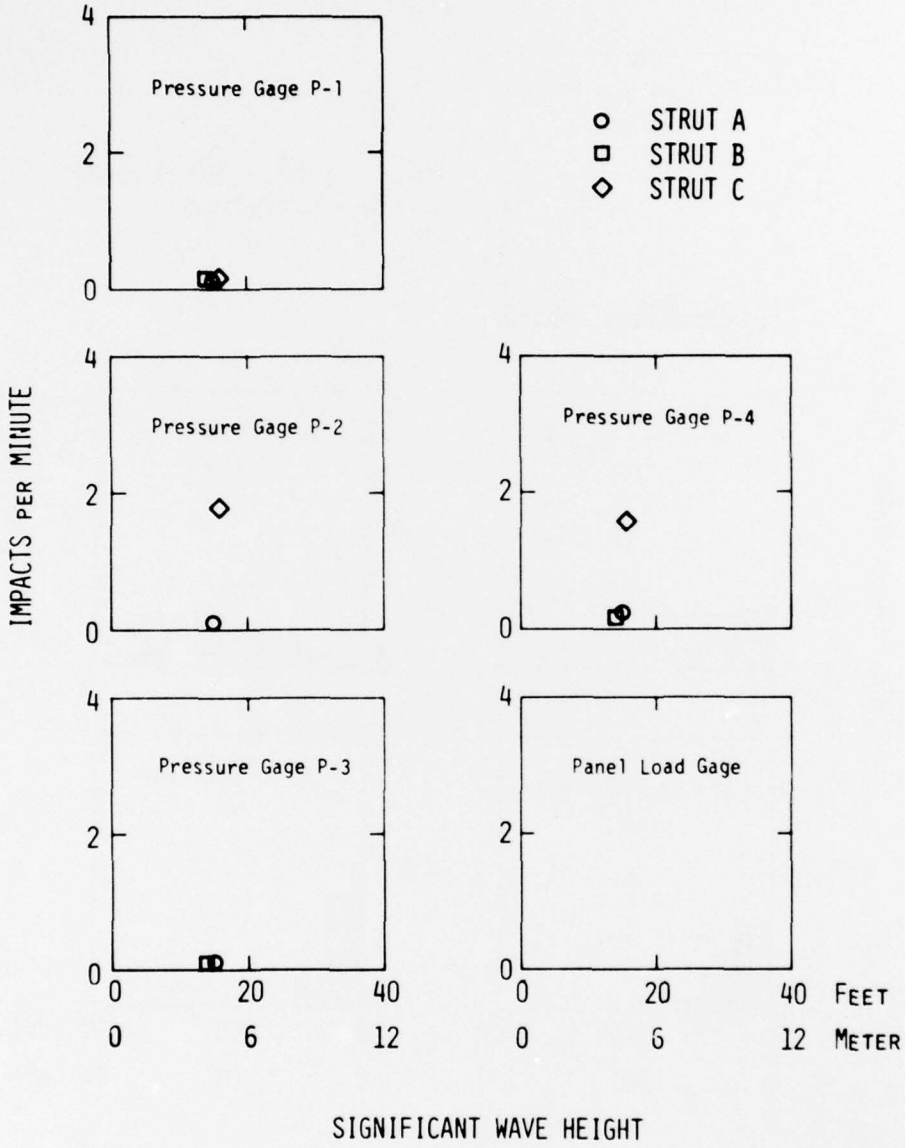

Figure 67 - Frequency of Impacting in Random Head Seas for SWATH 6
20 Knots

SWATH 6A - HEAD SEA STATE 6 - 28 KNOTS

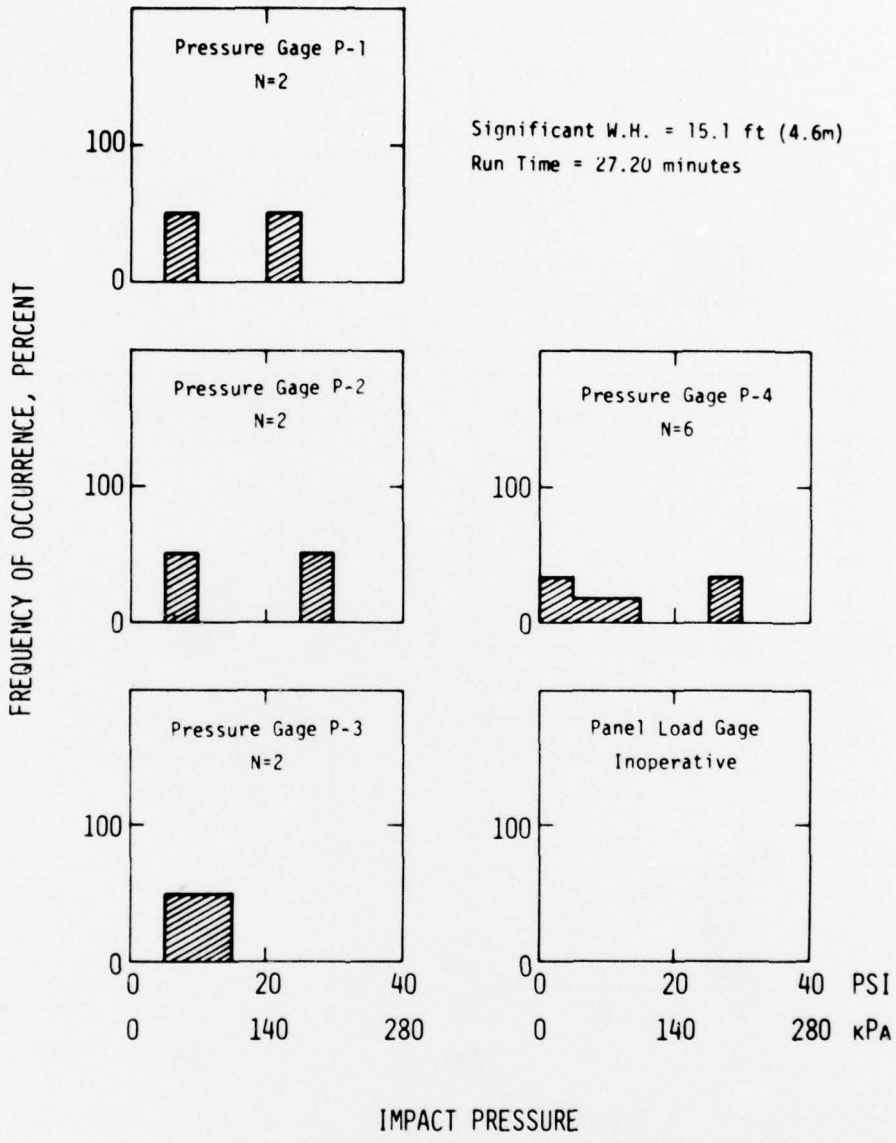

Figure 68 - Impact Pressure Histograms for SWATH 6A in Head Sea State 6 - 28 Knots

SWATH 6B - HEAD SEA STATE 6 - 28 KNOTS

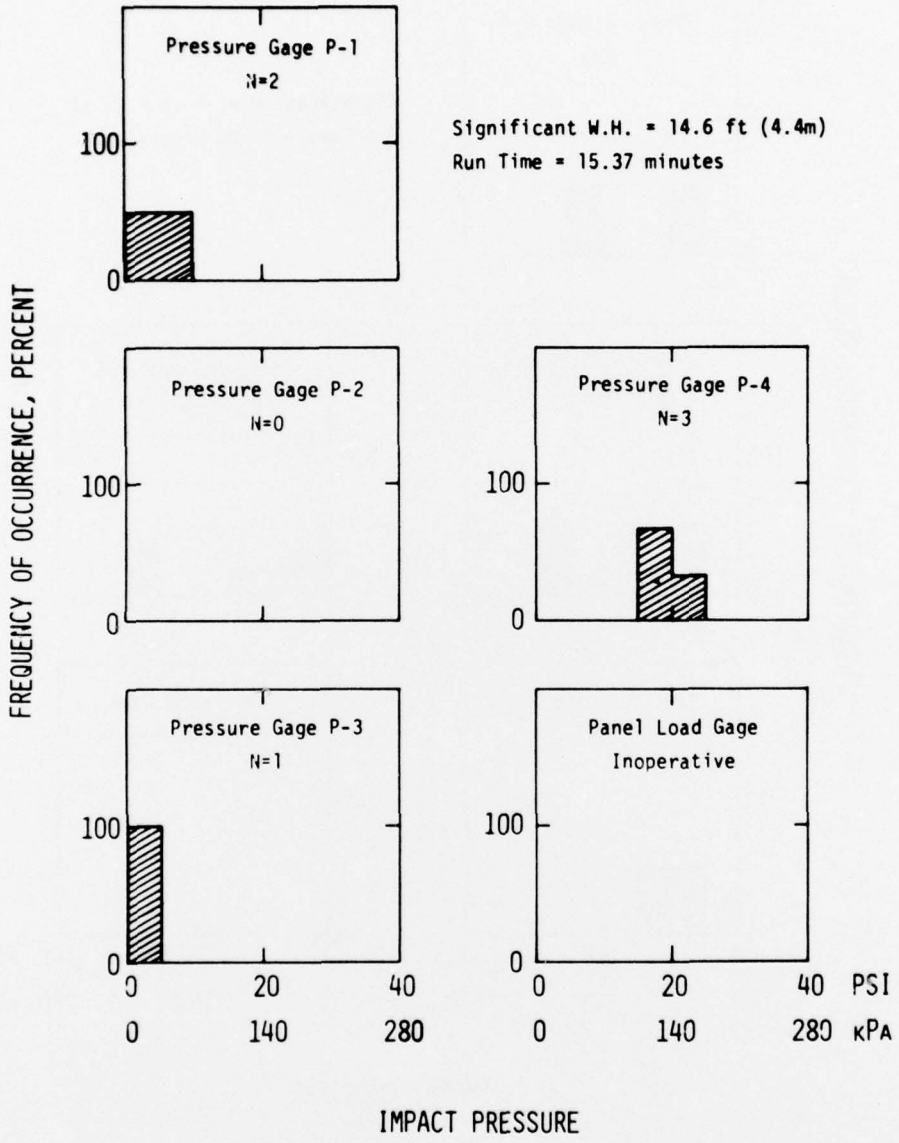

Figure 69 - Impact Pressure Histograms for SWATH 6B in Head Sea State 6 - 28 Knots

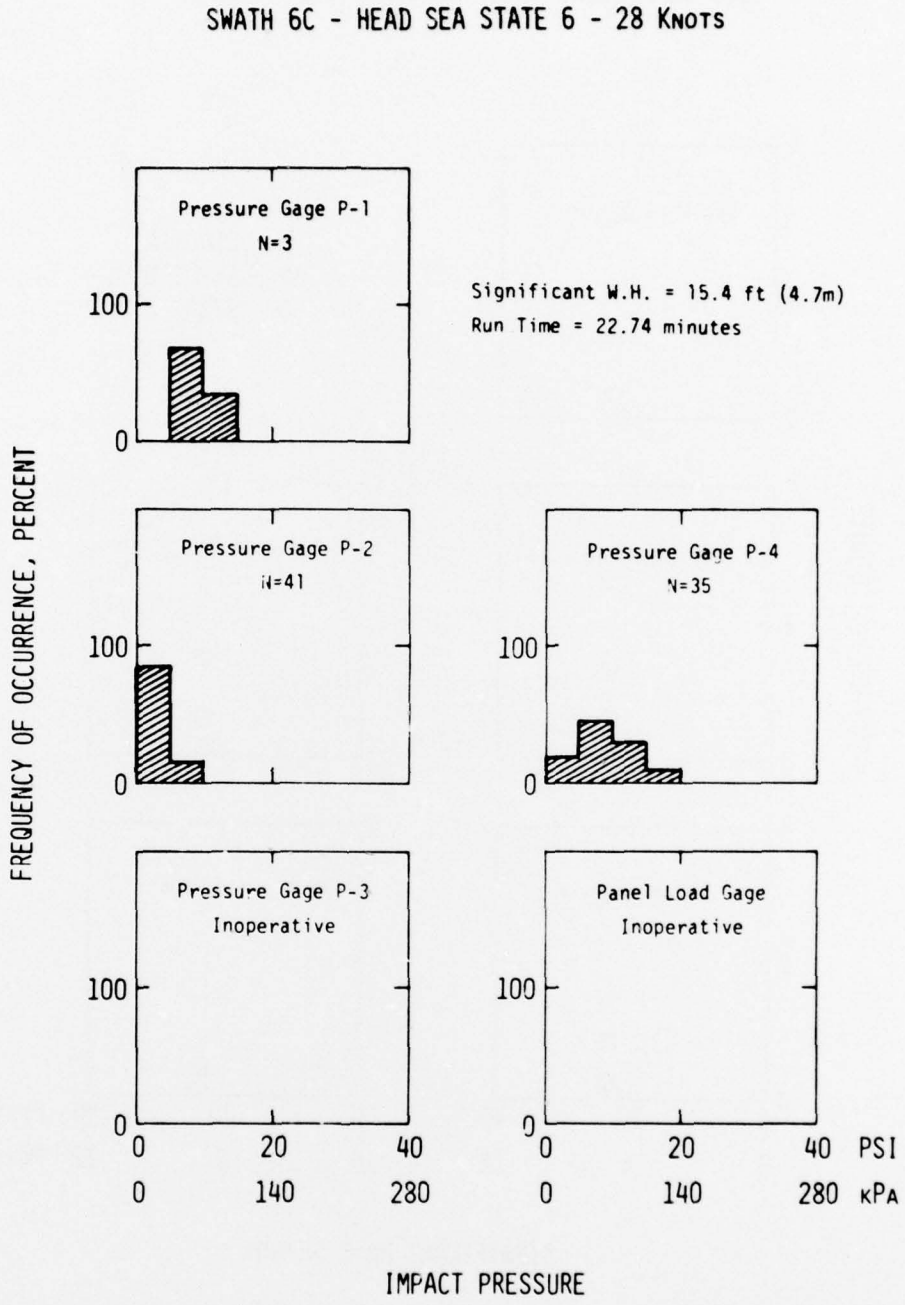

Figure 70 - Impact Pressure Histograms for SWATH 6C in Head Sea State 6 - 28 Knots

BOW QUARTERING SEAS - RANDOM WAVES - 20 KNOTS

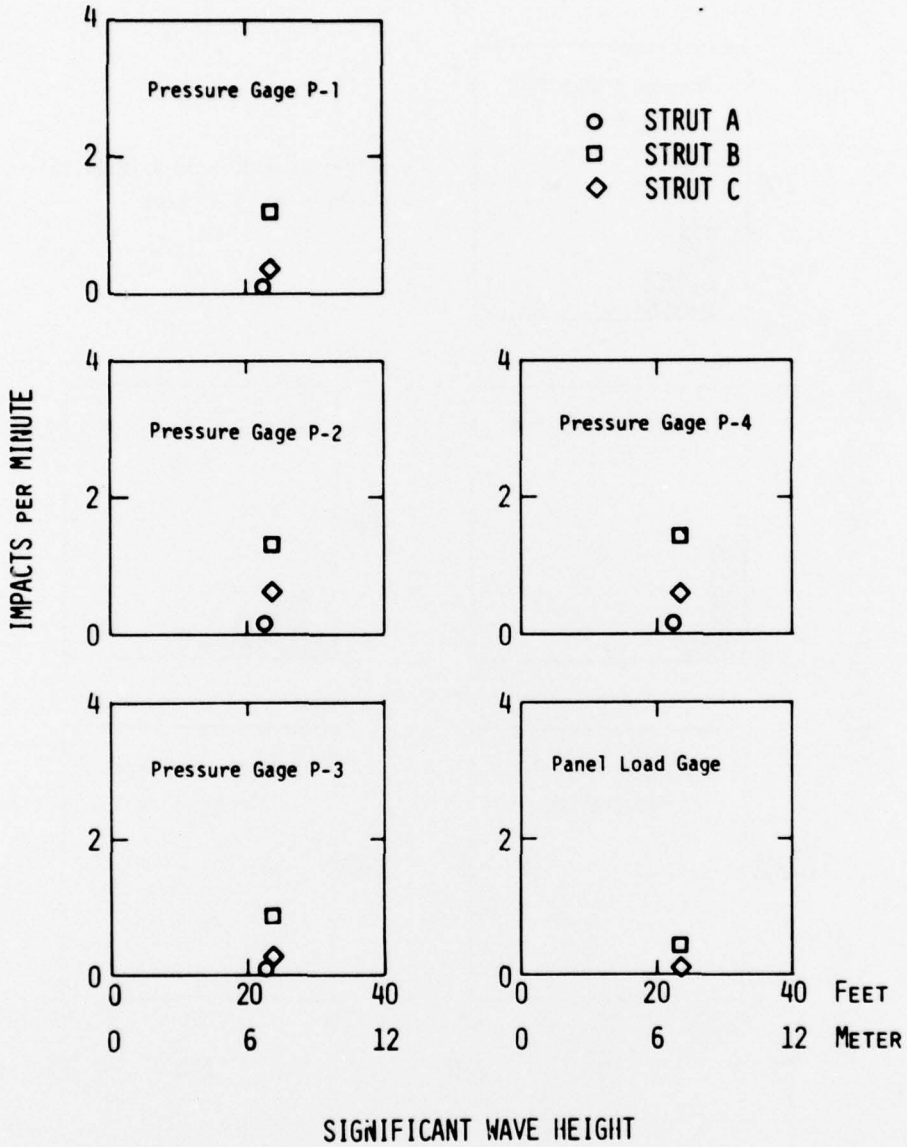

Figure 73 - Frequency of Impacting in Random Bow Quartering Seas for SWATH 6 - 20 Knots

SWATH 6A - BOW QUARTERING SEA STATE 7 - 20 KNOTS

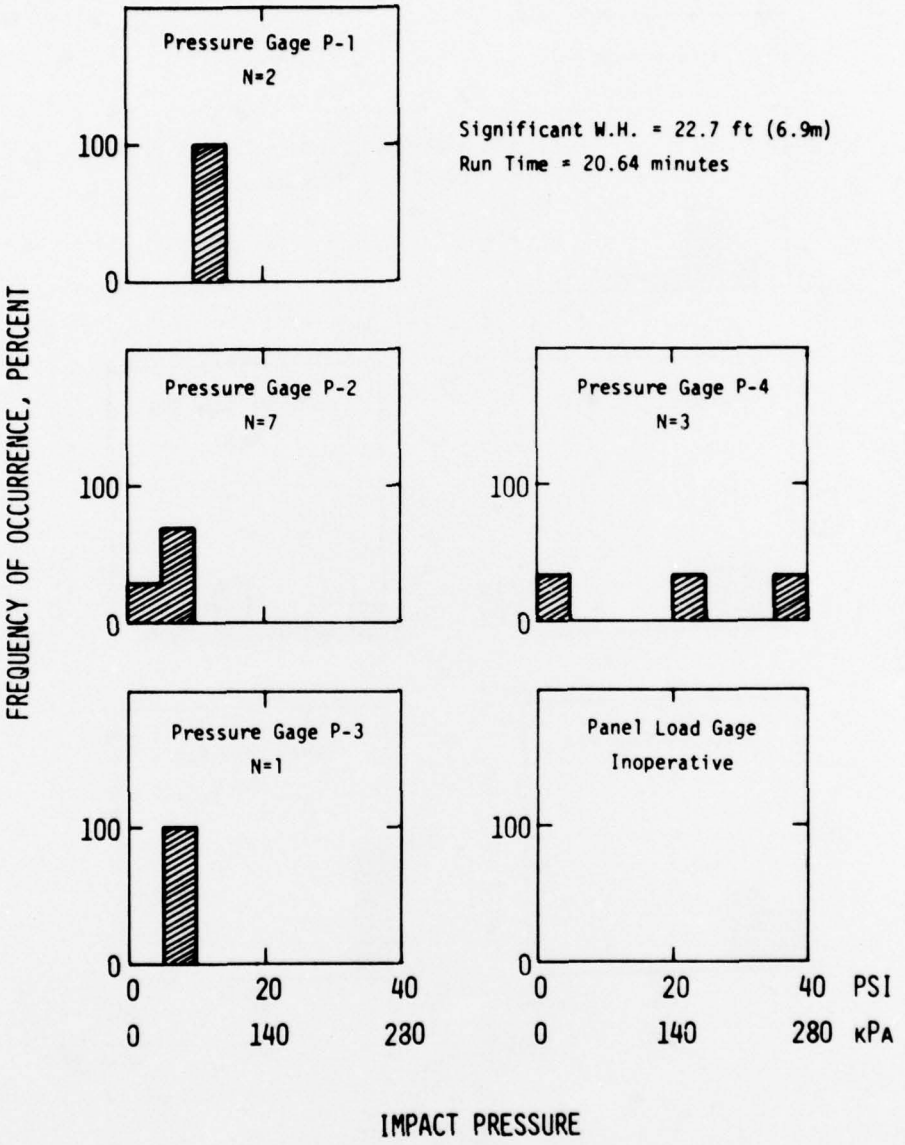

Figure 74 - Impact Pressure Histograms for SWATH 6A in Bow Quartering Sea State 7 - 20 Knots

SWATH 6B - BOW QUARTERING SEA STATE 7 - 20 KNOTS

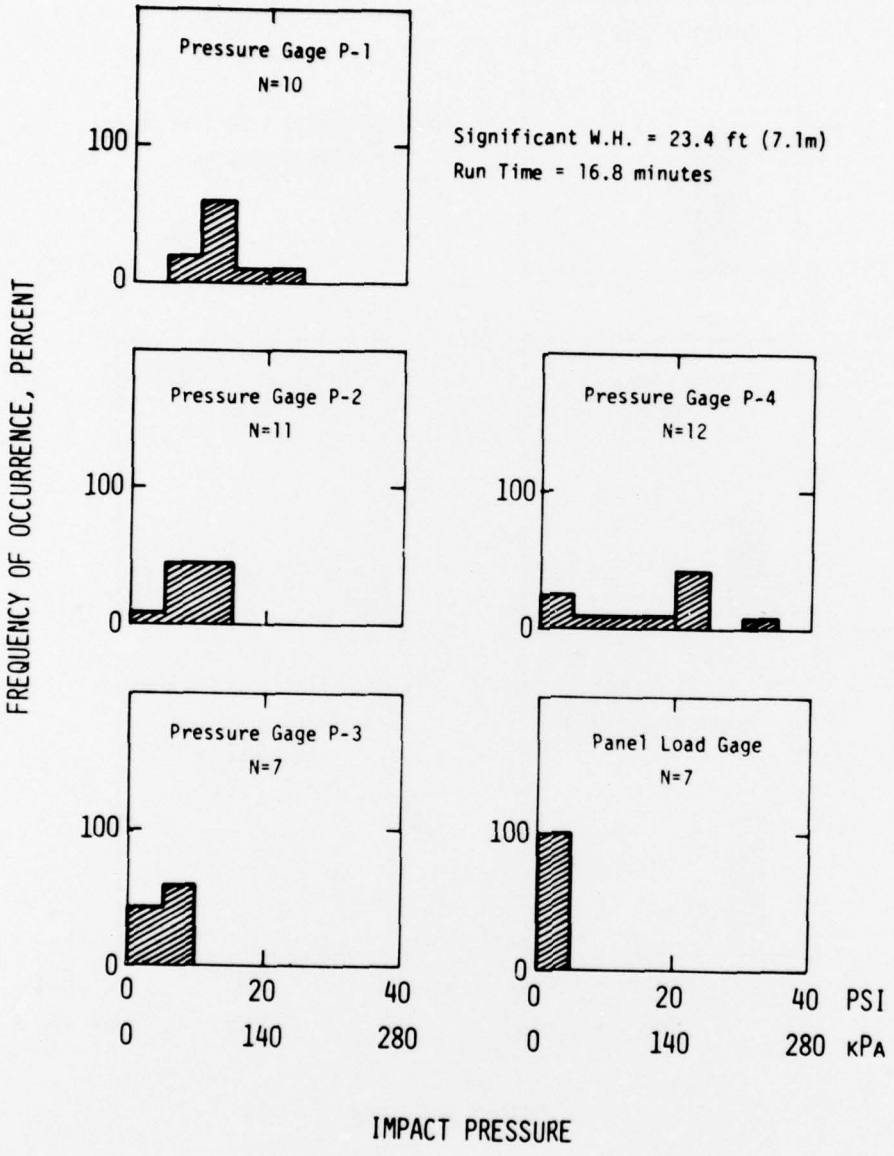

Figure 75 - Impact Pressure Histograms for SWATH 6B in Bow Quartering Sea State 7 - 20 Knots

SWATH 6C - BOW QUARTERING SEA STATE 7 - 20 KNOTS

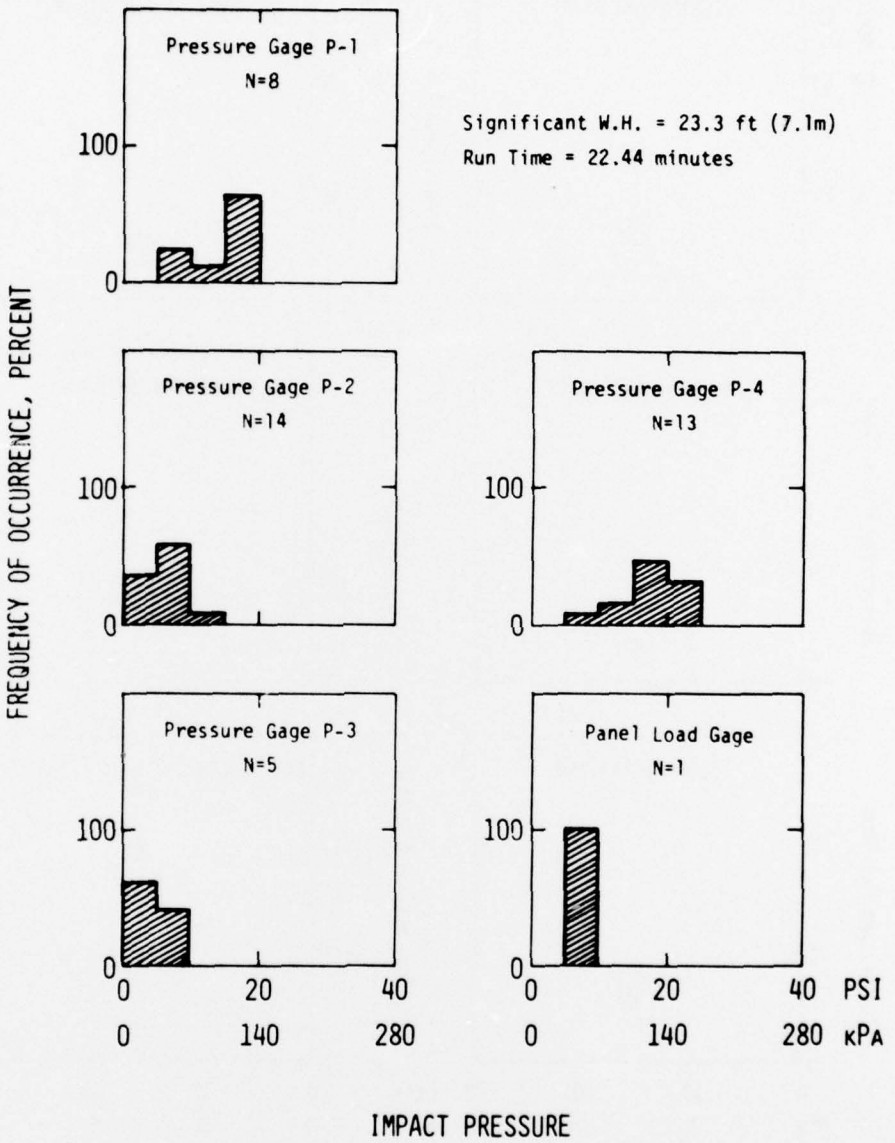

Figure 76 - Impact Pressure Histograms for SWATH 6C in Bow Quartering Sea State 7 - 20 Knots

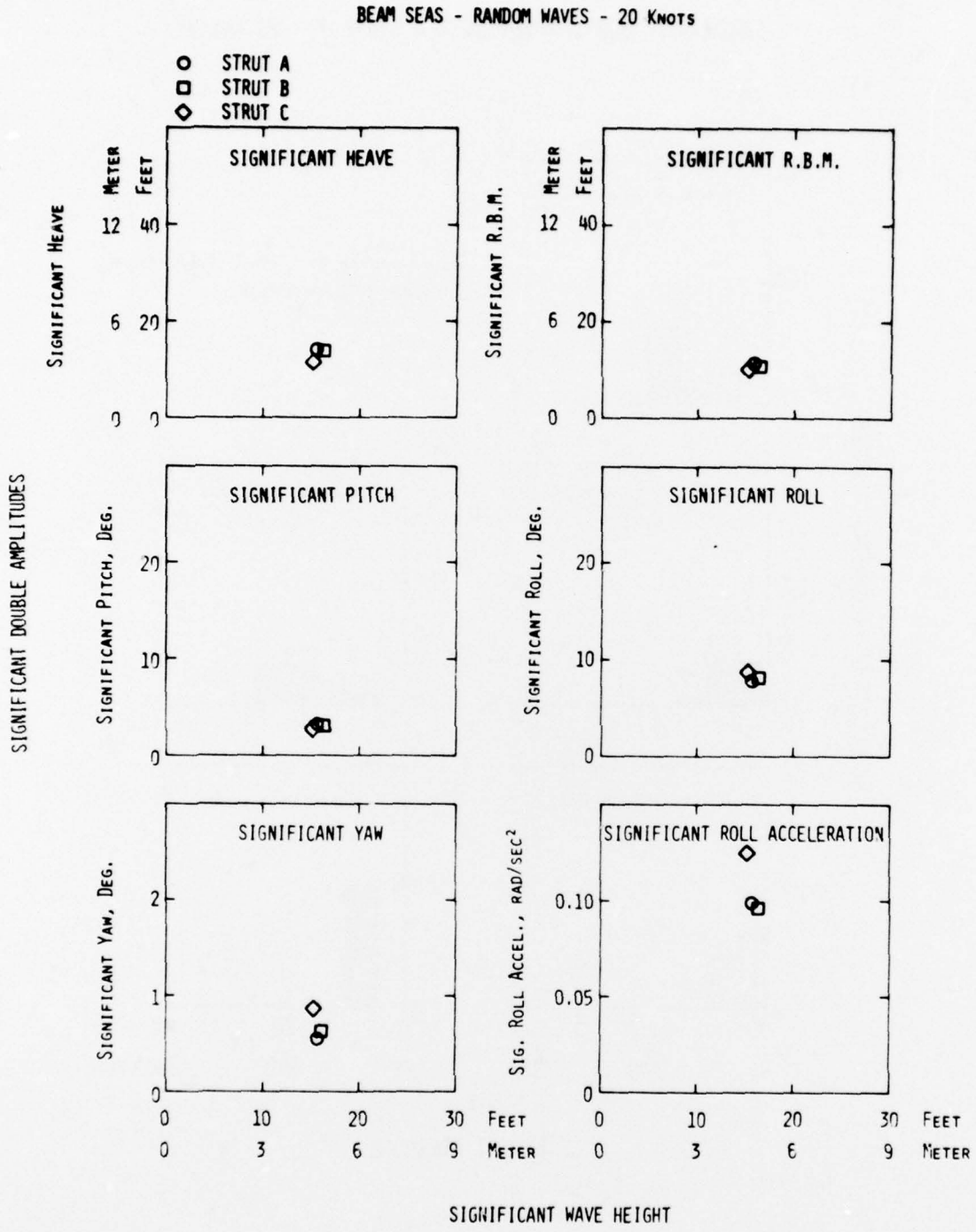

Figure 77 - Significant Double Amplitudes of Motions in Random Beam Seas for SWATH 6 - 20 Knots

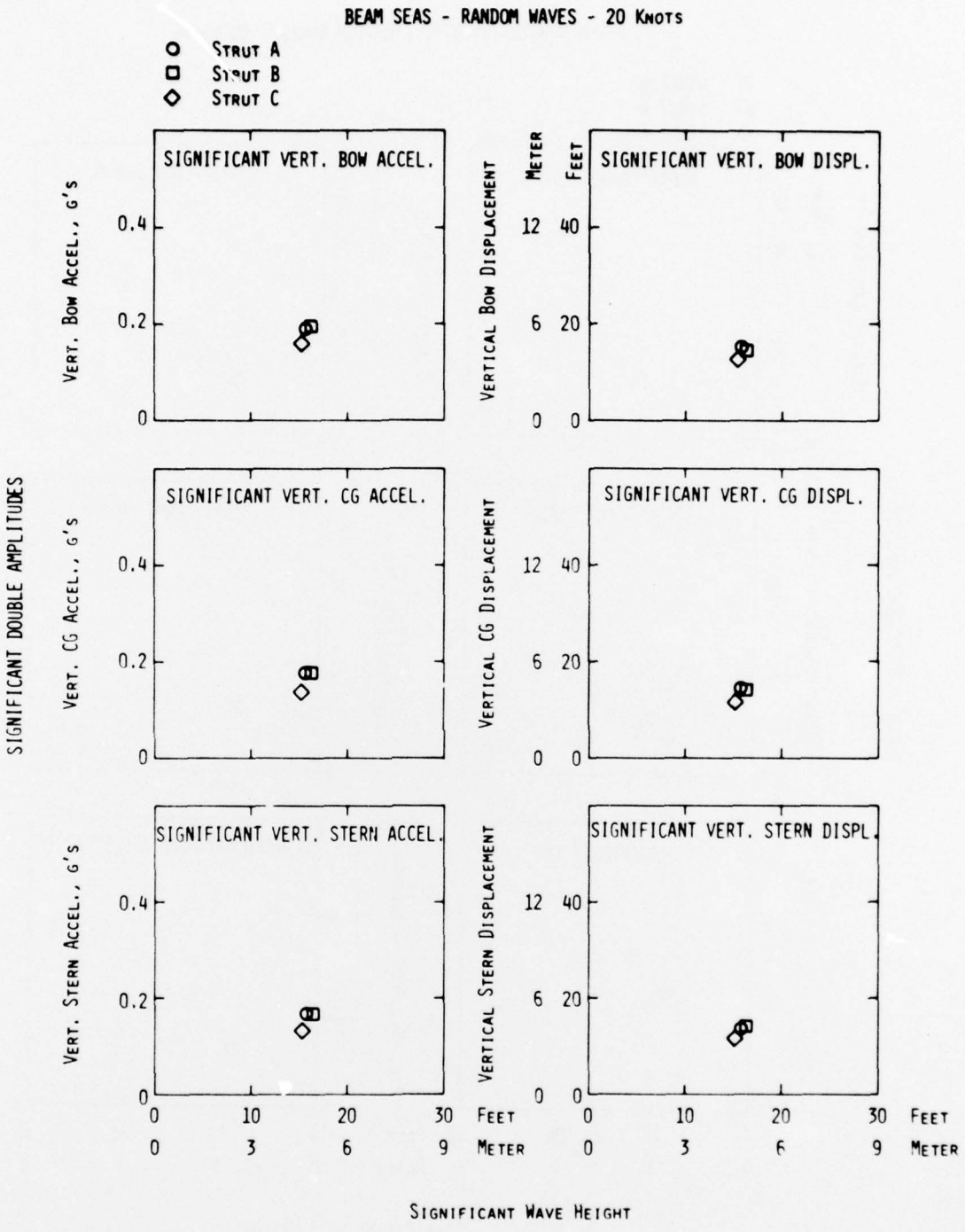

Figure 78 - Significant Double Amplitudes of Vertical Accelerations and Vertical Motions in Random Beam Seas for SWATH 6 - 20 Knots

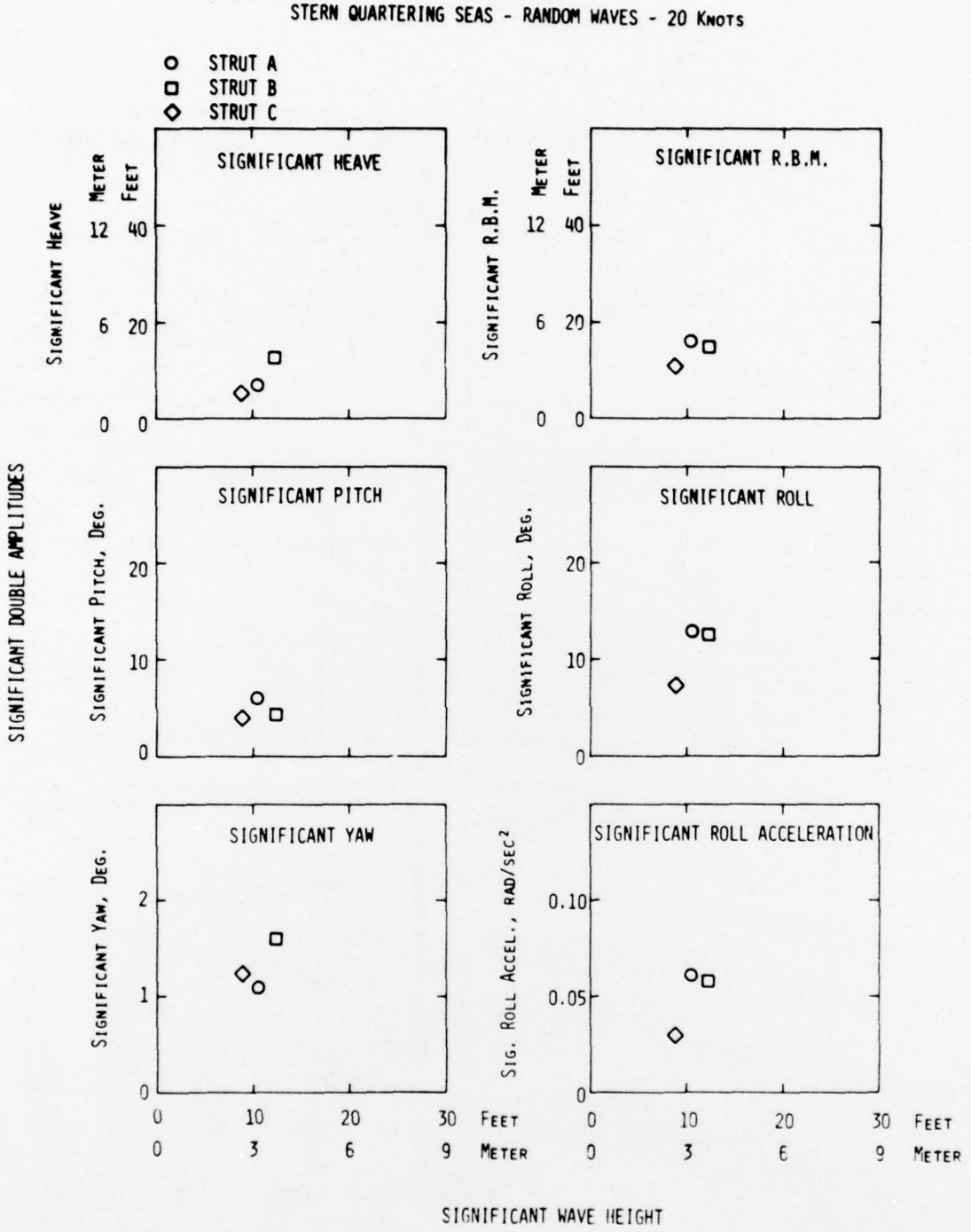

Figure 79 - Significant Double Amplitudes of Motions in Random Stern Quartering Seas for SWATH 6 - 20 Knots

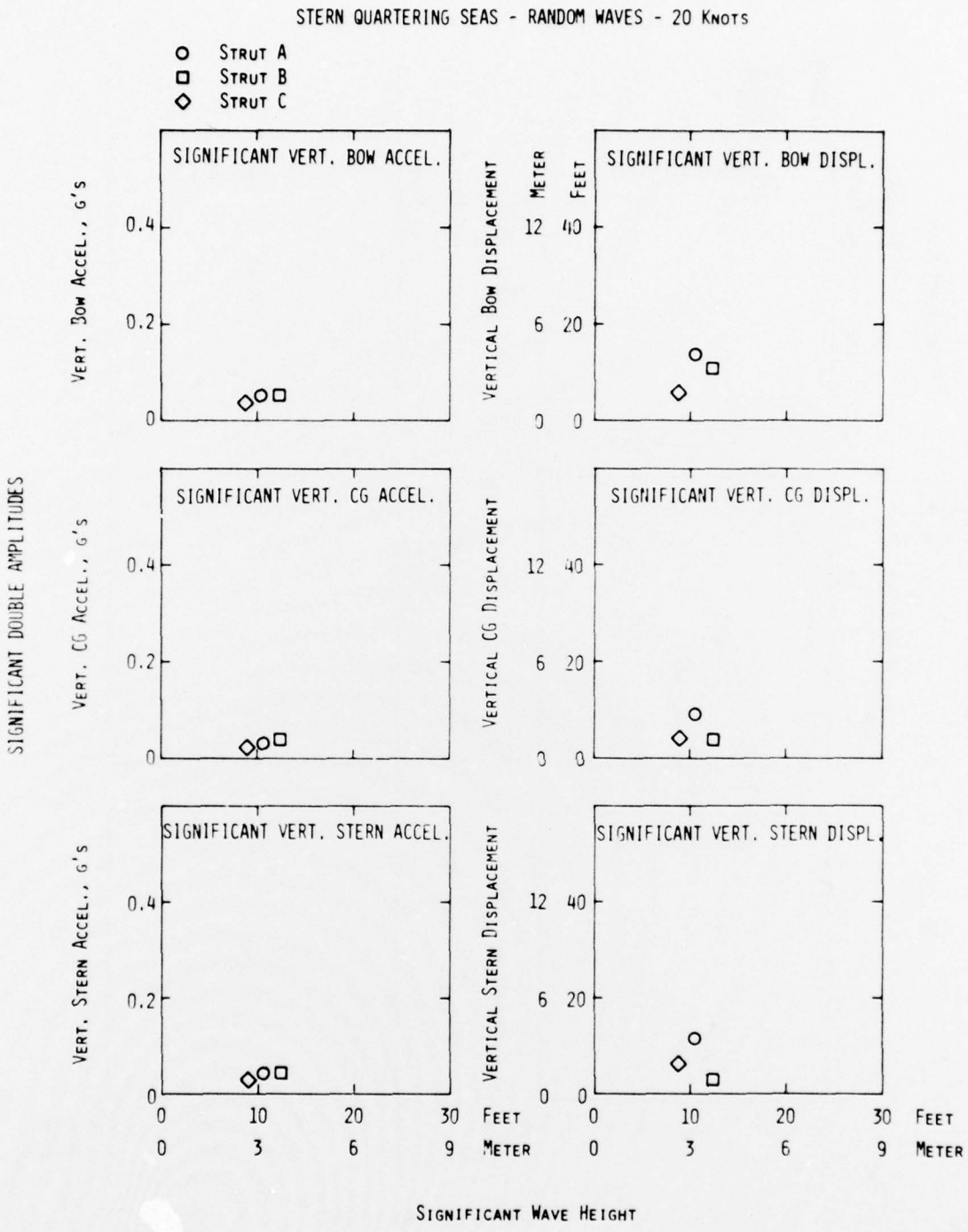

Figure 80 - Significant Double Amplitudes of Vertical Accelerations and Vertical Motions in Random Stern Quartering Seas for SWATH 6 - 20 Knots

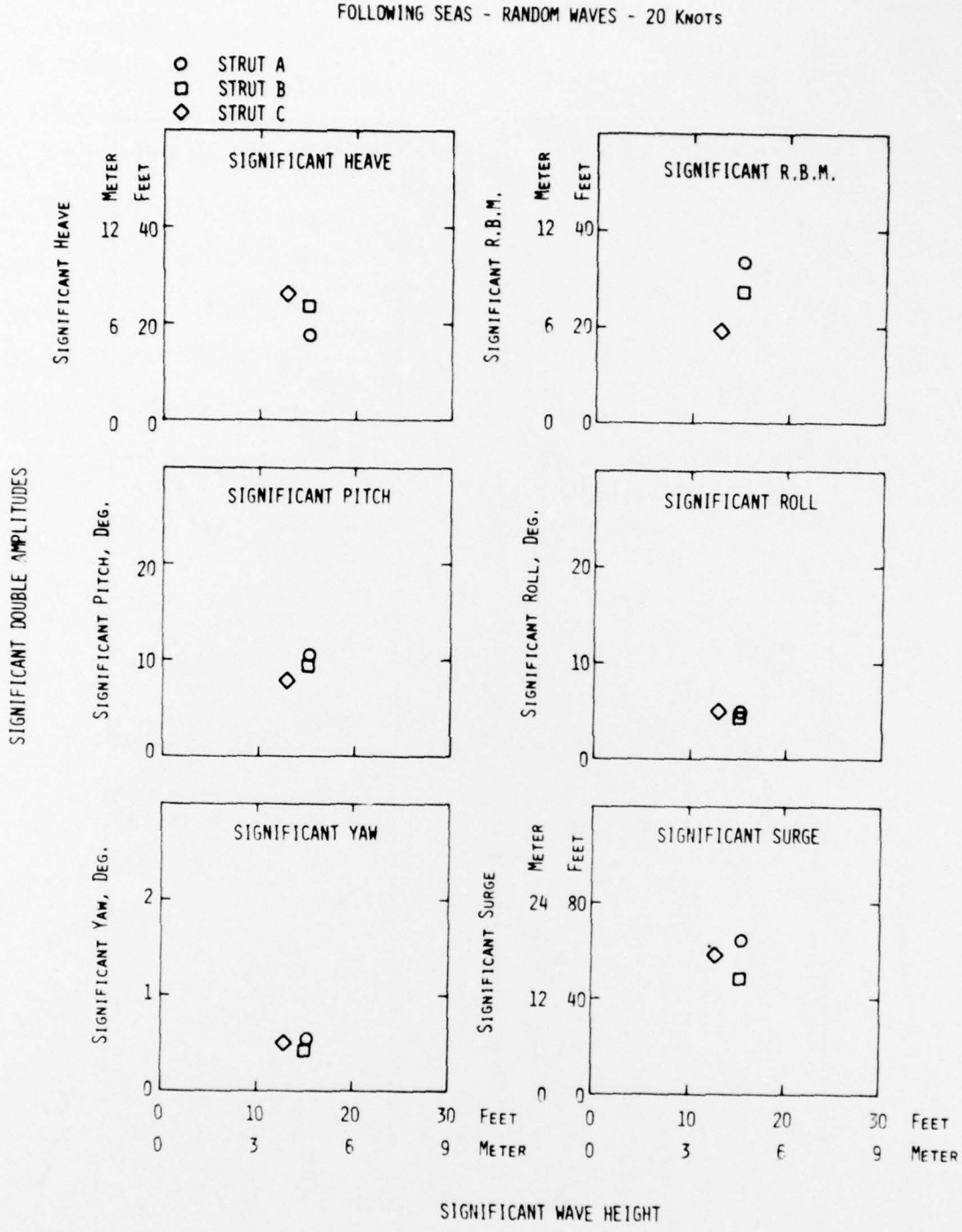

Figure 81 - Significant Double Amplitudes of Motions in Random Following Seas for SWATH 6 - 20 Knots

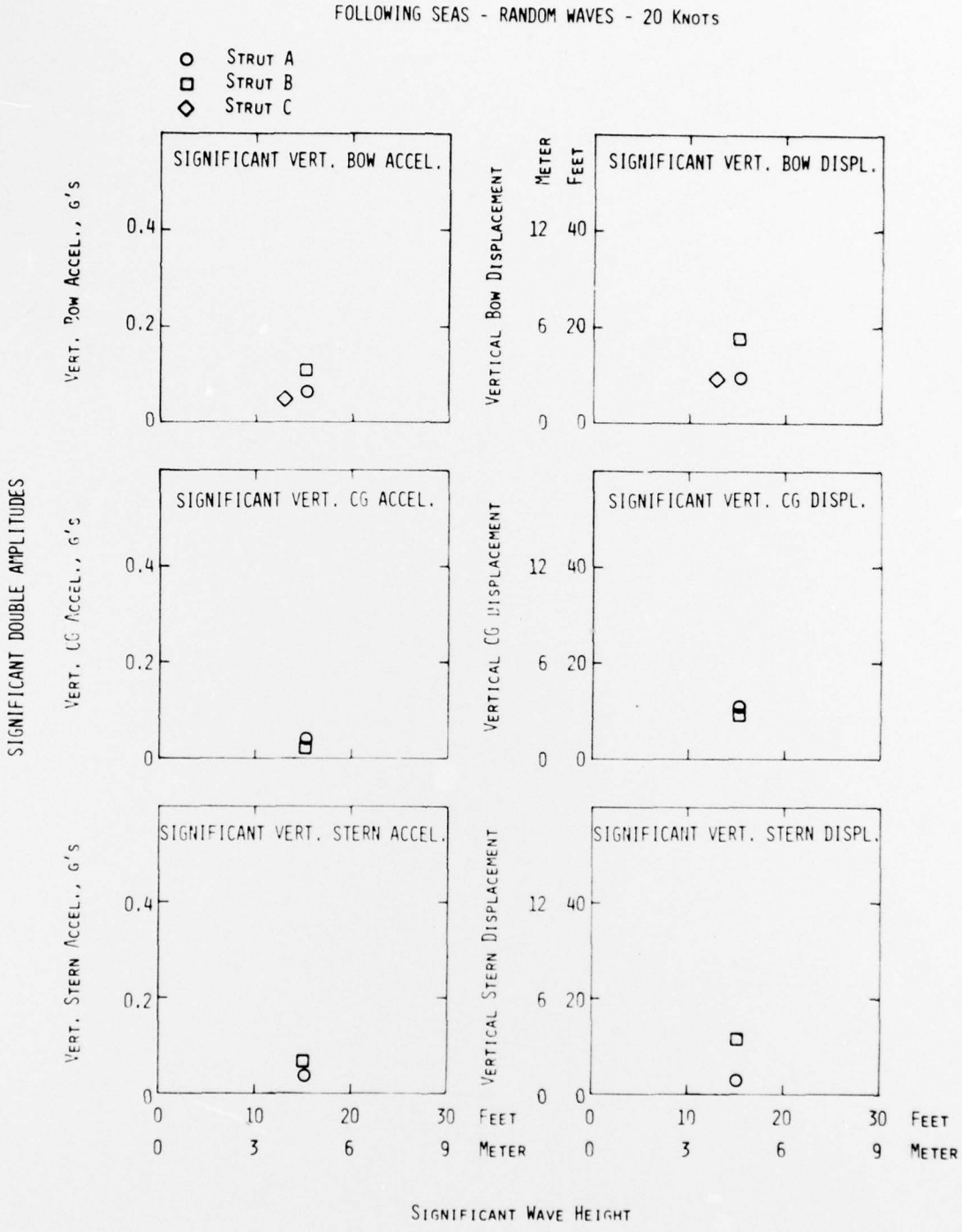

Figure 82 - Significant Double Amplitudes of Vertical Accelerations and Vertical Motions for SWATH 6 - 20 Knots

DTNSRDC ISSUES THREE TYPES OF REPORTS

(1) DTNSRDC REPORTS, A FORMAL SERIES PUBLISHING INFORMATION OF PERMANENT TECHNICAL VALUE, DESIGNATED BY A SERIAL REPORT NUMBER.

(2) DEPARTMENTAL REPORTS, A SEMIFORMAL SERIES, RECORDING INFORMATION OF A PRELIMINARY OR TEMPORARY NATURE, OR OF LIMITED INTEREST OR SIGNIFICANCE, CARRYING A DEPARTMENTAL ALPHANUMERIC IDENTIFICATION.

(3) TECHNICAL MEMORANDA, AN INFORMAL SERIES, USUALLY INTERNAL WORKING PAPERS OR DIRECT REPORTS TO SPONSORS, NUMBERED AS TM SERIES REPORTS; NOT FOR GENERAL DISTRIBUTION.